Kansas Geological Survey Technical Series 24

Midcontinent Carbonate Research

Virtual Symposium • Extended Abstracts

14–15 September 2021

Editors:
Diana Ortega-Ariza
Ibukun Bode-Omoleye
Franek J. Hasiuk
Sahar Mohammadi
Evan K. Franseen

Kansas Geological Survey • University of Kansas • Lawrence, Kansas

Midcontinent Carbonate Research Virtual Symposium Extended Abstracts

Editors: Diana Ortega-Ariza, Ibukun Bode-Omoleye,
Franek J. Hasiuk, Sahar Mohammadi, and Evan K. Franseen

Kansas Geological Survey
Technical Series 24
September 2021

ISBN 978-1-58806-337-2

Kansas Geological Survey
1930 Constant Avenue
Lawrence, KS 66047-3724

785.864.3965
www.kgs.ku.edu

KU KANSAS GEOLOGICAL SURVEY
The University of Kansas

Table of Contents

Preface 1

Assessment of the Arbuckle in Western Kansas Using Inversion of 3-D Seismic
Adeniyi Ajobiewe and George Tsoflias 2

Diagenesis of the Arbuckle Group on the Southern Midcontinent (Missouri and Oklahoma)
Phillip A. Bailey III, Britney J. Temple, and Jay M. Gregg 6

A Preliminary Characterization of Pore Heterogeneity and Permeability in Karst Carbonate Reservoirs
Ibukun Bode-Omoleye 10

Geometry of the Burlington Shelf During the Early Mississippian: Thickening Both Shoreward and Basinward Away from the Starved (Shaved?) Central Middle Shelf
Matthew G. Braun, Bradley D. Cramer, Brittany M. Stolfus, Madysen Gilbert, Megan N. Heath, Gwen L. Barnes, Ryan J. Clark, James E. Day, Brian J. Witzke, Nicholas J. Hogancamp, and Stephanie Tassier-Surine 13

Paleozoic Brine Reflux: Its Impact on Diagenesis and Basin-Brine Composition in Major Onshore Oil-and-Gas Basins of the United States
Robert H. Goldstein, David A. Fowle, and Randy L. Stotler 16

Tectonically Controlled Patterns of Contour-Current Deposition and Erosion in Outer Shelf, Lower Mississippian, Arkansas-Missouri-Oklahoma
C. Robertson Handford 20

Chemical and Engineering Properties of Kansas Limestone Aggregates: A Review of Data from Construction Material Inventories
Franek J. Hasiuk 24

Hydrothermal Fluid Flow and Burial History in the STACK Play of North-Central Oklahoma
Andrew M. Hollenbach, Sahar Mohammadi, Robert Goldstein, and Andreas Möller 28

Paleokarst Development and Controls in the Cambrian Potosi Dolomite and Eminence Formation, Illinois Basin
Yaghoob Lasemi and Zohreh Askari 31

Timing of Hydrothermal Fluid Flow Events in Kansas and Tri-State Mineral District
Sahar Mohammadi, Andrew M. Hollenbach, Robert H. Goldstein, and Andreas Möller 34

Regional Controls on Low-Latitude, Shallow-Water Heterozoan and Photozoan Carbonate Facies Distribution, Lower Mississippian, Continental U.S.
Diana Ortega-Ariza and Evan K. Franseen 38

Geological Influences upon the Mississippian Pitkin Limestone/ Caney Shale in the Arkoma Basin
Abbas Seyedolali, Kurt Rottmann, Emlio J. Torres Parada, William Full, and Brittany V. Stroud 42

Logging Reservoirs, Petroleum Systems, Wettability, and CCS Viability in Midcontinent Carbonates Using Gentle-Extraction Cryo-Trap Mass Spectrometry of Drill Cuttings' and Cores' Present-Day Volatiles
Michael P. Smith, Christopher Smith, Patrick Gordon, and Timothy Smith 44

Static Earth Modeling and CO_2 Storage in Lansing and Kansas City Groups, Huffstutter Field, Kansas, USA
Valerie Smith 48

Facies Architecture and Reservoir Characteristics of the Caney Shale, Ardmore Basin, Southern Oklahoma, USA
Yulun Wang, G. Michael Grammer, Jack Pashin, Jim Puckette, and Mileva Radonjic 52

Preface

This volume is the result of a virtual symposium on U.S. Midcontinent carbonate research hosted by the Kansas Geological Survey on September 14–15, 2021. The idea to hold the symposium was motivated by the importance of Midcontinent carbonate rocks in that they:

- have contributed to fundamental sedimentology and stratigraphy concepts
- host active and mature hydrocarbon reservoirs
- are targets for CO_2 sequestration
- serve as outcrop analogs for petroleum systems
- store paleoclimate and paleoenvironmental information
- are sources of construction and industrial materials

The goals of the symposium were to (1) have presentations on new and ongoing research on carbonate formations in the Midcontinent region, (2) foster discussion and the exchange of ideas, (3) explore opportunities for future collaborations, and (4) generate interest in having future meetings on a regular basis. The extended abstracts in this volume come from presentations that were given at the symposium. They cover Cambrian to Pennsylvanian carbonate rocks in the Midcontinent and comprise a diverse array of subjects, including sedimentologic, tectonic, geochemical, geophysical, diagenetic, reservoir, and aggregate studies.

We thank all of the speakers and participants for joining us in this symposium and sharing their research, thoughts, and ideas. We are extremely grateful to Julie Tollefson (KGS) for technical editing and production of this volume and to Blair Schneider (KGS) for symposium logistical help.

The Editors

Assessment of the Arbuckle in Western Kansas Using Inversion of 3-D Seismic

Adeniyi Ajobiewe and George Tsoflias
Department of Geology, University of Kansas, Lawrence, Kansas, USA

Introduction

The United States Department of Energy–National Technology Laboratory (DOE-NETL), under the Carbon Storage Assurance Facility Enterprise program (CarbonSAFE), has initiated projects that focus on the development of geologic storage sites in western Kansas for the storage of 50+ million metric tons (MMT) of CO_2 from industrial sources. Previous studies have identified the Cambrian-Ordovician Arbuckle Group as a deep saline aquifer with a potential for commercial-scale storage of CO_2. It consists mainly of dolomite with scattered beds containing chert, sand, and a minor amount of glauconite (Wallace, 1943). Arbuckle Group rocks in Kansas vary in thickness from north to south and are thickest in the southeastern corner — up to 1,340 ft. Regionally extensive and thick shales in the Morrowan, Atokan, and Cherokee intervals form primary seals for reservoir zones in the region (Watney et al., 2016).

The Patterson oil field in Kearny County, southwestern Kansas (fig. 1), was identified as a suitable site for CO_2 storage (Meng et al., 2020). The Arbuckle Group is the thickest of all candidate CO_2 storage zones at the Patterson Field. Two new 3-D seismic surveys were acquired over the Patterson and Hartland fields in 2019, and two deep wells were drilled through the Arbuckle down into the granitic basement (Meng et al., 2020). The 3-D seismic covered a combined 25.9 square miles of land with a bin size of 82.5 x 82.5 feet. The seismic dataset includes Offset Vector Tile (OVT) processed pre-stack time migrated (PSTM) gathers and stacked volumes. Figure 2 shows borehole logs along with formation tops at the Patterson KGS #5-25 well.

This study uses pre-stack and post-stack geophysical inversion methods to characterize the Arbuckle Group at Patterson Field. This research will aid the development of reservoir models for CO_2 flood simulations and serve as a reference point for future monitoring.

Methods and Results

Seismic-well tie: A seismic-well tie process was carried out using the Hampson-Russell software (CGG, 2021). This process used the Patterson KGS #5-25 well with associated sonic and density logs and the Patterson 3-D OVT data to generate a synthetic seismogram (fig. 2). Information about depths to the top of geologic formations was obtained through the Kansas Geological Survey (KGS) online oil and gas well database (KGS Oil and Gas Well Database). The generated synthetic

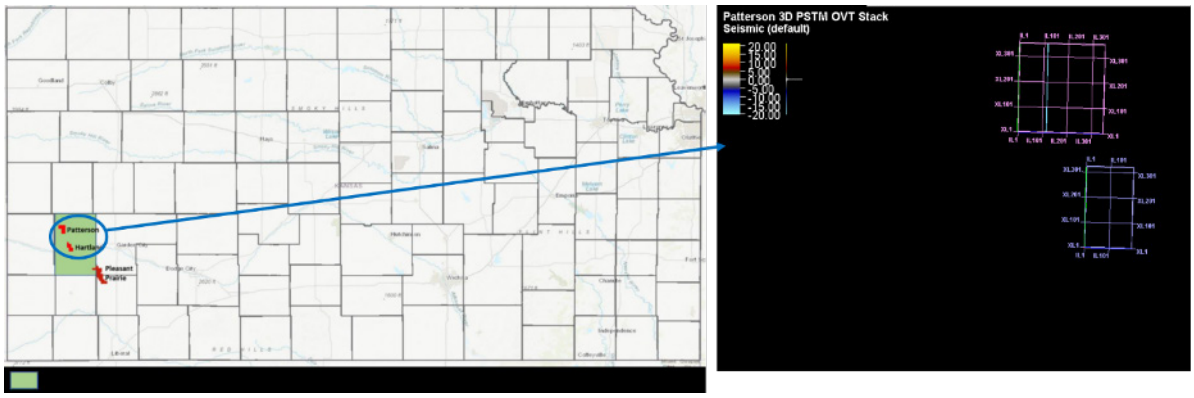

Figure 1. Location of the study area in Kearny County, Kansas. Patterson (pink outline) and Hartland (dark blue outline) 3-D surveys shown to the right (Map of Oil and Gas Data in Kansas).

seismogram was used as a link between these geological picks and the Patterson seismic data. A time-depth relationship obtained as a result shows that the top of the Arbuckle Group (about 5,762 ft true vertical depth [TVD]) is a negative amplitude reflection (trough) at about 1,032 ms on seismic. With a statistical wavelet extraction process outputting a 180° phase wavelet, the seismic data were determined to have a reverse polarity.

Inversion Results: The pre-stack and post-stack inversion results show consistent impedance characteristics of the Arbuckle Group. Both the pre- and post-stack impedance volumes delineate the top of the Arbuckle, whereas in the amplitude reflection data the Arbuckle top is a weak trough (fig. 2) not easily traced. The pre-stack impedance inversion yields higher resolution imaging and good agreement with borehole observations (fig. 3). Overall, the upper Arbuckle is lower in impedance than the lower Arbuckle and less heterogeneous. Lower impedance zones correlate with higher porosity and lower density zones, whereas the reverse relationship applies to higher impedance zones (fig. 3). This implies that the upper Arbuckle has more

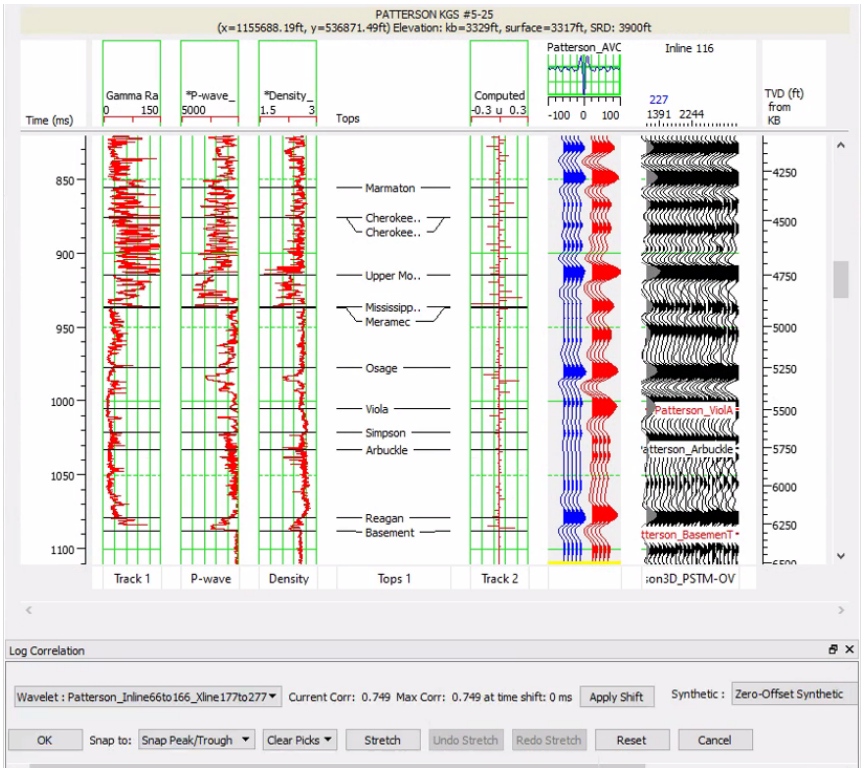

Figure 2. Seismic-well tie of the Patterson KGS #5-25 well using a well-extracted wavelet. The Arbuckle top corresponds to 1,032 ms two-way travel time (TWT), and synthetic-seismic correlation is 0.749.

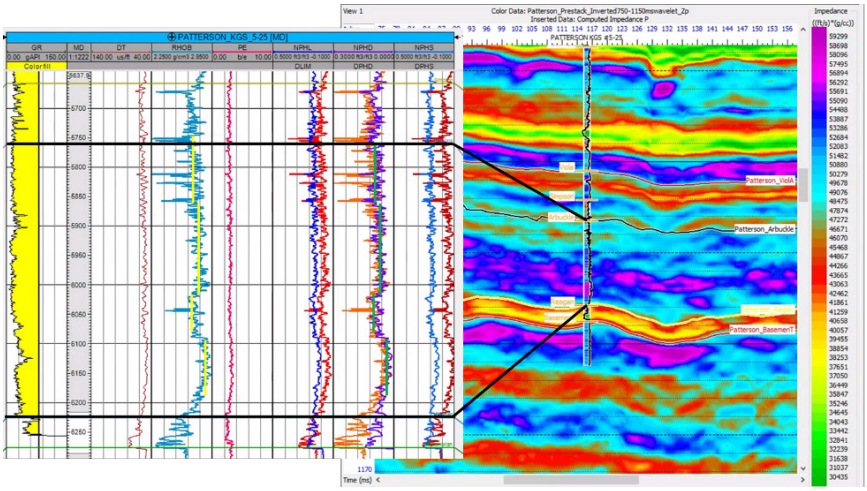

Figure 3. Patterson KGS #5-25 density and porosity well curves (left) and pre-stack impedance profile (Zp) of the inverted 3-D seismic at the well location (right).

porosity than the lower Arbuckle and the potential to hold larger CO_2 volume in place.

Based on the observed overall impedance contrast between the upper and lower Arbuckle zones seen in the inverted volume, a horizon that represents the boundary between upper and lower Arbuckle was picked (fig. 4). The picked horizon reveals variability in the thickness of the upper and lower impedance Arbuckle zones and the presence of a structural high and an adjacent low within the Arbuckle impedance; both appear to be basement-controlled and do not extend into shallower units. Maps of average impedance of the upper and lower Arbuckle zones show that the upper Arbuckle has predominantly lower impedances than the lower Arbuckle in most areas in the field (fig. 5).

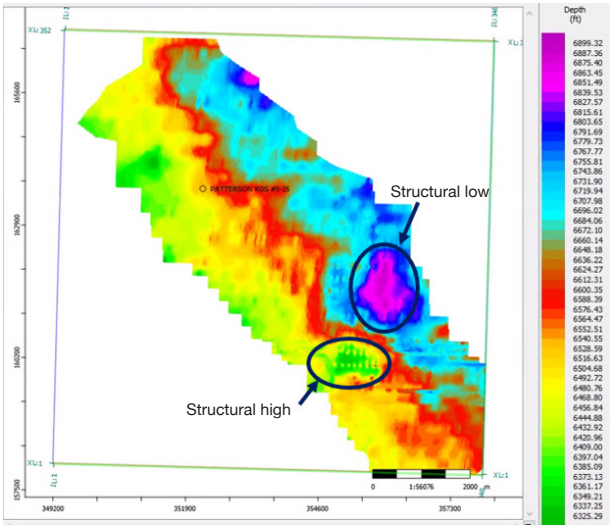

Figure 4. Depth structure map of the impedance boundary between the upper and lower Arbuckle.

Discussion and Conclusions

Within a unit with consistent mineral composition, variability in seismic impedance likely corresponds to variability in density and porosity distribution. As shown in fig. 3, large-scale porosity and density trends correspond to seismic impedance changes. At well KGS #5-25, higher porosity and lower density correspond to lower impedance values, predominantly seen in the upper Arbuckle. Conversely, the lower Arbuckle exhibits higher impedance with lower porosity and higher density zones. The impedance trends appear consistently throughout the seismic volume.

The upper Arbuckle should be targeted for the injection of CO_2 as it is likely more porous and better suited for fluid injection than the lower Arbuckle. In addition, the higher impedance variability of the lower Arbuckle may represent poor connectivity between porous and less porous zones, making it uncertain that injected CO_2 will flood the reservoir efficiently. This study demonstrates that seismic impedance inversion can offer insight to the internal architecture of the Arbuckle Group and help support CO_2 injection and storage projects. Pre-stack impedance inversion, as expected, provided superior imaging results to post-stack inversion, although both methods yield consistent results.

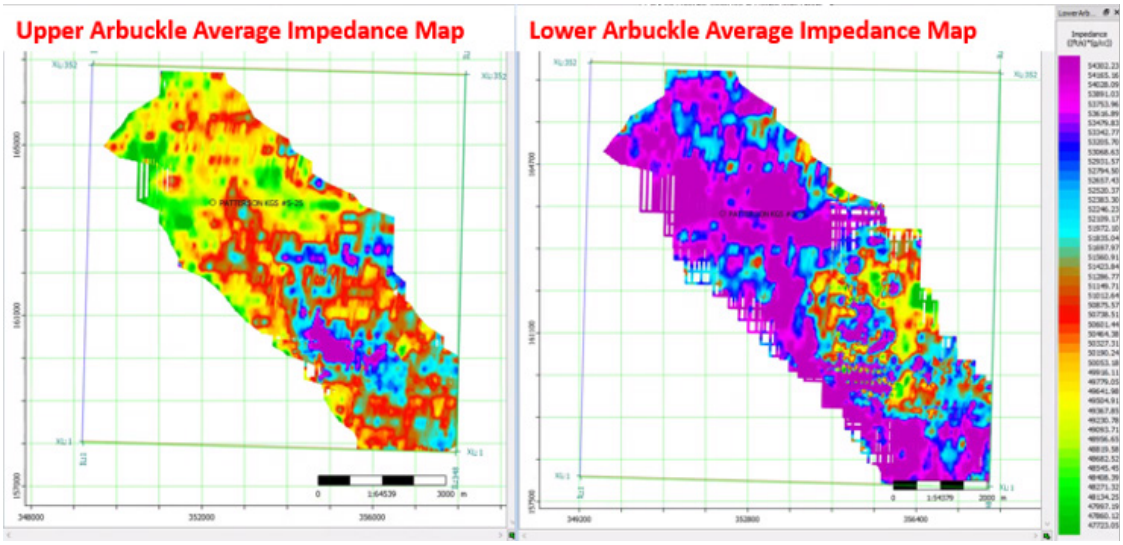

Figure 5. Average impedance maps of the upper and lower Arbuckle.

Acknowledgments

U.S. Department of Energy/NETL, DE-FE0029264 and collaborators E. Holubnyak, J. Meng, F. Hasiuk, J. Hollenbach, D. Wreath, and Berexco.

References

Meng, J., Holubnyak, Y., Hasiuk, F., Hollenbach, J., and Wreath, D., 2020, Geological characterization of the Patterson CO_2 storage site from 3-D seismic data: Midcontinent Geoscience. v. 1, p. 52–90.

Wallace, L., 1943, The stratigraphy and structural development of the Forest City basin in Kansas: Kansas Geological Survey Bulletin, 51, 142 p.

Watney, W. L., Rush, J., and Raney, J., 2016, Modeling CO_2 sequestration in saline aquifer and depleted oil reservoir to evaluate regional CO_2 sequestration potential of Ozark Plateau aquifer system, south-central Kansas, final report, Award Number: DE-FE0002056: Kansas Geological Survey, https://doi.org/10.2172/1262271.

Diagenesis of the Arbuckle Group on the Southern Midcontinent (Missouri and Oklahoma)

Phillip A. Bailey III[1], Britney J. Temple[2], and Jay M. Gregg[3]
[1] RZG LLC, Zebulon, North Carolina, USA
[2] Consultant, Oklahoma City, Oklahoma, USA
[3] Oklahoma State University, Stillwater, Oklahoma, USA

Introduction

The Arbuckle Group carbonates are an important petroleum reservoir and are used to store wastewater emplaced through injection wells in Oklahoma. Additionally, the Arbuckle may have been a major conduit for metalliferous fluids affecting the Ozark region and contributing to the Tri-State Mississippi Valley-type (MVT) mineral district of Oklahoma, Kansas, and Missouri as well as the MVT deposits of the Ozark region of Missouri and Arkansas (Gregg and Shelton, 2012).

The Arbuckle comprises part of the Sauk megasequence and was deposited under epeiric sea conditions on a shallow-water platform as a series of third- to fifth-order depositional cycles. These strata are further defined by regional and subregional unconformities (Palmer et al., 2012). Depositional environments ranged from supratidal to shallow subtidal and transitioned to an off-platform setting southward into the Arkoma basin and Oklahoma aulacogen (Perry, 1989). Strata included in the Arbuckle Group are temporally equivalent to the Ellenburger Group in Texas and the Knox Group of the Appalachian basin. Petrographic and geochemical evidence for late diagenetic alteration of Arbuckle-age carbonates exists throughout the Midcontinent (Gregg and Shelton, 2012).

Methods and Results

Seven subsurface cores penetrating the Arbuckle Group were described and sampled at the Oklahoma Geological Survey Petroleum Information Center (OPIC) in Norman, Oklahoma, and the Missouri Geological Survey McCracken Core Library in Rolla, Missouri (fig. 1). Petrographic analysis, including cathodoluminescence (CL), was conducted on 98 thin sections made from samples taken from the cores.

All of the cores examined in this study are completely dolomitized except for those lithologies that have been replaced by chert. Chert frequently replaces oolitic grainstones in these units, preserving the original limestone depositional texture. Less frequently, void space is lined by drusy quartz crystals, particularly in the lower part of the Arbuckle. Occasionally, sulfide minerals (pyrite, sphalerite, and galena) are observed either as open-space-filling crystals or replacing carbonate lithologies. Replacement dolomite in subtidal mudstones, intertidal grainstones, and peritidal laminates is typically unimodal, very fine to medium crystalline planar-s dolomite. Occasionally, replacement dolomite is characterized by medium to coarse crystalline planar to nonplanar dolomite crystals. Typically, the planar to nonplanar dolomite is observed with void-filling rhombic and saddle dolomite cements.

Porosity typically is filled by coarse crystalline rhombic and saddle dolomite cement followed, occasionally, by coarse crystalline, open-space-filling, blocky calcite. Less frequently, dolomite cement is interspersed with quartz cement. Dolomite cements in southwestern Missouri and northeastern Oklahoma (fig. 1) display a distinctive CL zonation pattern consisting of four major compositional zones as described by Voss et al. (1989). West of Tulsa, Oklahoma, (fig. 1) dolomite cements occupying open pore spaces display a complex zonation of up to six compositional zones alternating from dull to bright CL.

This study analyzed 214 fluid inclusions for T_h, T_m, or both. Out of those, 127 fluid inclusions, for which both the T_h and T_m values were obtained, were grouped

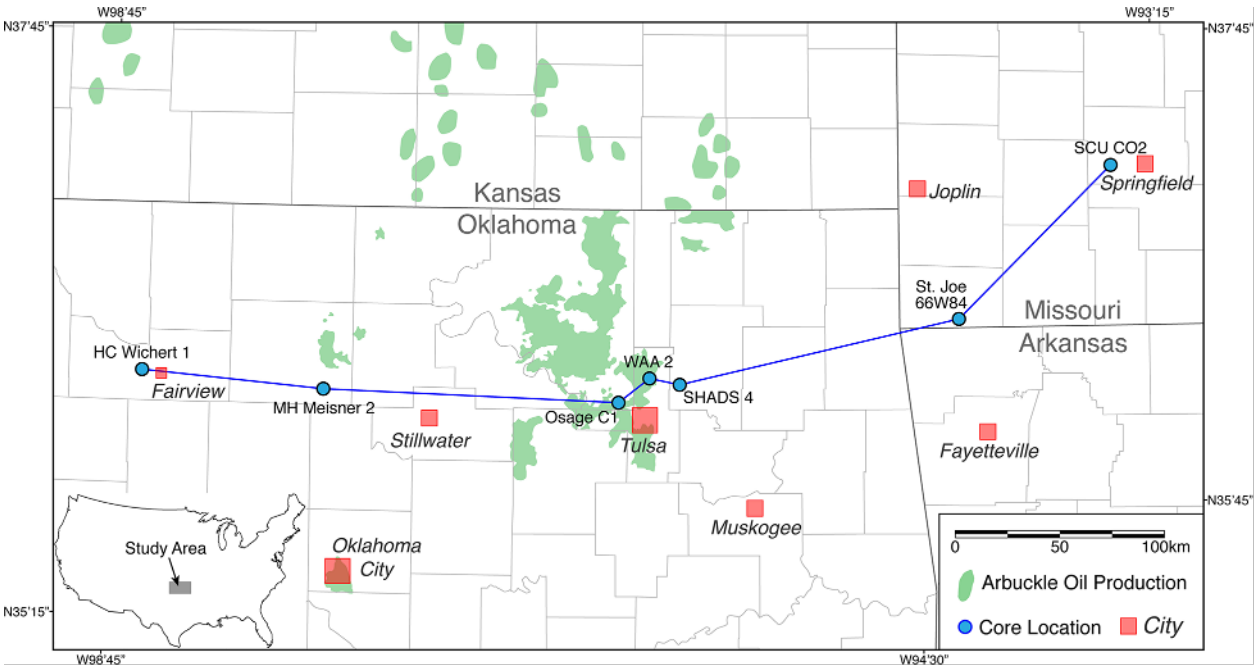

Figure 1. Map of the study area showing core locations and Arbuckle oil production.

as assemblages and plotted (fig. 2a). Fluid inclusion values in void-filling rhombic and saddle dolomite cements range from 90° to 155°C with calculated salinities ranging from 10 to 27 wt.% NaCl equivalent. Tables with individual fluid inclusion measurements and average measurements for assemblages are available in Temple (2016) and Bailey (2018).

Very fine to medium crystalline planar dolomites replacing microbial laminate, burrowed mudstone, and grainstone lithologies display carbon and oxygen isotope values ranging from $\delta^{13}C$ = -4.7 to -0.5‰ and $\delta^{18}O$ = -6.4 to -3.0‰, respectively (fig. 2b). Medium to coarse crystalline planar to nonplanar dolomite replacing these lithologies display carbon and oxygen isotope values ranging from $\delta^{13}C$ = -3.8 to -1.1‰ and $\delta^{18}O$ = -8.0 to -5.3‰, respectively. Dolomite cements display $\delta^{13}C$ values ranging from -3.5 to -0.6‰ and $\delta^{18}O$ values ranging from -10.5 to 4.2‰ (fig. 2b). Tables with C and O isotope values are available in Temple (2016) and Bailey (2018).

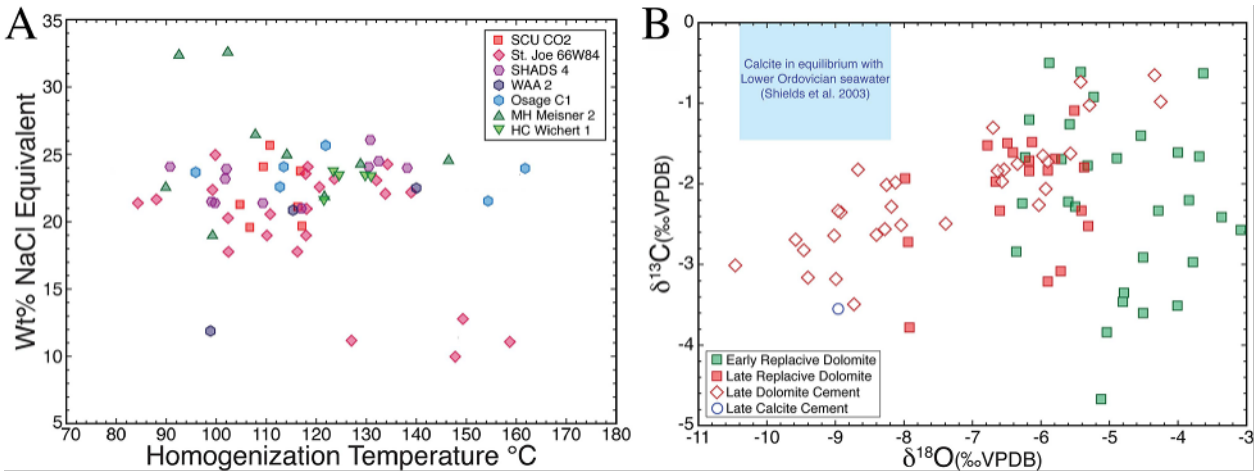

Figure 2. (a) Fluid inclusion assemblages. Homogenization temperatures (T_h) plotted against calculated wt.% NaCl equivalent. (b) Values of $\delta^{18}O$ plotted against $\delta^{13}C$. Values for calcite in equilibration with Ordovician seawater (Shields et al., 2003) are shown.

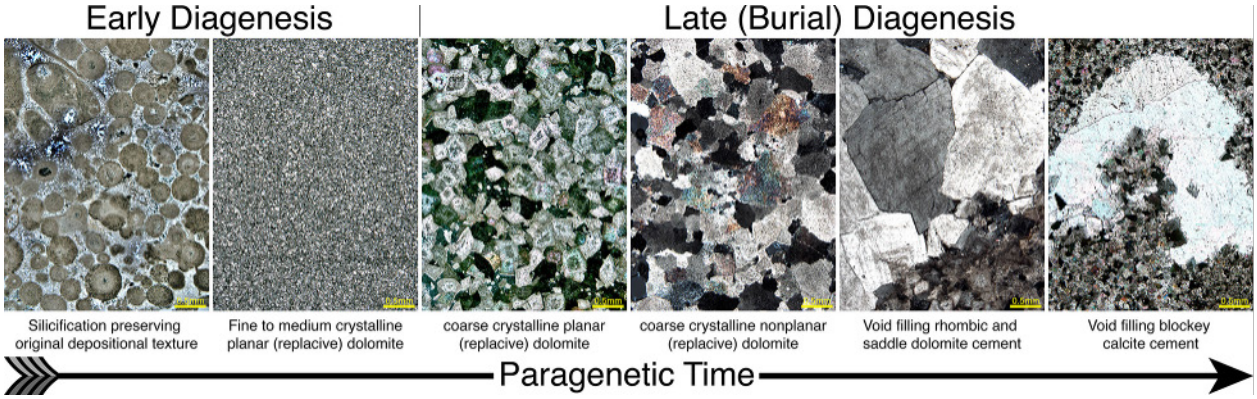

Figure 3. Paragenesis of diagenetic events in the Arbuckle Group, southern Midcontinent.

Discussion and Conclusions

Early diagenesis of the original Arbuckle limestone sediments involved both silicification and dolomitization (fig. 3). Silicification preserved some of the original depositional fabric of the limestones. The timing of silica replacement likely was prior to dolomitization, as the fine texture of allochems are preserved. Dolomitization largely destroyed detailed depositional textures in the original Arbuckle limestones. Very fine to medium planar dolomite textures replacing Arbuckle limestones are interpreted as early diagenetic (Sibley and Gregg, 1987). This is consistent with carbon and oxygen isotope values that suggest equilibration with early Ordovician seawater.

Dolomites exhibiting medium to coarse crystalline planar to nonplanar textures in the Arbuckle section are interpreted as later diagenetic in origin. These late diagenetic textures frequently are associated with solution-enlarged porosity that is filled by rhombic and saddle dolomite cement and occasionally followed by coarse blocky calcite cement (fig. 3). This interpretation is consistent with nonplanar textures (Sibley and Gregg, 1987), fluid inclusion homogenization temperatures (fig. 2a), and depleted oxygen isotope values (fig. 2b).

The findings of this study are consistent with previous research suggesting basin fluid flow events on the Midcontinent of North America corresponding with Ouachita tectonism during the Late Pennsylvanian subperiod and Permian Period. Basinal brines are thought to have migrated northward from the Arkoma and/or the Anadarko basins by means of a gravity (topographical) driven fluid flow system (Appold and Garven, 1999).

References

Appold, M. S., and Garven, G., 1999, The hydrology of ore formation in the Southeast Missouri District: Numerical models of topography-driven fluid flow during the Ouachita Orogeny: Economic Geology, v. 94, p. 913–936.

Bailey, P. A., 2018, Diagenesis of the Arbuckle Group in northeastern and north-central Oklahoma, U.S.A. [M.S.]: Oklahoma State University, 75 p.

Gregg, J. M., and Shelton, K. L., 2012, Mississippi Valley-type mineralization and ore deposits in the Cambro-Ordovician Great American Carbonate Bank; *in* J. R. Derby, R. D. Fritz, S. A. Longacre, W. A. Morgan, and C. A. Sternach, eds., The Great American Carbonate Bank: The Geology and Economic Resources of the Cambro-Ordovician Sauk Megasequence of Laurentia: AAPG Memoir 98, p. 163–186.

Palmer, J., Thompson, T. L., Seeger, C., Miller, J. F., and Gregg, J. M., 2012, The Sauk Sequence from the Reelfoot Rift to Southwestern Missouri; *in* J. R. Derby, R. D. Fritz, S. A. Longacre, W. A. Morgan, and C. A. Sternach, eds., The Great American Carbonate Bank: The Geology and Economic Resources of the Cambro-Ordovician Sauk Megasequence of Laurentia: AAPG Memoir 98, p. 1,013–1,030.

Perry, W., 1989, Tectonic evolution of the Anadarko Basin region, Oklahoma: United States Geological Survey Bulletin, v. 1866-A, 28, p. A1–A16.

Shields, G. A., Carden, G. A., Veizer, J., Meidla, T., Rong, J. Y., and Li, R. Y., 2003, Sr, C, and O isotope geochemistry of Ordovician brachiopods: A major

isotopic event around the Middle-Late Ordovician transition: Geochimica et Cosmochimica Acta, v. 67, p. 2,005–2,025.

Sibley, D. F., and Gregg, J. M., 1987, Classification of dolomite rock textures: Journal of Sedimentary Petrology, v. 57, p. 967–975.

Temple, B. J., 2016, Petrology and geochemistry of the Lower Ordovician and Upper Cambrian (Arbuckle) carbonates, NE Oklahoma and SW Missouri [M.S.]: Oklahoma State University, 78 p.

Voss, R. L., Hagni, R. D., and Gregg, J. M., 1989, Sequential deposition of zoned dolomite and its relationship to sulfide mineral paragenetic sequence in the Viburnum Trend, southeast Missouri: Carbonates and Evaporites, v. 4, p. 195–209.

A Preliminary Characterization of Pore Heterogeneity and Permeability in Karst Carbonate Reservoirs

Ibukun Bode-Omoleye
Kansas Geological Survey, University of Kansas, Lawrence, Kansas, USA

Introduction

The Cambrian-Ordovician Arbuckle Group strata in Kansas are interpreted as broad shallow-shelf subtidal to peritidal deposits that were exposed during the post-Arbuckle Sauk-Tippecanoe unconformity (Cole, 1975). Production and wastewater disposal have historically taken place within the upper Arbuckle fractured-karstic carbonate units, with reservoir distribution controlled by basement structural patterns and subaerial exposure. Despite the importance of the Arbuckle as a mature hydrocarbon reservoir and as a highly utilized saline aquifer for the disposal of both industrial waste and oilfield brines, very few studies have taken a regional approach to studying its rock properties as they relate to the stratal packages within the unit. The goal of this study is to review and document current knowledge of petrophysical and rock property complexities that affect fluid flow and create internal heterogeneity within the Arbuckle. Due to recent carbon capture, utilization, and storage (CCUS) activities within the study area, modern well log suites (e.g., nuclear magnetic resonance [NMR] and formation micro image [FMI] logs) have been acquired and used to identify pore structure and rock type variability (Doveton and Watney, 2015). These log suites are calibrated with core description and measurements to identify controls on permeability in the Arbuckle. The objectives are to characterize the varied distribution of reservoir facies that have implications for (1) predicting compartmentalization for hydrocarbon production, (2) identifying targeted intervals for possible captured carbon storage, and (3) dispersal patterns of injected fluids and their relations to seismic events.

Methods and Results

Data collected from cores and well logs from Arbuckle intervals in southern Kansas (fig. 1) show the rocks comprising mostly dolomitized rocks that are overprinted with karst and fractures at certain intervals. Dominant facies include peloidal grainstones, mudstones, oolitic packstones, stromatolitic boundstones, and breccia (fig. 2a). Franseen and Byrnes (2012) showed in their regional study of the Arbuckle Group that despite the presence of karst and other later diagenetic events in the upper Arbuckle, matrix porosity dominates several intervals. Similarly, King and Goldstein (2018) identified early- and late-stage diagenetic events that reduce and generate porosity in a series of dissolution and cementation events, with substantial primary and secondary porosity persisting throughout the unit. Hence, stratigraphic architecture is still expected to provide a first-order constraint on the spatial continuity of reservoir facies, porosity, permeability, saturations, and other petrophysical attributes within certain intervals.

Pore networks within the lithofacies consist of any of the following pore types: (1) matrix (intercrystalline, moldic, fenestral, and vuggy), (2) karst porosity, and (3) fracture porosity. Pore types generally depend on vertical stratigraphic position and then subsequent diagenetic overprint and structural setting. Whole core measurements from the Wellington #1-32 and Cutter KGS #1 wells indicate absolute permeability values ranging from 0.1 md to 200 md in matrix-dominated fabrics with no vuggy component. Porosity and permeability are variable in the karst- and breccia-related textures and are generally higher in brecciated rocks with additional vuggy porosity (2.74 mD to 317 mD). Fractures cut across all facies, and only significantly enhance permeability when the fractures are open and numerous. Available well data included gamma ray (GR), neutron porosity (NPHI), photoelectric factor (PEF), and bulk density (RHOB) for mineralogy and lithology evaluation. Compressional

and shear slowness (DTC, DTXX, DTYY), resistivity arrays, NMR T2 distribution, and core porosity provide both direct and indirect estimations of porosity and pore structure. NMR T2 distribution partitioning was used to process binary facies and define a cutoff for megaporosity by the summation of times from 1,024 to 2,048 ms relaxation time bins (Doveton and Watney, 2015; Deng et al., 2019) (fig. 3). The presence of vugs is confirmed in image logs, and drill-stem test measurements from cores provide preliminary information about larger-scale permeability distribution in the Arbuckle.

Discussion and Conclusions

The review of petrophysical characterization in the published literature from several Arbuckle wells and newly assessed data from CCUS wells show a

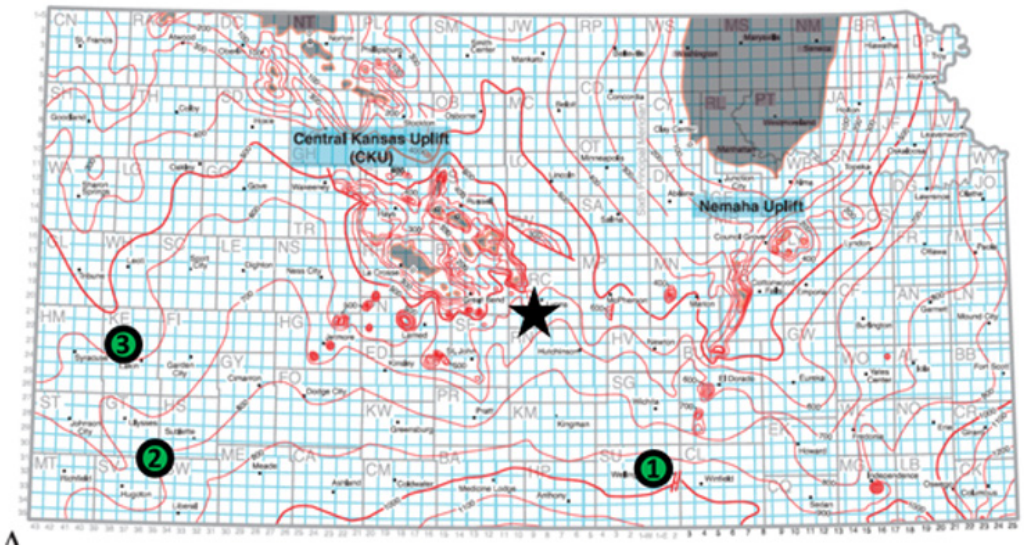

Figure 1. Isopach map of Arbuckle Group strata (base Simpson to Precambrian) for the state of Kansas from well data. Contour interval 100 ft (30 m). The Arbuckle is absent in areas that are shaded in gray (modified from Cole, 1975). Core data from a Lyons County well (black star) used in Franseen and Byrnes (2012) forms the basis for lithostratigraphic classification. Other wells with advanced well log suites (green circles outlined in black) are used for this preliminary study. Core data are integrated from (1) KGS Cutter #1 (API:15-189-22781), (2) Wellington #1-32 (API:15-191-22591), and (3) Patterson KGS 5-25: (API:15-093-21979).

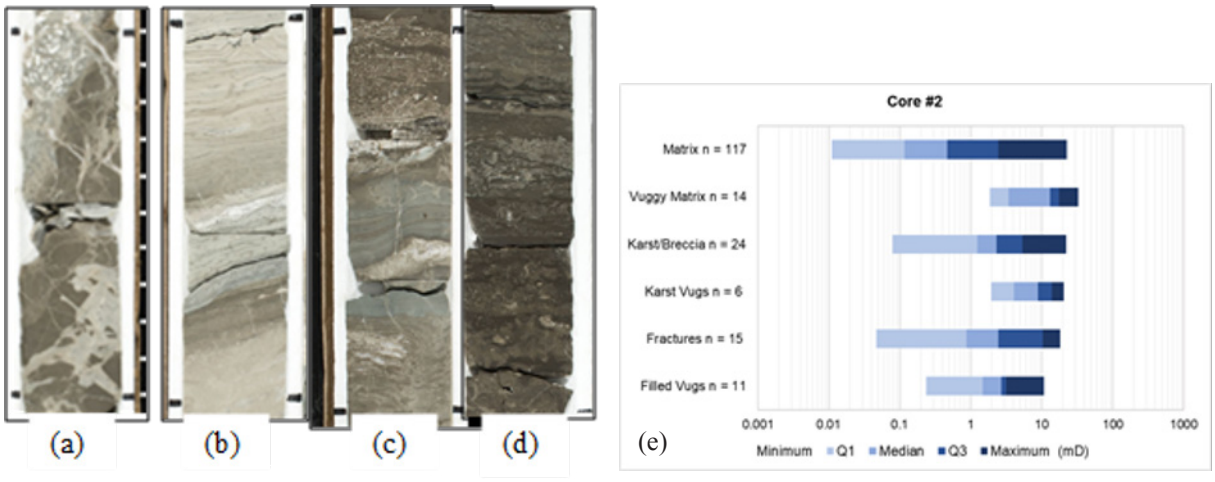

Figure 2. Dominant facies in the Arbuckle Group in Kansas (Wellington #1-32 well): (a) breccia, (b) laminated stromatolitic boundstone, (c) mixed packstone-grainstone, and (d) peloidal packstone-grainstone, respectively. (e) Range of permeability in the Cutter KGS #1 well based on identified dominant pore types from core with n *indicating the number of measurements taken for each category.*

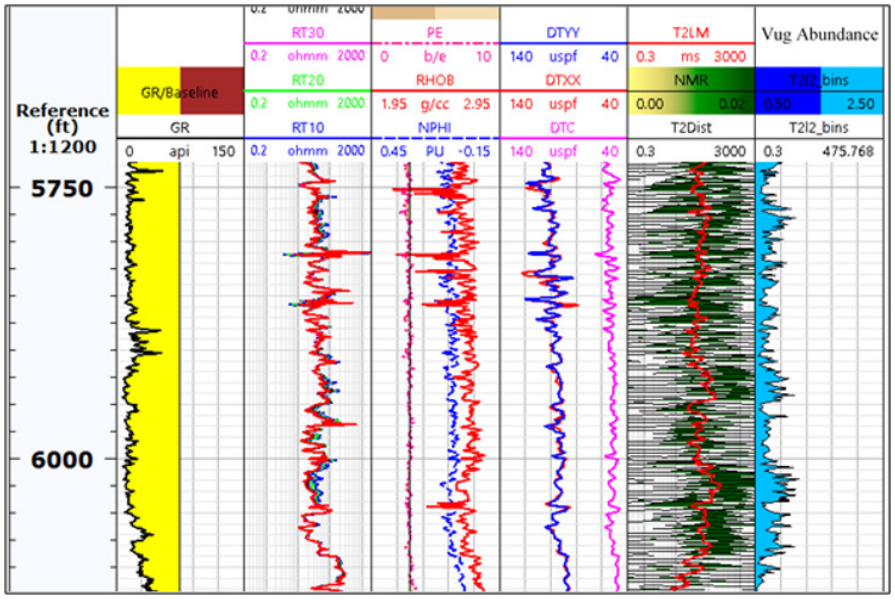

Figure 3. Well-log data set and vuggy facies labels for the Arbuckle from Patterson KGS #5-25 well (API: 15-093-21979). The log tracks from left to right correspond to GRTC (with shale baseline); resistivity (RT10, RT20, RT30, RT60, and RT90); PE and NPHI/RHOB; DTC, DTXX, and DTYY; NMR T2 distribution in waveform with T2 log mean; and binarized facies showing distribution of vuggy porosity.

complex distribution of reservoir and non-reservoir facies with varying thicknesses across the study area. The upper Arbuckle shows karst facies in several of the wells; however, matrix porosity still dominates several intervals. A combination of mineralogy-sensitive well logs was able to differentiate lithology, whereas lithology-independent logs were used to identify different pore structure to include vuggy porosity, matrix porosity, and unconnected porosity. Integrating NMR T2 distribution waveforms and conventional logs for vuggy facies classification in carbonate rocks has been successful for rock typing and vuggy prediction (Doveton and Watney, 2015; Deng et al., 2019). The alternating packaging of porous and non-porous lithologies at different scales and the different porosity types result in variable vertical and lateral heterogeneity that could control fluid flow patterns. Continued work will examine the implications this has for reservoir architecture, lateral continuity of facies, and possible communication of fluids between fractured units. Detailed studies of the Cambrian-Ordovician Ellenburger Formation show a variety of karst and matrix facies, with diagenetic overprint that is complex and produces strong spatial heterogeneity within the reservoir systems (Loucks, 2008). Similar studies exist within the Arbuckle (Goldstein and King, 2018), and future characterization of rock properties would benefit from integrating the distribution of dolomitization and karst processes to understand the effects of genesis on relative timing and the effects on reservoir character.

References

Cole, V. B., 1975, Subsurface Ordovician–Cambrian rocks in Kansas: Kansas Geological Survey, Subsurface Geology Series 2, 18 p.

Deng, T., Xu, C., and Jobe, D., 2019, A comparative study of three supervised machine-learning algorithms for classifying carbonate vuggy facies in the Kansas Arbuckle Formation: Petrophysics, v. 60, no. 6, p. 838–853. SPWLA-2019-v60n6a8.

Doveton, J., and Watney, L., 2015, Textural and pore size analysis of carbonates from integrated core and nuclear magnetic resonance logging: An Arbuckle study: Interpretation, v. 3, no. 1, SA77–SA89. https://doi.org/10.1190/INT-2014-0050.1.

Franseen, E. K., and Byrnes, A. P., 2012, Arbuckle Group platform strata in Kansas: A synthesis; *in* J. R. Derby, R. D. Fritz, S. A. Longacre, W. A. Morgan, and C. A. Sternbach, eds., The great American carbonate bank: The geology and economic resources of the Cambrian–Ordovician Sauk megasequence of Laurentia: AAPG Memoir 98, p. 1,031–1,047.

King, B. D. and Goldstein, R. H., 2018, History of hydrothermal fluid flow in the Midcontinent, USA: The relationship between inverted thermal structure, unconformities and porosity distribution. Geological Society, London, Special Publications, v. 435, no. 1, p. 283–320.

Loucks, R. G., 2008, Review of the lower Ordovician Ellenburger group of the Permian basin, west Texas, https://bit.ly/3himKJV.

Geometry of the Burlington Shelf During the Early Mississippian: Thickening Both Shoreward and Basinward Away From the Starved (Shaved?) Central Middle Shelf

Matthew G. Braun[1], Bradley D. Cramer[1], Brittany M. Stolfus[1], Madysen Gilbert[1,2], Megan N. Heath[1], Gwen L. Barnes[1], Ryan J. Clark[3], James E. Day[4], Brian J. Witzke[1], Nicholas J. Hogancamp[5,6], Stephanie Tassier-Surine[3]

[1] Department of Earth and Environmental Sciences, University of Iowa, Iowa City, Iowa, USA
[2] Current address: Nicholas School of the Environment, Duke University, Durham, North Carolina, USA
[3] Iowa Geological Survey, University of Iowa, Iowa City, Iowa, USA
[4] Department of Geography, Geology, and the Environment, Illinois State University, Normal, Ilinois, USA
[5] Hess Corporation, Houston, Texas, USA
[6] Department of Earth and Atmospheric Sciences, University of Houston, Houston, Texas, USA

Introduction

The latest Devonian to Early Mississippian (Famennian to Osagean) was marked by significant changes in the ocean-atmosphere-biosphere system that included two major biogeochemical events. Following the end-Devonian mass extinction, this interval recorded two of the largest positive $\delta^{13}C$ excursions of the Phanerozoic: the Hangenberg excursion (which occurs at the Devonian-Carboniferous boundary) and the Kinderhook-Osage Boundary Excursion (KOBE), which spans the K-O boundary (fig. 1). Some of the best-exposed strata of this age are located in the U.S. Midcontinent, notably the Iowa, Illinois, and Missouri tri-state region, which includes the type area for the Kinderhookian Stage.

The predominantly siliciclastic deposits of the Famennian gave way to a broad carbonate platform, known as the Burlington shelf, which dominated Midcontinent stratigraphy during the Mississippian (Witzke and Bunker, 2001, 2002). Depositional strike on the shelf was northeast–southwest, with inner shelf facies in central Iowa transitioning to proximal and central middle shelf facies in southeast Iowa and northern Missouri, distal middle shelf facies in western Illinois and central Missouri, and eventually transitioning to outer shelf and shelf break facies farther to the south and southeast (fig. 2). Rather than a single clinoform geometry of simple thinning into the basin across the shelf edge, strata across the Burlington shelf demonstrate a dumbbell shape with strata thinning most significantly from the proximal middle shelf to the central middle shelf before thickening again into the distal middle shelf (fig. 3). This geometry is evident through successive sea-level cycles spanning the latest Famennian through at least the middle Osagean and is a prominent feature of Mississippian stratigraphy of the upper Midwest. Further complicating stratigraphic correlations is the presence of the sub-Burlington unconformity, a southeastward expanding hiatal surface present at the K-O boundary in the tri-state and Mississippi River valley areas (Lane and Brenckle, 2001; Witzke and Bunker, 2002). Often, the unconformity is marked by hardgrounds, and no obvious erosional surfaces have been identified; the magnitude of the unconformity is greatest along the central middle shelf region, where a significant portion of upper Kinderhook and lower Osage strata are missing (Witzke and Bunker, 2002).

Methods and Results

Outcrops and cores were selected at key facies/depth transitions across the Burlington shelf (figs. 2–3) and examined using an integrated high-resolution stratigraphic approach. When possible, all

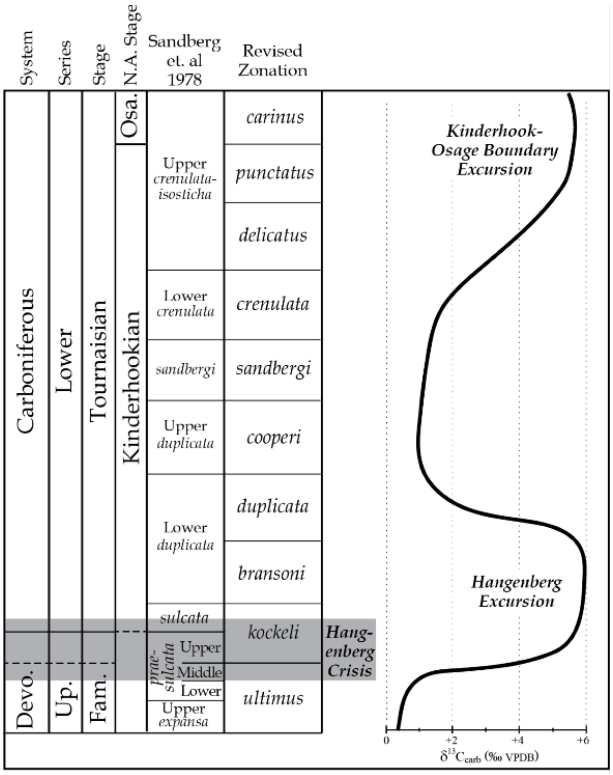

Figure 1. General conodont zonation and carbon isotope curve for the Devonian-Carboniferous boundary and Lower Mississippian interval (modified from Cramer et al., 2019).

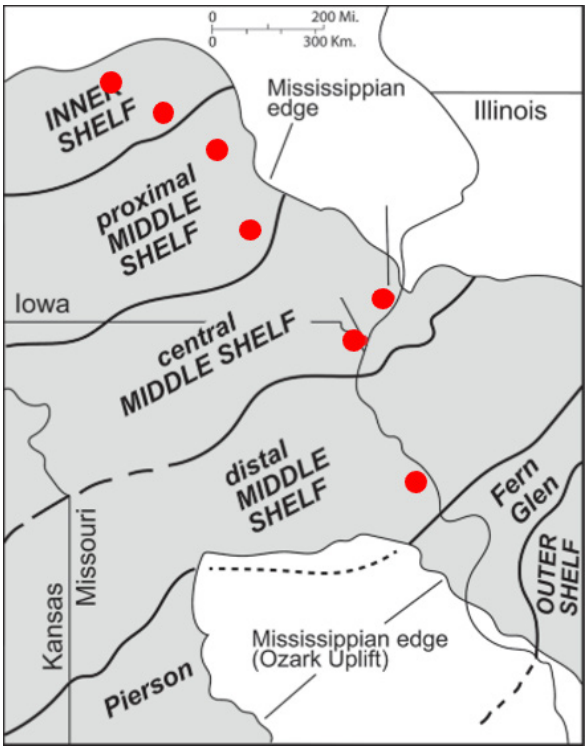

Figure 2. General facies trends in the tri-state area. Transect line corresponds to the cross section of fig. 3. Red dots indicate approximate location of key outcrops and cores examined (modified from Witzke and Bunker, 2002).

sampling was completed concurrently to produce a cohesive lithostratigraphic, sequence stratigraphic, biostratigraphic, and chemostratigraphic framework. Samples for conodont biostratigraphy were collected at a 1–2 m resolution, with higher-resolution sampling (0.5 m or less) conducted at major inflections in the $\delta^{13}C$ record or at expected sequence boundaries. A bulk rock sampling procedure was used to produce a continuous $\delta^{13}C$ chemostratigraphic record through the studied succession that is independent of the brachiopod distribution. Samples were generally collected at 30 cm intervals; however, at the stratigraphic intervals expected to record $\delta^{13}C$ excursions, the resolution was increased to 10 cm.

The inner shelf facies of central Iowa preserve an expanded record of the KOBE with peak $\delta^{13}C$ values of +6‰; however, the Hangenberg excursion is not recorded. Conversely, in the distal middle shelf facies of the tri-state area, the KOBE is absent, while an expanded record of the Hangenberg excursion (peak $\delta^{13}C$ values of +5‰) is recorded.

Discussion and Conclusions

Preliminary results indicate the magnitude of the sub-Burlington unconformity is larger than previously thought in the tri-state region, as a significant portion of upper Kinderhook to lower Osage strata and the entire KOBE are missing. The development of this unconformity is enigmatic as no obvious erosional surfaces, subaerial exposure patterns, or evidence for tectonic influences have been recognized. As this hiatal surface is typically marked by hardgrounds, the unconformity is likely related to changes in sedimentation dynamics and sediment starvation in the middle shelf region. Sediment derived from the inner shelf would have accumulated in the proximal middle shelf region or instead bypassed the central middle shelf to be deposited in the distal middle shelf. Additionally, if sedimentation rates in the central middle shelf were slow enough, frequent storms may have eroded any autochthonous sediment and transported it into deeper regions of the basin. This development of a starved/shaved central middle shelf

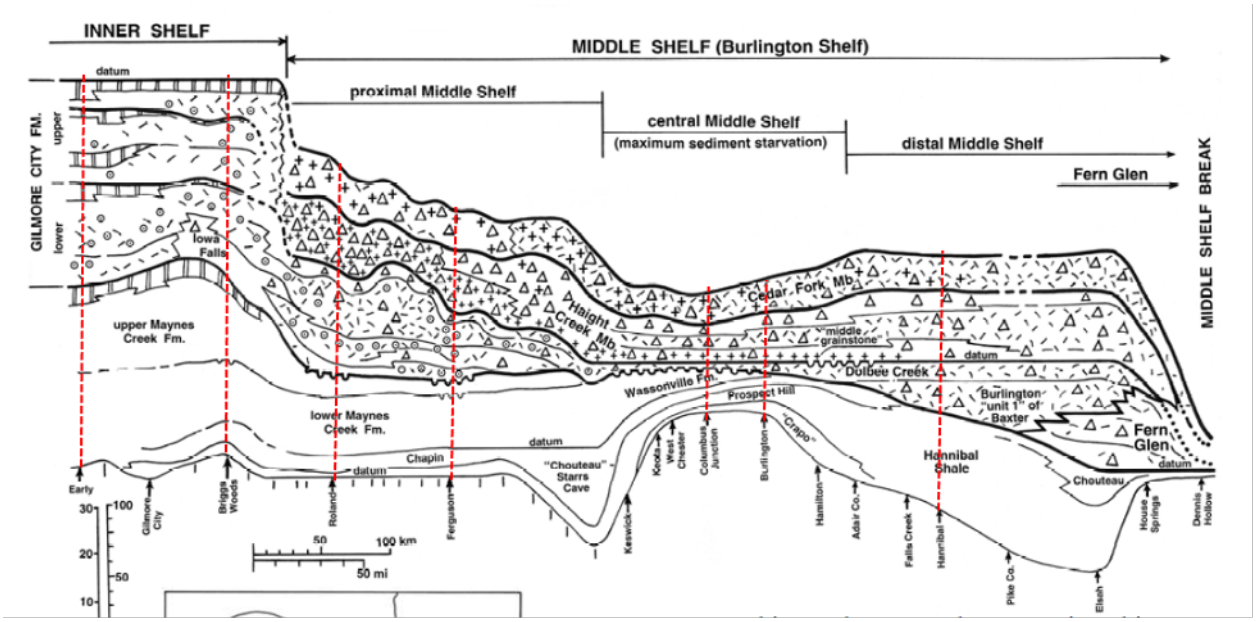

Figure 3. Northwest-to-southeast transect of Lower Mississippian strata in the tri-state area. Note the thinning of strata within the central middle shelf region forming a dumbbell-like pattern; red lines indicate approximate location of key outcrops and cores examined (modified from Witzke and Bunker, 2002).

region may explain the enigmatic dumbbell-like geometry of the Burlington shelf.

References

Cramer, B. D., Clark, R. J., and Day, J. E., 2019, The Devonian-Carboniferous boundary in the type area of the Mississippian: Iowa Geological Survey Guidebook Series 30, 80 p.

Lane, H. R., and Brenckle, P. L, 2001, Type Mississippian subdivisions and biostratigraphic succession; *in* P. H. Heckel, ed., Stratigraphy and Biostratigraphy of the Mississippian Subsystem (Carboniferous System) in its Type Region, the Mississippi River Valley of Illinois, Missouri, and Iowa: Illinois State Geological Survey, Guidebook 34, p. 83–107.

Witzke, B. J., and Bunker, B. J., 2001, Comments on the Mississippian stratigraphic succession in Iowa; *in* P. H. Heckel, ed., Stratigraphy and Biostratigraphy of the Mississippian Subsystem (Carboniferous System) in its Type Region, the Mississippi River Valley of Illinois, Missouri, and Iowa: Illinois State Geological Survey, Guidebook 34, p. 63–75.

Witzke, B. J., and Bunker, B. J., 2002, Bedrock geology in the Burlington area, southeast Iowa; *in* B. J. Witzke, S. A. Tassier-Surine, R. R. Anderson, B. J. Bunker, and J. A. Artz, eds., Pleistocene, Mississippian, & Devonian Stratigraphy of the Burlington, Iowa, Area: Iowa Department of Natural Resources, Geological Survey, Guidebook Series 23, p. 23–51.

Paleozoic Brine Reflux: Its Impact on Diagenesis and Basin-Brine Composition in Major Onshore Oil-and-Gas Basins of the United States

Robert H. Goldstein[1], David A. Fowle[1], and Randy L. Stotler[2]
[1]KICC, Department of Geology, University of Kansas, Lawrence, Kansas, USA
[2]Department of Earth and Environmental Sciences, University of Waterloo, Waterloo, Ontario, Canada

Introduction

The U.S. Midcontinent, Delaware, Midland, and Williston basins are productive sedimentary basins, each with Paleozoic histories of evaporite deposition. Typically, the evaporites are considered the seal for hydrocarbons, but herein we make the case that the deposition of evaporites provided a source for brines and that those brines sank deeply into underlying rocks to charge each basin with residual evaporite brines. Those brines were diagenetically reactive during their initial sinking and had an impact on porosity distribution. After heating and varying degrees of alteration of the original brine chemistry through rock-water interaction and mixing at depth, the brines migrated again, this time upward. There is an extensive late diagenetic record of the hot brines having been injected into less deeply buried rocks, impacting porosity in the most important hydrocarbon reservoirs, affecting thermal maturity in shallowly buried rocks, and localizing Mississippi Valley-type (MVT) lead-zinc deposits.

Brines in North American Cratonal Evaporite Basins

In the Midcontinent, mid-Permian marine evaporites, such as the Hutchinson salt, are well known and widespread. New studies of the brine chemistry currently residing in the subsurface (Stotler et al., 2021) and earlier studies (Musgrove and Banner, 1993) indicate a family of fluids in Pennsylvanian, Mississippian, and Ordovician strata that is highly saline and has chemistries indicating an origin as a residual evaporite brine during deposition of the Permian evaporites. Those brines are widespread and have penetrated downward into the Pennsylvanian section and the Western Interior Plains Aquifer System (WIPAS), which encompasses the entire sub-Pennsylvanian section in the region. The original compositions of the residual evaporite brines have been modified by rock-water interaction and mixing processes.

Upper Permian evaporites are widespread in the Delaware and Midland basins of west Texas and New Mexico. Brine compositions in these basins show a family of brines with high salinities, positive $\delta^{18}O_{VSMOW}$ (+2‰ to +9‰), Br/Cl consistent with evaporative concentration, and $^{87}Sr/^{86}Sr$ all pointing to evaporation of Permian seawater that was followed by deep penetration of brines into the basin (McNeal, 1965; Engle et al., 2016; Saller and Stueber, 2018). The brine chemistries are complicated by rock-water interaction and later mixing with meteoric water. Deep penetration into the basin is indicated by brines being present in the Cambrian-Ordovician Ellenburger Group.

In the Williston basin of North Dakota, Montana, and Saskatchewan, there are extensive Devonian (Prairie) and Mississippian (Charles) evaporites. Highly saline brines in the basin have Cl/Br:Na/Br relationships that are consistent with the evaporation of seawater rather than salt dissolution (Iampan and Rostron, 2000). Distribution of the brines suggests both Devonian and Mississippian events of brine generation and sinking to charge the basin.

What is the Diagenetic Impact of Sinking Brines?

Midcontinent Paleozoic carbonate reservoirs commonly show a record of diagenetic phases that precipitated from Permian sinking brines. Close to the source, in stratigraphic sequences that are not far below Permian evaporites, abundant dolomitization

from low-temperature brines of Permian age is well known. The best-studied example of this is in the Hugoton embayment, where the Krider and Winfield dolomites contain low-temperature, highly saline fluid inclusions and give Permian U-Pb ages (Luczaj and Goldstein, 2000). Down section, in Pennsylvanian carbonate reservoirs, much of the early porosity is reduced by calcite cement with the same salinity and low-temperature fluid inclusion results as that which precipitated the dolomite up section. Based on the isotopic composition of the calcite and using the fluid inclusion temperatures, the $\delta^{18}O_{VSMOW}$ of the fluid that precipitated that calcite was +0.5 to +4.9‰. These compositions are distinctly more positive than normal Permian seawater and require evaporative fractionation. The observations indicate that large-scale sinking of Permian residual evaporite brines led to dolomitization up section, and as the fluids evolved in composition during sinking, calcite precipitation down section.

The best-known example of the impact of sinking of residual evaporite brines is in the Delaware and Midland basins. This is the site of the famous seepage-reflux model (Adams and Rhodes, 1960; Saller, 2018), where sinking of brines that were generated in Permian evaporative lagoons led to dolomitization of shelf carbonates. Our recent work on the Wolfcamp in the center of the Delaware basin (Dobber and Goldstein, 2020) shows a first phase of fracture-filling calcite cement with fluid inclusion salinities approximately 12 wt.% NaCl eq., calculated $\delta^{18}O_{VSMOW}$ for water of precipitation of about +4.0 to +5.5‰, and $^{87}Sr/^{86}Sr$ slightly more radiogenic than Ochoan seawater. The Wolfcamp from the eastern margin of the Midland basin shows that both calcite and anhydrite cement precipitated from sinking Permian brines (DeZoeten and Goldstein, 2017). Fluid inclusion salinities are high, 17.4–18.5 wt.% NaCl eq., $^{87}Sr/^{86}Sr$ is similar to Ochoan seawater, and the calculated $\delta^{18}O_{VSMOW}$ of the water is +6.4 to +9.6‰, which is clear evidence of seawater evaporation.

The observations support a chemical evolution of residual evaporite brines as they sink, interact with the rocks, and experience microbial metabolic reactions. This can be modeled in the reactive transport program X1t (fig. 1). Refluxing residual evaporite brines dolomitize on the way down, removing Mg++ from the brine and releasing Ca++ to the brine. In the presence of high sulfate in the fluid, this leads to precipitation of anhydrite. Where organic matter substrate and nutrients allow, microbial reactions can reduce sulfate and affect alkalinity to drive precipitation of calcite cement.

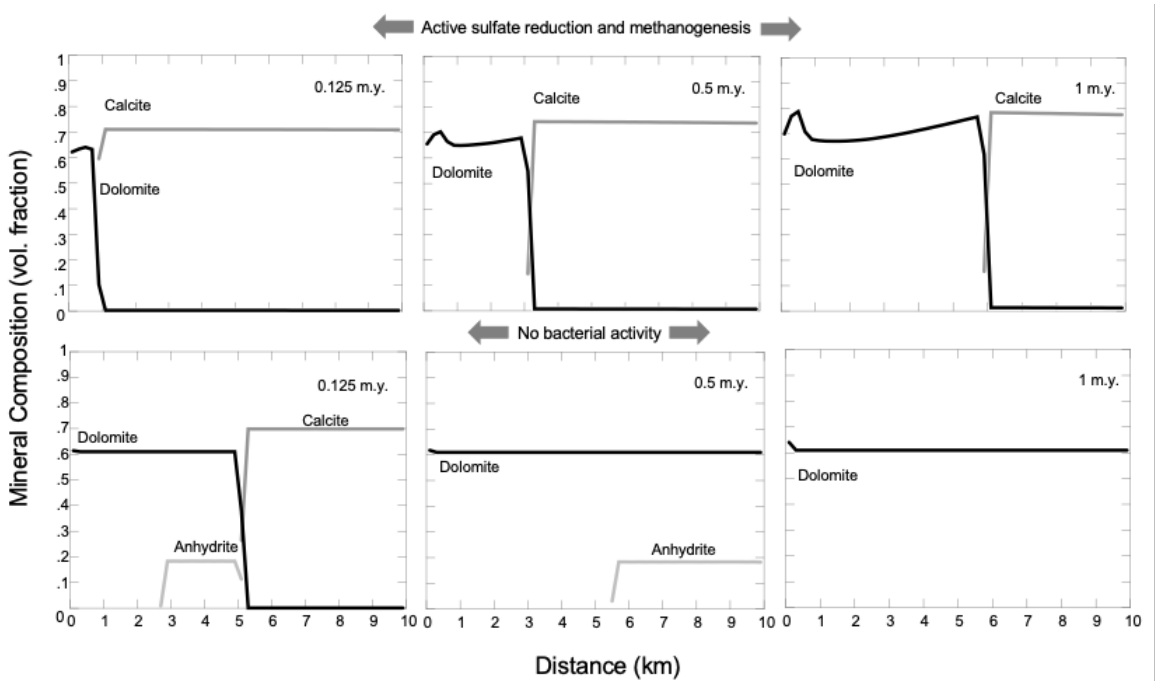

Figure 1. Reactive transport modeling of refluxing brine with and without microbial kinetics.

And Then Brines Rise

Once brines have penetrated deeply into a basin, one might expect that they would stay in place because of their high density — but they rise to impact reservoir rocks once again. In the basins studied here, many areas have experienced injection of warm basin brines into the cooler, more shallowly buried carbonate reservoir rocks. These hydrothermal fluids dissolve carbonate and silica phases and precipitate baroque dolomite, calcite, megaquartz, and lead and zinc sulfides. Fluid inclusion data show high temperatures, consistent with a deep source, but the salinities are largely the same as those that were present when the brines were at low temperature and sinking from the surface. $^{87}Sr/^{86}Sr$ values show slightly radiogenic values, evidence of rock-water interaction at depth. Composition of fluid inclusions still preserve the Cl/Br and positive $\delta^{18}O_{VSMOW}$ of a residual evaporite brine, although with some modification from fluid mixing and rock-water interaction (e.g., Shelton et al., 2009). Locally, the warm brines cause thermal maturation of shallowly buried source rocks, and they may also be responsible for migration of petroleum from the deeply buried parts of basins to shallow reservoirs.

The main drivers for forcing deep fluids into shallow rocks appear to be tectonic. In the Midcontinent, Pennsylvanian-Permian uplift of the Ouachitas provided the topography to generate hydrologic head to drive fluids into the foreland basin and out the other side (e.g., Goldstein et al., 2019). Ancestral Rockies deformation provided pathways for fluid flow. In the Williston basin, it was largely Laramide uplift that drove fluid flow (Goldstein and Mitchell, 2013). In the Delaware and Midland basins, Laramide deformation opened the system to allow fluid flow, but most fluid flow was likely driven by the Eocene-Oligocene volcanic phase and Miocene to present-day basin-and-range uplift (Hiemstra and Goldstein, 2014). Despite different tectonic drivers, each basin shows the impact of warm brines injected into cooler rocks.

References

Adams, J. E., and Rhodes, M. L., 1960, Dolomitization by seepage refluxion: American Association of Petroleum Geologists Bulletin, v. 44, p. 1,912–1,920.

DeZoeten, E., and Goldstein, R. H., 2017, Diagenetic history of the Wolfcamp A in the Eastern Midland basin, Texas: AAPG Datapages, Inc. Search and Discovery Article #51395.

Dobber, A. W., and Goldstein, R. H., 2020, Diagenetic controls on reservoir character of the Lower Permian Wolfcamp and Bone Spring Formations in the Delaware basin, West Texas: URTeC: 3181 Unconventional Resources Technology Conference (URTeC), doi:10.15530/urtec-2020-3181, 23 p.

Engle, M. A., Reyes, F. R., Varonka, M. S., Orema, W. H., Ma, L., Ianno, A. J., Schell, T. M., Xu, P., and Carroll, K. C., 2016, Geochemistry of formation waters from the Wolfcamp and "Cline" shales: Insights into brine origin, reservoir connectivity, and fluid flow in the Permian Basin, USA: Chemical Geology, v. 425, p. 76–92, doi:10.1016/j.chemgeo.2016.01.025.

Goldstein, R. H., and Mitchell, R. W., 2013, Diagenesis, fluid, and thermal history of carbonate mudrocks; An example from the Lower Lodgepole Formation, Williston basin: AAPG Search and Discovery Article #90163.

Goldstein, R. H., King, B. D., Watney, W. L., and Pugliano, T. M., 2019, Drivers and history of late fluid flow and impact on Midcontinent reservoir rocks; *in* M. Grammer, J. Gregg, J. Puckette, P. Jaiswal, M. Pranter, S. Mazzullo, and R. Goldstein, eds.,Mississippian reservoirs of the Mid-Continent, U.S.A: AAPG Memoir 122, doi:10.1306/13632157M116585.

Hiemstra, E. J., and Goldstein, R. H., 2014, Repeated injection of hydrothermal fluids into downdip carbonates: A diagenetic and stratigraphic mechanism for localization of reservoir porosity, Indian Basin field, New Mexico, USA; in S. Agar and S. Geiger, eds., Fundamental controls on fluid flow in carbonates: Geological Society, London Special Publication, v. 406, http://dx.doi.org/10.1144/SP406.1.

Iampen, H. T., and Rostron, B. J, 2000, Hydrogeochemistry of pre-Mississippian brines, Williston Basin, Canada–USA: Journal of Geochemical Exploration, v. 69–70, p. 29–35.

Luczaj, J. A., and Goldstein, R. H., 2000, Diagenesis of the Lower Permian Krider dolomite, southwest Kansas: Fluid-inclusion, U-Pb, and fission-track evidence for reflux dolomitization during latest Permian time: Journal of Sedimentary Research, v. 70, p. 762–773.

McNeal, R. P., 1965, Hydrodynamics of the Permian basin; in A. Young and J. E. Galley, eds., Fluids in subsurface environments: AAPG Memoir 4, p. 308–326.

Musgrove, M., and Banner, J. L., 1993, Regional ground-water mixing and the origin of saline fluids: Midcontinent, United States: Science, v. 259, p. 1,877–1,882.

Saller, A. H., 2018, Dolomitization and anhydrite precipitation by highly evaporated seawater in moderately deep subsurface, Permian basin: AAPG Datapages, Inc. Search and Discovery Article #11127.

Saller, A. H., and Stueber, A. M., 2018, Evolution of formation waters in the Permian basin, United States: Late Permian evaporated seawater to Neogene meteoric water: AAPG Bulletin, v. 102, no. 3, p. 401–428.

Shelton, K. L., Gregg, J. M., and Johnson, A. W., 2009, Replacement dolomites and ore sulfides as recorders of multiple fluids and fluid sources in the southeast Missouri Mississippi Valley-type district: Halogen-$^{87}Sr/^{86}Sr$-$\delta^{18}O$-$\delta^{34}S$ systematics in the Bonneterre Dolomite: Economic Geology, v. 104, p. 733–748.

Stotler, R. L., Kirk, M. F., Newell, K. D., Goldstein, R. H., Frape, S. K., and Gwynne, R., 2021, Stable bromine isotopic composition of coal bed methane (CBM) produced water, the occurrence of enriched 81Br, and implications for fluid flow in the Midcontinent, USA: Minerals 2021, v. 11, no. 4: 358. https://doi.org/10.3390/min11040358.

Tectonically Controlled Patterns of Contour-Current Deposition and Erosion in Outer Shelf, Lower Mississippian, Arkansas-Missouri-Oklahoma

C. Robertson Handford
Consulting Sedimentologist, Huntsville, Alabama, USA

Introduction

Over the past decade, several studies have challenged long-standing depositional and biostratigraphic interpretations of Lower Mississippian carbonates in northwest Arkansas-southwest Missouri-northeast Oklahoma (Thompson and Fellows, 1970; Lane, 1978; Manger and Thompson, 1982) and proposed the following:

- Mass transport processes played a role in the deposition of mud-dominated bodies previously interpreted as Waulsortian-like mounds (Chandler, 2001; Childress and Grammer, 2015; Evans and Basssett, 2013).
- Syndepositional tectonic activity influenced Kinderhookian-Osagean deposition (Mazzullo and Wilhite, 2015), and basinward thinning was not due to condensed sedimentation but to erosion and exposure over the crest of a foreland bulge uplift.

In this paper, I address the stratigraphic relationships, thickness patterns, facies characteristics, and structural framework to propose a new depositional model for the Lower Mississippian in north Arkansas, southwest Missouri, and northeast Oklahoma (fig. 1). The results support syndepositional tectonic activity as a major driver and suggest that deep outer-shelf contour currents account for depositional and erosional patterns, sedimentary structures, stratal features, and basinward thinning.

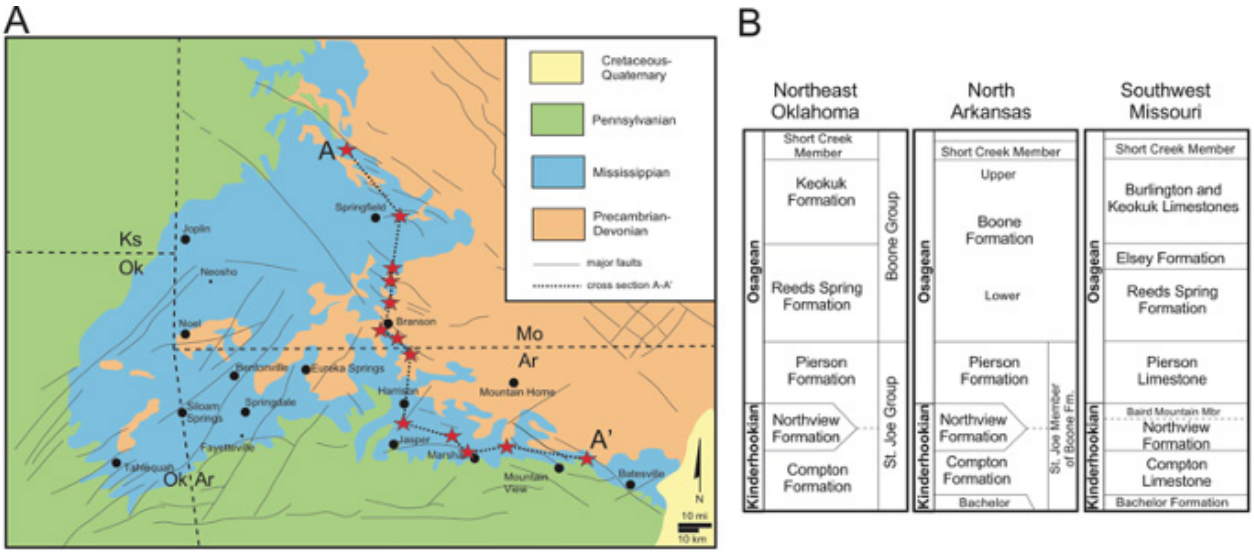

Figure 1. (a) Study area showing Mississippian outcrop belt, major faults, and cross-section line shown in fig. 2. (b) Generalized Lower Mississippian stratigraphic column in study area (modified from Thompson and Fellows, 1970). This paper follows the nomenclature shown here.

Methods and Results

The following methods were used in this study:

- Graphically log many of the same outcrops studied by Thompson and Fellows (1970) and Mazzullo et al. (2013) to identify the major facies and stacking patterns and to interpret depositional processes.
- Construct a regional stratigraphic cross section (fig. 2) showing interpreted sequences, lateral and vertical facies associations, and correlations constrained by the conodont zonation of Thompson and Fellows (1970) and Boardman et al. (2013).
- Construct a regional isopach map of the St. Joe Formation (Bachelor, Compton, Northview, and Pierson formations of Missouri) and superimpose the major fault zones of Cox (2009) to determine possible tectonic controls over deposition (fig. 3a).

The Burlington crinoidal limestones (shelf-margin) pass basinward (south) into relatively deep-water chert with turbidites (Highlandville) and thin Compton-Pierson mudstone-wackestone (Branson north), but these pass southward into thick crinoidal packstones (Baird Mountain quarry and Branson Airport) before thinning basinward to a featheredge (fig. 2). Thus, a relatively thick, convex-upward limestone body comprising St. Joe (Compton-Pierson) limestones is present south of the main Burlington shelf-margin complex and draped by Reeds Spring chert. Correlations show that St. Joe limestones and conodont zones thin basinward, but several zones are missing locally because of erosion and truncation (Thompson and Fellows, 1970; Boardman et al., 2013; Mazzullo and Wilhite, 2015). The Bolivar-Mansfield and Chesapeake fault zones underlie significant thickness changes, indicating a relationship between faulting and deposition.

A regional isopach map of the St. Joe Formation (Bachelor-Compton-Northview-Pierson) with an overlay of the major fault zones of Cox (2009) clearly confirms a relationship between stratigraphic thickness and faulting (fig. 3a). Isopach contours follow the northwest and northeast fault trends and indicate that faults were active prior to or during deposition. Fundamental principles favor deposition of the thickened siliciclastic Northview Formation in a topographic low where accommodation was high. Thus, the northwest-southeast area between the Bolivar-Mansfield (BMFZ) and Chesapeake (CHFZ) fault zones was structurally low (graben?) and deeper than areas north and south of the faults. Thick St. Joe carbonate deposition was favored across structural highs (horsts?), where the seafloor was elevated, providing a more suitable habitat for heterozoan carbonate production. Thus, a northwest-southeast trending belt of crinoid-rich carbonates exceeding 70 ft in thickness formed south of the CHFZ (fig. 3a). The basinward side of this belt is cut by northeast-trending faults, which also affected seafloor topography, productivity, deposition, and erosion. In general, basinward thinning coincides with converging

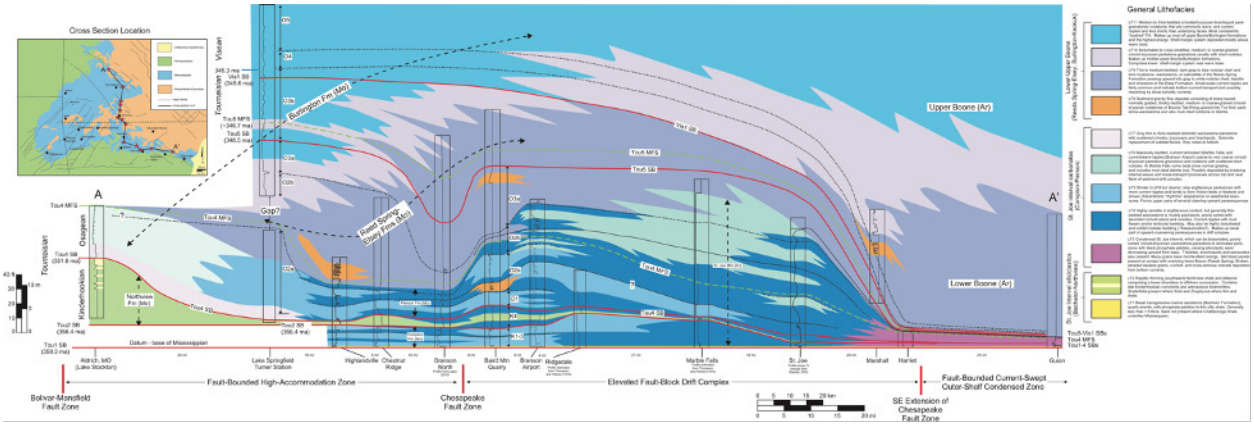

Figure 2. Stratigraphic cross section A–A' of measured sections. Correlations include conodont zone boundaries (K1-O5) of Thompson and Fellows (1970), interpreted third-order Tournaisian sequence boundaries (SB), maximum flooding surfaces (MFS), and parasequences. Measured sections by this author, Thompson and Fellows (1970), Shanks (1976), and Lopez (2013). Graphic profiles in measured sections indicate higher energy increasing to the left.

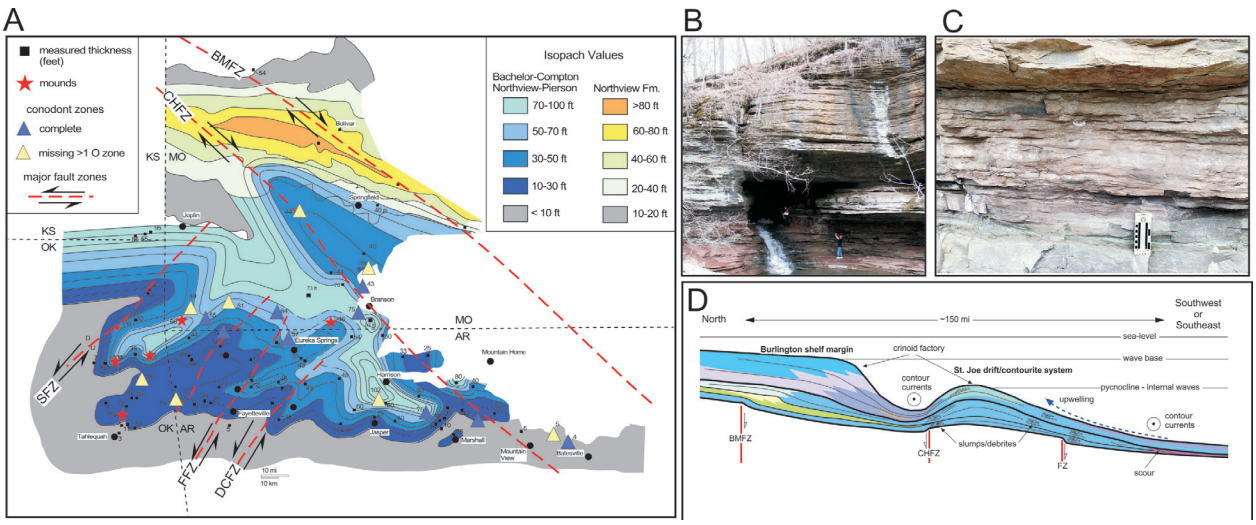

Figure 3. (a) Isopach map of St. Joe interval with major fault zones of Cox (2009). Isopach values from numerous sources. (b–c) Evenly bedded to nodular, rippled, and flaser-bedded Compton-Pierson limestones. (d) Idealized depositional profile during Osagean time.

conodont zones (condensed), but in some places it is characterized by missing conodont zones, reworked, mixed conodonts, and stratal truncation. I propose that erosion by deep-water bottom currents and depressed sediment production were largely responsible for basinward thinning to the south. Complete conodont zones are more characteristic where the St. Joe Formation is thick.

St. Joe limestones are typically thin to medium bedded, relatively continuous, and include nodular bedding (*Thalassinoides*?), current-ripples, and flaser-lenticular bedding (fig. 3b-c) deposited by contour currents (Rebesco et al., 2014). Some beds have sharp bases and graded bedding, which is characteristic of turbidity current processes. Debrites and slump features are present along fault zones and the flanks of the thick St. Joe body. *Zoophycos* is common in the lower Pierson and upper part of the Northview formations and indicates a relatively deep-water setting. Small to large Waulsortian mounds, in situ and displaced, are present near major faults. Sediment waves and truncation surfaces are present in the Pierson–Reeds Spring transition and indicate sediment transport and erosion by contour currents.

Discussion and Conclusions

In summary, deposition of the Lower Mississippian was driven by the interaction of syndepositional tectonic activity, multi-factory carbonate production, contour-current reworking, and erosion of crinoid-rich sediments, local sediment gravity-flow processes, and wave activity. Interactions led to the accumulation of a variably thick sediment-drift body that was a self-sourcing sediment factory but molded by contour-current reworking and erosion (fig. 3d). This model corroborates basinward-thinning of Lower Mississippian strata but as controlled by juxtapositioning of contour-current deposition and erosion around regional fault-controlled sea-floor perturbations in a relatively deep outer shelf. Faulting was probably syndepositional. Contour currents locally scoured beds and concomitantly deposited crinoid-rich sediment as migrating sediment waves.

References

Boardman, D. R., II, Thompson, T. L., Godwin, C., Mazzullo, S. L., Wilhite, B. W., and Morris, B. T., 2013, High-resolution conodont zonation for Kinderhookian (Middle Tournaisian) and Osagean (Upper Tournaisian-Lower Visean) strata of the western edge of the Ozark Plateau, North America: Shale Shaker, September-October, p. 98–151.

Chandler, S. L., 2001, Carbonate Olistoliths, St. Joe and Boone Limestones (lower Mississippian) Northwestern Arkansas: M. S. thesis, University of Arkansas, Fayetteville.

Childress, M., and Grammer, G. M., 2015, High resolution sequence stratigraphic architecture of a

mid-continent Mississippian outcrop in southwest Missouri: Shale Shaker, v. 66, p. 206–234.

Cox, R. T., 2009, Ouachita, Appalachian, and Ancestral Rockies deformations recorded in mesoscale structures on the foreland Ozark plateaus: Tectonophysics, v. 474, p.674–683.

Evans, K. R., and Bassett, D. J., 2013, Devonian and Mississippian tectonism in western Missouri; syndepositional sedimentation and backstepping of the Mississippian shelf margin; *in* D. J. Bassett, ed., Association of Missouri Geologists Field Trip Guidebook, 60th Annual Meeting. Association of Missouri Geologists, p. 19–80.

Harbaugh, J. W., 1957, Mississippian bioherms in northeast Oklahoma: American Association of Petroleum Geologists Bulletin, v. 41, p. 2,530–2,544.

Lane, H. R., 1978, The Burlington shelf (Mississippian, north-central United States): Geologica et Paleontologica, v. 12, p. 167–176.

Lopez, M. R. T., 2013, High-resolution stratigraphy of Lower Mississippian strata at Branson North, Missouri: M.S. thesis, Oklahoma State University, Stillwater, 150 p.

Manger, W. L., and Thompson, T. L., 1982, Regional depositional setting of Lower Mississippian Waulsortian mound facies, southern Midcontinent, Arkansas, Missouri and Oklahoma; *in* K. Bolton, H. R. Lane, and D. V. LeMone, eds., Symposium on the Paleoenvironmental Setting and Distribution of the Waulsortian Facies: El Paso Geological Society and University of Texas at El Paso, p. 43–50.

Mazzullo, S. J., Boardman, D. R., Wilhite, B. W., Godwin, C., and Morris, B. T., 2013, Revisions of outcrop lithostratigraphic nomenclature in the Lower to Middle Mississippian subsystem (Kinderhookian to basal Meramecian series) along the shelf-edge in southwest Missouri, northwest Arkansas, and northeast Oklahoma: Shale Shaker, v. 63, no. 6, p. 414–454.

Mazzullo, S. J., and Wilhite, B., 2015, New insights into lithostratigraphic architecture of subsurface Lower to Middle Mississippian petroliferous strata in southern Kansas and northern Oklahoma: AAPG Search and Discovery Article #51198.

Post, E. J., 1982, Conodont biostratigraphy of the St. Joe Formation (Lower Mississippian), north-central Arkansas: M.S. thesis, University of Arkansaas, Fayetteville, 74 p.

Rebesco, M., Hernandez-Molina, F. J., Van Rooij, D., and Wahlin, A., 2014, Contourites and associated sediments controlled by deep-water circulation processes: State-of-the-art and future considerations: Marine Geology, v. 352, p. 111–154.

Shanks, J. L., 1976, Petrology of the St. Joe Limestone at its type area north-central Arkansas: M.S. thesis, University of Arkansas, Fayetteville, 49 p.

Thompson, T. L., and Fellows, L. D., 1970, Stratigraphy and conodont biostratigraphy of Kinderhookian and Osagean rocks of southwestern Missouri and adjacent areas: Missouri Geological Survey and Water Resources, Report of Investigations No. 45, 263 p.

Troell, A. R., 1962, Lower Mississippian bioherms of southwestern Missouri and northwestern Arkansas: Journal of Sedimentary Petrology, v. 32, p. 629–664.

Chemical and Engineering Properties of Kansas Limestone Aggregates: A Review of Data from Construction Material Inventories

Franek J. Hasiuk
Kansas Geological Survey, University of Kansas, Lawrence, Kansas, USA

Introduction

Construction materials are a commonly overlooked sector in economic geology despite their ubiquity in our modern world. It is common for more than 75% of concrete and asphalt to be composed of crushed rock, sand, and/or gravel. Although the scarcity of these resources has received attention in the news media, what is often less appreciated is that the quality of aggregates can also negatively affect their performance as construction materials. For example, in southwest Iowa, Pennsylvanian-aged sediments are known to produce pavements that have shorter life spans due to the high clay content of these "cyclothemic" limestones (Dubberke, 1983). Microporosity has been shown to be high in poorer-performing crushed rocks in Iowa. This has led the Iowa Department of Transportation to have three quality-related metrics for approval of coarse aggregate sources (Ridzuan, 2016): low alumina (as shown on X-ray fluorescence), low microporosity (as shown by less than 30 mL on the Iowa Pore Index Test), and pure mineralogy (calcite or dolomite based on X-ray diffractometry).

Methods

Construction Material Inventories (CMI) were conducted by the Kansas Department of Transportation in conjunction with the U.S. Federal Highway Administration for roughly one-third of Kansas counties (36 of 105) from 1963 to 1982. These reports contain general geological descriptions of the material-bearing units in these counties to guide aggregate prospecting. Geographic locations of specific deposits (fig. 1) are described using the Public Land Survey System (PLSS), and the reports include the geological context of deposits as well as the results of engineering tests on materials samples. Engineering test data include material type

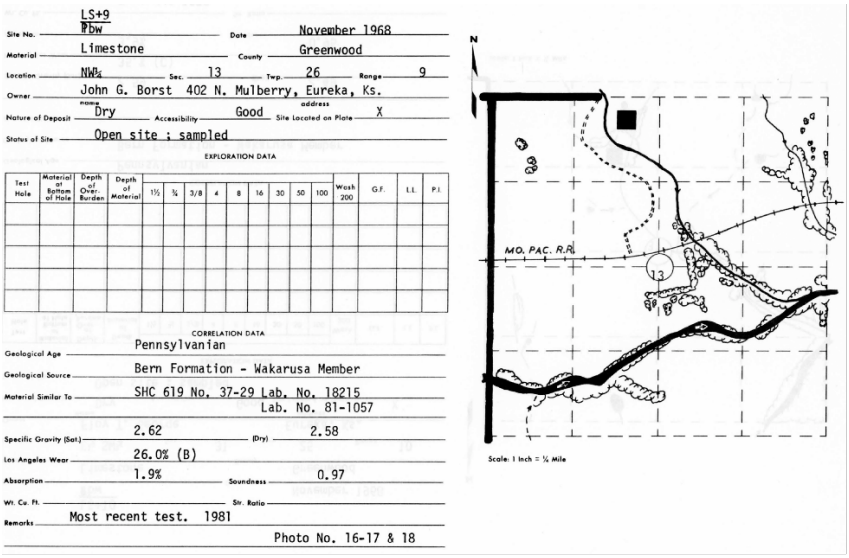
Site No. LS+9 Pbw — Date November 1968
Material Limestone — County Greenwood
Location NW¼ Sec. 13 Twp. 26 Range 9
Owner John G. Borst 402 N. Mulberry, Eureka, Ks. (name, address)
Nature of Deposit Dry — Accessibility Good — Site Located on Plate X
Status of Site Open site ; sampled

EXPLORATION DATA

Test Hole	Material at Bottom of Hole	Depth Over-Burden	Depth of Material	1½	¾	3/8	4	8	16	30	50	100	Wash 200	G.F.	L.L.	P.I.

CORRELATION DATA
Geological Age Pennsylvanian
Geological Source Bern Formation - Wakarusa Member
Material Similar To SHC 619 No. 37-29 Lab. No. 18215
Lab. No. 81-1057
Specific Gravity (Sat.) 2.62 (Dry) 2.58
Los Angeles Wear 26.0% (B)
Absorption 1.9% Soundness 0.97
Wt. Cu. Ft. Str. Ratio
Remarks Most recent test. 1981
Photo No. 16-17 & 18

Figure 1. Example material site data sheet for a location in Greenwood County, Kansas (Meyers and Blackwell, 1982). The sheet contains information about the location (both as PLSS coordinates and a hand-drawn map) as well as geological and engineering property data.

(e.g., sand and gravel, limestone, volcanic ash), specific gravity, Los Angeles abrasion (a proxy for hardness), absorption (a proxy for porosity), weight per cubic yard (i.e., bulk density), and other data, though not all sites have engineering data or values for all data.

Data from all CMIs were manually digitized. However, location data were supplemented by visually estimating locations on site maps to the third quarter-call (e.g., northeast corner of the southeast corner of the southwest corner of section 36). Locations were geocoded using LEO7.0 (Gagnon and Look, 2008) from the Kansas Geological Survey to obtain latitude/longitude values from PLSS data for representation in a geographical information system. In total, the CMI database included 2,326 geocoded sites and data from 1,631 tests. Test results included a unique value for each of the properties listed above (e.g., specific gravity, LA abrasion).

In addition, an internal KGS database of geochemical data (KGS-Chem) from Kansas rocks was analyzed. These data were digitized from a card catalog by Dobbs and Goodman during 1998–2000 (Adkins-Heljesen, personal communication, 2019). No other report detailing the methods used to collect these data was identifiable. The KGS-Chem database consists of 4,166 rows, each containing available data for location (PLSS and LEO-derived latitude/longitude), geological context, material type, major element oxides, and other data obtainable from X-ray fluorescence.

Results and Discussion

The purpose of this study was to assess limestones, so the CMI and KGS-Chem databases were trimmed to only such lithologies. Of the CMI sites, 797 were "limestone" lithology (34%). This percentage was higher than that for the KGS-Chem database, which was 26% "limestone" (n = 1,068). These limestone sites spanned the Paleozoic outcrop belt in eastern Kansas (fig. 2) and were composed mostly of Pennsylvanian and Permian samples, with minor amounts of data from Cretaceous and Mississippian formations. Because every engineering property or chemical measurement in the databases was assigned to a geological formation, it is possible to provide a statistical description of the variation in these properties (figs. 3, 4).

Absorption is an engineering property that describes the ratio of water absorbed by a material to the material weight (AASHTO T85). Knowing the density of the material, we can estimate that 1% absorption equals about 3% porosity, 5% absorption equals about 12% porosity, 10% absorption equals about 21% porosity. CMI data show a stratigraphic trend of increasing absorption in younger stratigraphic intervals (fig. 3a). Ridzuan (2016) has shown that porosity of less than about 8% (equivalent to about 3% absorption) corresponds to lower microporosity and thus higher performance in pavements.

LA abrasion is an engineering property defined as the ratio of the original mass of 5 kg of coarse

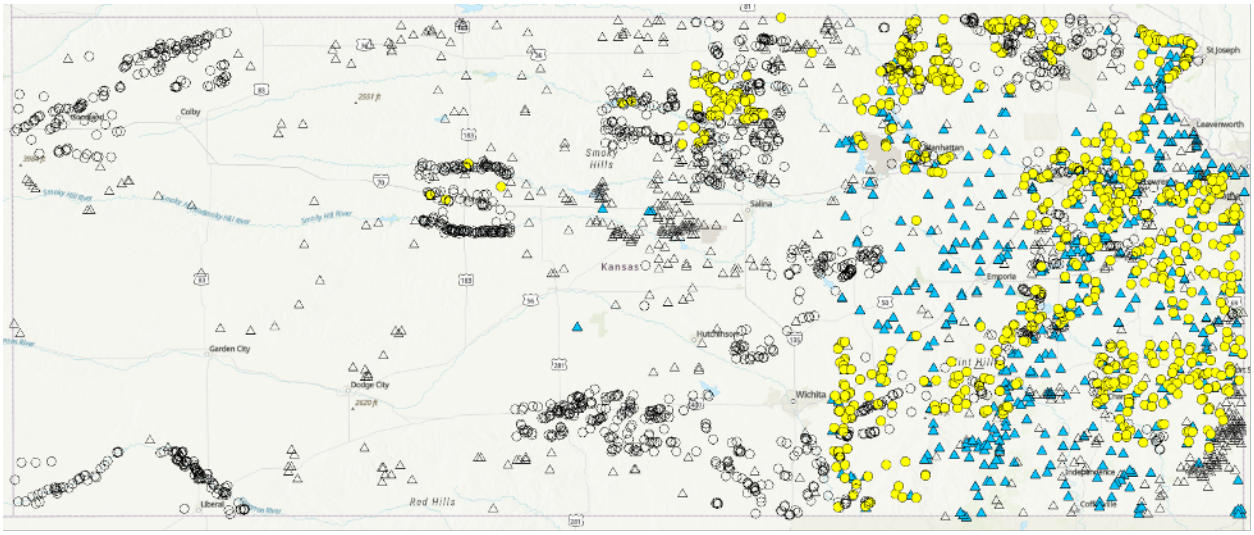

Figure 2. Map showing the distribution of localities in both CMI (circles) and KGS-Chem (triangles) databases. Filled symbols show locations of limestone samples; open symbols show locations of other material types (e.g., volcanic ash, sand and gravel, chert).

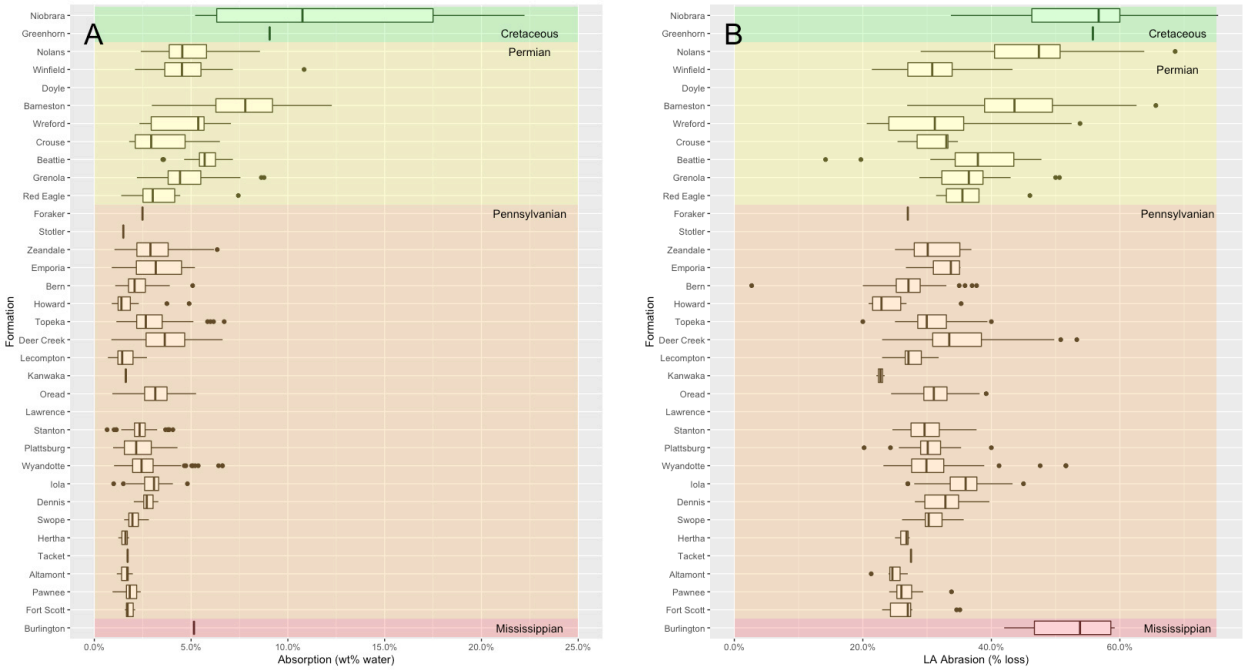

Figure 3. Summary plots from the CMI database showing variation in two engineering properties within formations (colors represent geological periods): (a) absorption (a proxy for porosity) and (b) LA abrasion (a proxy for hardness).

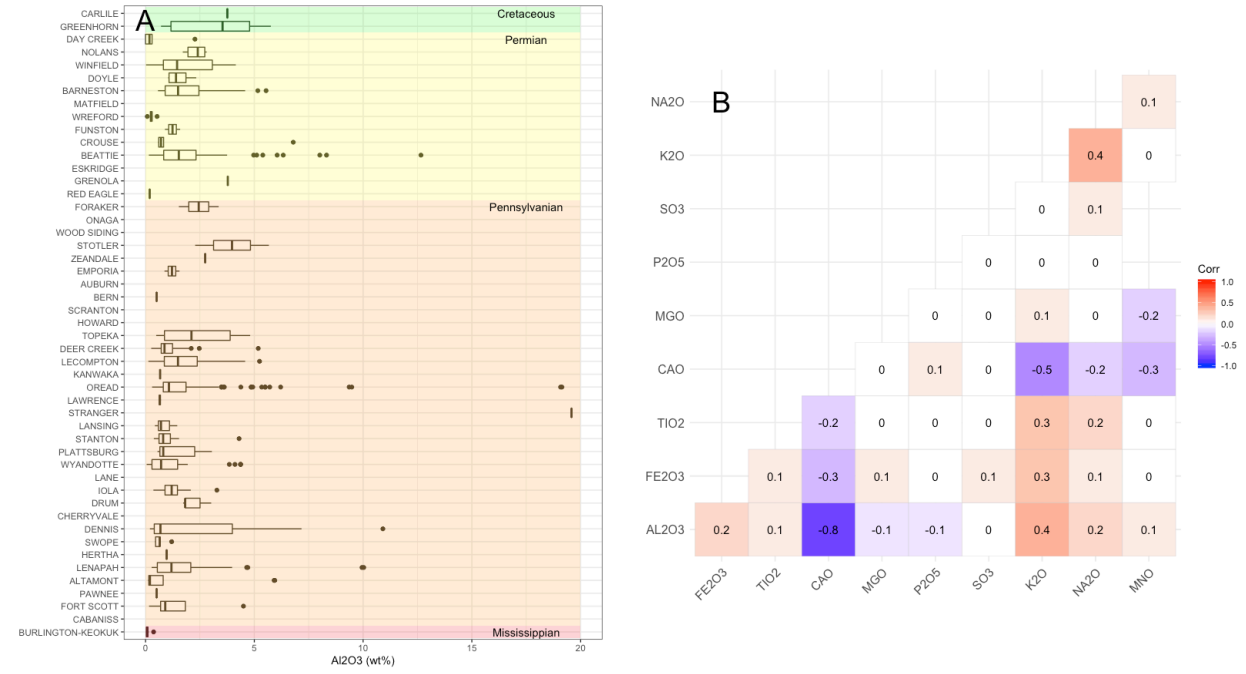

Figure 4. Example summary plots from limestone samples in the KGS-Chem database: (a) alumina content box plots by formation (colors represent geological periods) and (b) correlation matrix for major element oxides. The strongest correlation is the negative correlation between CaO and Al_2O_3 (R = -0.8).

aggregate to the mass remaining after the aggregate is rotated in a drum for 15 minutes with solid steel balls. Stratigraphically, Pennsylvanian and all but two of the Permian samples averaged between 25% and 35% mass loss (fig. 3b), while the remaining Permian samples had values greater than 40% and the Cretaceous and Mississippian samples greater than 50%.

Alumina content was reported in KGS-Chem as wt% Al_2O_3. Stratigraphically, this property can be seen (fig. 4a) to vary much less than either absorption or LA abrasion (fig. 3). In Iowa, a cutoff of 0.6 wt% Al_2O_3 is used for carbonate coarse aggregate (Dawson, 2011). Among all oxides reported, the strongest covariance (R = -0.8) was seen between Al_2O_3 and CaO, suggesting mixing between shale and limestone end members (fig. 4b).

Conclusions

CMI and KGS-Chem data can be used to identify candidate horizons with favorable chemical and engineering properties. Additional work is continuing to (1) refine stratigraphic interpretations to the member level (where possible), (2) publish these databases as interactive web maps, and (3) collect new data to fill in gaps both stratigraphically and spatially.

References

Dawson, M. R., 2011, A method to rapidly predict service life and susceptibility to deicing salt deterioration of aggregates used in Portland cement concrete: Mid-Continent Transportation Research Symposium, 19 August, Ames, Iowa.

Dubberke, W., 1983, Factors relating to aggregate durability in Portland cement concrete: Iowa Department of Transportation Report HR-2022.

Gagnon, G., and Look, K., 2008, LEO Version 7: A legal description to geographic coordinate conversion program for Kansas: Kansas Geological Survey. http://www.kgs.ku.edu/software/LEO/index.html.

Meyers, L. D., and Blackwell, D. A., 1982, Construction Materials Inventory of Greenwood County, Kansas: Kansas Department of Transportation, Construction Materials Inventory, v. 36, 144 p.

Ridzuan, M. F. A., 2016, Understanding the geological basis of the Iowa Pore Index: M.S. thesis, Iowa State University, 72 p.

Hydrothermal Fluid Flow and Burial History in the STACK Play of North-Central Oklahoma

Andrew M. Hollenbach[1,2], Sahar Mohammadi[1], Robert Goldstein[2], and Andreas Möller[2]
[1]Kansas Geological Survey, KICC, Lawrence, Kansas, USA
[2]University of Kansas, KICC, Department of Geology, Lawrence, Kansas, USA

Introduction

One of the inherent challenges of reservoir geology is assessing whether thermal history is simply controlled by burial or whether hydrothermal fluid flow perturbed the ambient burial temperature. A fluid is considered hydrothermal when it is warmer than ambient burial temperature. To identify a record of hydrothermal fluid flow, the paleo-temperature must be shown to have exceeded the ambient burial temperature at the time. As ambient burial temperature increases and decreases over time, making this determination is challenging. Here, we demonstrate a workflow to recognize the hydrothermal signature through U-Pb dating of diagenetic calcite, fluid inclusion analysis to get the temperature of precipitation, and use of the U-Pb date to calculate what the ambient burial temperature would have been at the time. Results reveal a record of hydrothermal fluid flow in the Mississippian rocks of the STACK play in north-central Oklahoma.

Methods and Results

This study uses the Pan Am Barnes D#2 core. Our research synthesizes petrographic analysis, laser ablation inductively coupled plasma mass spectrometry (LA-ICP-MS), fluid inclusion microthermometry, carbon and oxygen isotopic data, and stratigraphy to compare fluid inclusion homogenization temperatures to calculated ambient burial temperature for the time of mineral precipitation.

Petrographic study was conducted in plane-polarized, cross-polarized, reflected, and ultraviolet light and cathodoluminescence to define lithology and mineral paragenesis. The earlier part of the paragenesis begins with dolomite replacement, framboidal pyrite, and replacement calcite, followed by dissolution, replacement quartz, silicification, calcite, and stylolitization. The later part of the paragenesis includes precipitation of anhydrite in nodules, multiple events of chalcedony, partial replacement of anhydrite with megaquartz, dolomite, fracturing, dissolution of anhydrite, and multiple generations of calcite.

A sample of calcite cement (CS) from 8,891.5 ft (2,710.13 m; Osagean) in the core precipitated late in the paragenesis and provides a robust dataset. This calcite reduces a dissolved area of an earlier anhydrite. It differs petrographically and geochemically from calcite and dolomite cements that precipitated earlier in the paragenesis and may have predated compaction.

Carbon and oxygen isotopic values for calcite and dolomite in the various paragenetic stages and stratigraphic depths show a broad range. $\delta^{18}O$ values in calcite cement range from -3.5 to -8.5‰ VPDB, and $\delta^{13}C$ values range from 3.46 to -6.28‰ VPDB (fig. 1). The CS is paragenetically later than the other calcite samples and has the most negative $\delta^{18}O$ value of -8.5‰ VPDB; $\delta^{13}C$ is 2‰ VPDB.

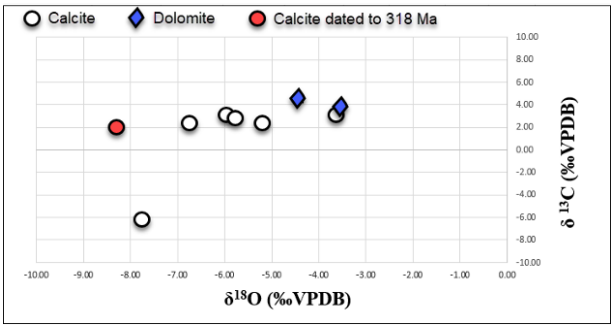

Figure 1. $\delta^{18}O$ and $\delta^{13}C$ values (per mil VPDB) for carbonate minerals in the Pan Am Barnes D#2 core in north-central Oklahoma. The datum point labeled red corresponds to the CS in this study, dated about 318 Ma; Tera-Wasserburg plot shown in fig. 2.

This study used fluid inclusion microthermometry to determine paleo-fluid temperature in the CS. We measured homogenization temperatures in primary two-phase aqueous fluid inclusions that ranged from 95° C to 115° C. T_m ice salinities of 13–18 wt. % NaCl eq. were also acquired.

We measured the age of the CS by LA-ICP-MS. That yielded a U-Pb radiometric date for precipitation of the calcite and entrapment of the fluid inclusions of 318 ± 9 Ma (fig. 2). This absolute date indicates that the calcite precipitated in its location during the Late Mississippian (Chesteran) or Early Pennsylvanian (Morrowan) (Cohen et al., 2013).

Discussion and Conclusions

Homogenization temperatures of primary fluid inclusions of 95° C to 115° C are consistent with the late position in the paragenesis and indicative of precipitation at high temperature. Because of the stratigraphic position adjacent to the underlying Woodford Shale, which is well known for its total organic carbon (TOC), it is generally assumed that the fluid of precipitation was near saturation with respect to methane. This would negate the need for a pressure correction for the fluid inclusion homogenization temperatures. These values of 95° C to 115° C, while still regarded as minimum entrapment temperatures, are likely close to the actual temperatures at which the calcite precipitated.

Given the dated calcite sample's $\delta^{18}O$ value of -8.5‰ VPDB and the fractionation factors for $\delta^{18}O$ calcite-water at the measured temperatures, this calcite would be interpreted to have precipitated from a ^{18}O-enriched aqueous fluid with $\delta^{18}O$ of 5–7‰ VSMOW. These compositions are consistent with known basin brines in the region (e.g., Musgrove and Banner, 1993).

The laser probe ICP-MS U-Pb date of 318 ± 9 Ma can be used to calculate the burial depth at the Late Mississippian to Early Pennsylvanian time of precipitation (Cohen et al., 2013). The maximum stratigraphic thickness measured between the sample and the uppermost Morrowan strata is 0.5 km. That thickness is then expanded to correct for compaction that may have taken place since precipitation. Using the backstripping algorithm in the Matlab-based program BasinVis 2.0 (Lee et al., 2020) and working backward from the maximum burial of 4.5 km during the

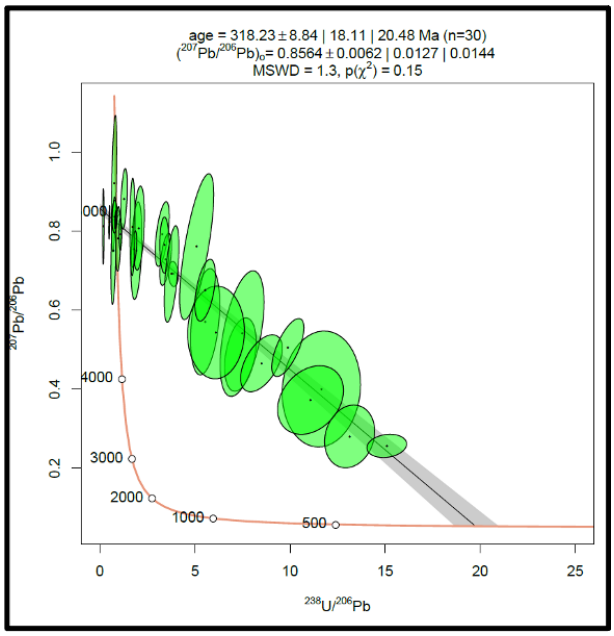

Figure 2: Tera-Wasserburg plot for calcite using LA-ICP-MS in the Pan Am Barnes D#2 core in north-central Oklahoma. The calcite sample was collected from a depth of 8,891.5 ft (2,710.13 m) in the STACK play of north-central Oklahoma.

Cretaceous (Pawlewicz, 1989), maximum burial depth at the time of calcite precipitation increases from 0.5 km to yield the uncompacted maximum depth of 0.84 km.

Maximum burial depth at the time of precipitation is then used with a geothermal gradient and paleosurface temperature to calculate the maximum possible ambient burial depth temperature at the time of precipitation. Assuming a surface temperature of 20° C (Habicht, 1979) and a liberally high geothermal gradient of 40° C (Newell, 1997; Macarewich et al., 2021), combined with the maximum uncompacted burial depth of 0.84 km, yields a maximum ambient burial temperature of 54° C at the time of precipitation. Because minimum paleo-fluid temperature measured by fluid inclusion microthermometry is 41° C above maximum ambient burial temperature, we conclude that the calcite precipitated from a hydrothermal fluid.

The results show that hydrothermal fluid was injected into the Mississippian rocks of the STACK play as early as the Late Mississippian to Early Pennsylvanian. The date corresponds to the development of the Ouachita fold-and-thrust belt, Ancestral Rocky Mountain uplift, and rapid subsidence of the Anadarko basin region. The source of the hydrothermal fluid is

currently not clear, but two primary hypotheses are (1) advective flow out of the Anadarko foredeep driven by orogenic uplift in the hinterland or compaction and (2) vertical flow from deeper strata or the basement.

The timing of hydrothermal fluid migration dated 318 Ma contributes to many years of discussion of the nearby Mississippi Valley-type ore deposits from Tri-State, southeast Missouri, central Missouri, and northern Arkansas. The origin of hydrothermal fluids that led to ore deposition have commonly been ascribed to the tectonic drive of the Marathon/Ouachita Orogeny, yet typical radiometric dates of gangue minerals in these districts and paleomagnetic dates do not coincide with the Pennsylvanian ages of the main phases of Ouachita deformation and burial of its foreland basin. Instead of yielding Early Pennsylvanian ages, many of these systems yield Late Pennsylvanian or Permian ages. The new date and evidence for hydrothermal fluid flow show that hydrothermal activity began as early as the Late Mississippian to Early Pennsylvanian, supporting the idea of a Ouachita tectonic driver. The discrepancies between timing of various events of hydrothermal fluid flow are a focus of further research (Mohammadi et al., this volume).

References

Cohen, K. M., Finney, S. C., Gibbard, P. L., and Fan, J. X., 2013, The ICS International Chronostratigraphic Chart. Episodes 36: p. 199–204.

Habicht, J. K. A., 1979, Paleoclimate, paleomagnetism, and continental drift: American Association of Petroleum Geologists, Studies in Geology, no. 9, 31 p.

Lee, E. Y., Novotny, J., and Wagreich, M., 2020, Compaction trend estimation and applications to sedimentary basin reconstruction (BasinVis 2.0): Applied Computing & Geosciences, v. 5, 100015.

Macarewich, S. I., Poulsen, C. J., and Montañez, I. P., 2021, Simulation of oxygen isotopes and circulation in a late Carboniferous epicontinental sea with implications for proxy records: Earth and Planetary Science Letters, v. 559, 116770.

Mohammadi, S., Hollenbach, A. M., Goldstein, R. H., and Möller, A., 2021, Timing of hydrothermal fluid flow events in Kansas and Tri-State Mineral District; *in* D. Ortega-Ariza, I. Bode-Omoleye, F. J. Hasiuk, S. Mohammadi, and E. K. Franseen, eds., Midcontinent Carbonate Research Virtual Symposium Extended Abstracts: Kansas Geological Survey, Technical Series 24, p. 34–37.

Musgrove, M. L., and Banner, J. L., 1993, Regional ground-water mixing and the origin of saline fluids: Midcontinent, United States: Science, v. 259, no. 5103, p. 1,877–1,882.

Newell, K. D., 1997, Comparison of maturation data and fluid-inclusion homogenization temperatures to simple thermal models: Implications for thermal history and fluid flow in the midcontinent: Current Research in Earth Sciences, Kansas Geological Survey, Bulletin 240, part 2, 16 p.

Pawlewicz M. J., 1989, Thermal maturation of the eastern Anadarko basin, Oklahoma; in Evolution of Sedimentary Basins — Anadarko Basin: U.S. Geological Survey Bulletin 1866, p. C1–C12. https://pubs.usgs.gov/bul/1866c/report.pdf.

Paleokarst Development and Controls in the Cambrian Potosi Dolomite and Eminence Formation, Illinois Basin

Yaghoob Lasemi and Zohreh Askari
Illinois State Geological Survey, University of Illinois at Urbana-Champaign, Champaign, Illinois, USA

Introduction

The Cambrian (Furongian) Potosi Dolomite and the Eminence Formation in the Illinois basin are part of the Knox Group in Illinois and constitute the lower part of the Knox Supergroup in Indiana (fig. 1). The Potosi in Illinois is a relatively pure dolomite unit, which conformably overlies the relatively impure Franconia Formation. The uppermost Cambrian Eminence Formation conformably overlies the Potosi and consists mainly of dolomite and sandy dolomite intercalated with thin shale and siltstone beds. In southwestern Indiana, the Franconia, Potosi, and Eminence stratigraphic units of Illinois cannot easily be differentiated with confidence; thus. the Potosi is a combined stratigraphic unit (Shaver et al., 1986; Thompson et. al., 2016) comprising these three units (fig. 1). The Potosi Dolomite ranges from 100 ft (30 m) in northern Illinois to more than 600 ft (183 m) thick in southern Illinois; the Eminence Formation is nearly 50 ft (15 m) in the north and thickens to more than 1,350 ft (411 m) in the south. The Potosi typically contains abundant drusy quartz; small quartz druse is also present in the Eminence Formation (Buschbach, 1975; Palmer et al., 2012).

The Potosi Dolomite contains vugular, fractured, and brecciated intervals (Freiburg and Leetaru, 2012; Lasemi et al., 2012; Lasemi and Askari, 2014; Leetaru et al., 2014). These diagenetic aspects of the Potosi were assumed to be related to paleokarst due to subaerial exposure at the top of the Eminence Formation (Freiburg and Leetaru; 2012; Leetaru et al., 2014). However, this interpretation is questioned because subaerial paleokarst features are present throughout the Knox succession but are absent at or near the top of the Eminence Formation. Here we focus on facies, porosity development, and correlation of the Potosi and Eminence in the subsurface of the Illinois basin and interpret the characteristics

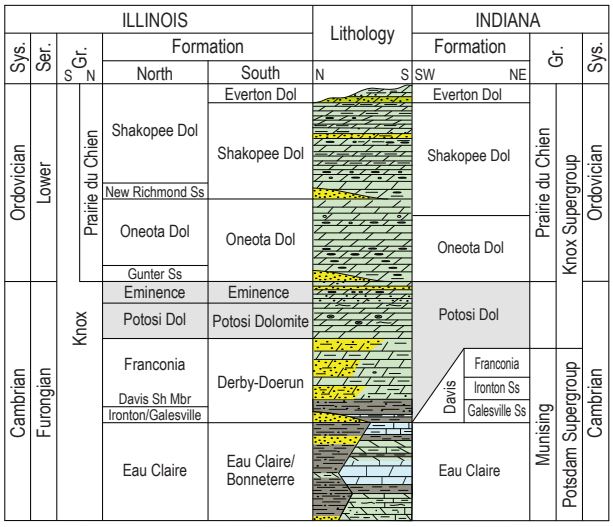

Figure 1. Stratigraphic column of the Cambrian-Ordovician succession in southern Illinois (from Kolata, 2005) and southwestern Indiana (from Thompson et. al., 2016).

of the porous intervals as buried paleokarst features unrelated to unconformity.

Methods and Results

Facies and stratigraphic variability of the Potosi were studied using the available subsurface data, including geophysical logs, cores, and well samples. The Potosi and Eminence consist mainly of fine to coarsely crystalline dolomite containing relics of bioclasts, ooids, and peloids suggesting pervasive dolomitization of shallow marine mudstone to grainstone facies. They are commonly dense (fig. 2a-b) but contain intercalations of vugular, brecciated, fractured, and/or cavernous intervals, which commonly contain chert and partially to completely mineralized cavities (fig. 2c-d). The pore spaces are generally lined with diagenetic quartz (drusy in places), calcite, or dolomite. The diagenetic fractures

are prevalent throughout the Potosi and Eminence (fig. 3), but commonly they are absent at or close to the top of the Eminence Formation. Individual highly porous intervals are up to 10 ft (3 m) thick, showing very high/abnormally high porosity (figs. 2a and 3). Throughout the Illinois basin, lost circulation intervals are encountered when drilling the Potosi Dolomite; well record data indicate that several hundred barrels of drilling fluid are often lost during drilling in these zones.

Discussion and Conclusions

Presence of lost circulation zones in the Potosi and Eminence suggest well-connected voids giving rise to excellent reservoir permeability. Drusy quartz and vuggy, fractured, and cavernous intervals are not limited to the Potosi but are present throughout the Knox succession (fig. 3), suggesting a widespread diagenetic event. Freiburg and Leetaru (2012) and Leetaru et al. (2014) interpreted the vuggy and brecciated zones of the Potosi in Macon County, central Illinois, as diagenetically altered early vadose or phreatic karstification due to subaerial exposure at the top of the Eminence Formation. Nevertheless, this interpretation is questioned because subaerial paleokarst features are absent at or near the top of the Eminence Formation. In addition, vugular and fractured/cavernous intervals are not limited to the Potosi and are present within the Knox succession (e.g., Greb et al., 2012; Lasemi and Askari,

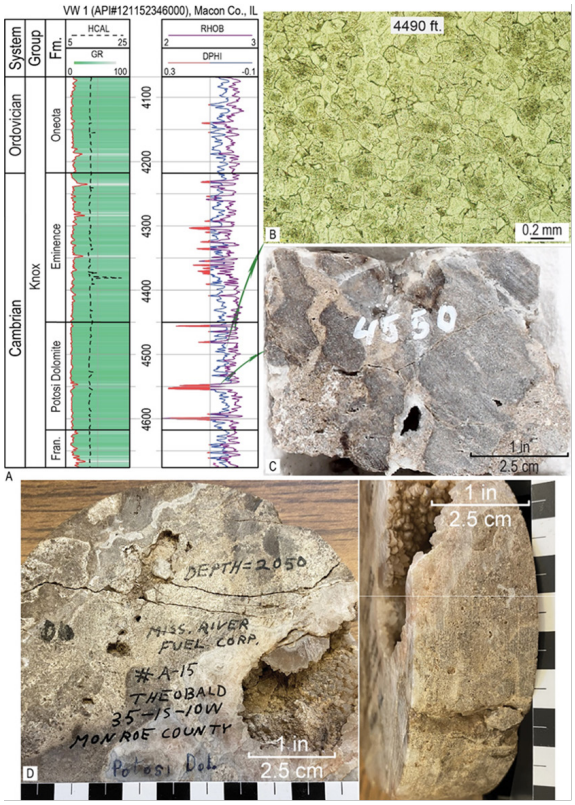

Figure 2. ADM VW 1 Well, Macon County, Illinois: (a) gamma ray, density, and density porosity log signatures; note high/abnormally high porosity intervals in red color; (b) photomicrograph in plane light of dense dolomite; and (c) core photograph of the fractured/ cavernous interval. (d) Fractured and cavernous porosity, Theobald No. 1 Well, Monroe County, Illinois.

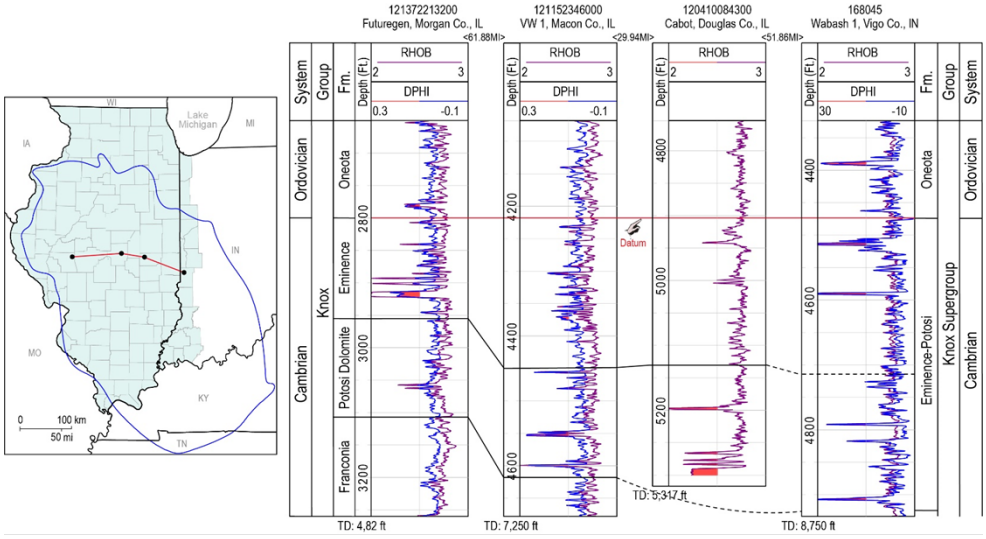

Figure 3. Stratigraphic variability of Eminence and Potosi from Morgan County, Illinois, to Vigo County, Indiana, (the blue line in the inset index map displays the outline of the Illinois basin). Abbreviations: RHOB — bulk density; DPHI — density porosity %. Note very high/abnormally high porosity that commonly represents vugular and fractured/cavernous intervals.

2014). We interpret the porous zones in the Potosi and Eminence as buried paleokarst features unrelated to unconformity. The development of this buried paleokarst and related secondary porosity appear to have been related to multiple stages of diagenesis and early to late-stage dolomite formation with reservoir quality later enhanced by carbonate dissolution and brecciation (Lasemi and Askari, 2020). It was likely controlled by basinal and hydrothermal fluid flow through the initial pore system (e.g., Gregg and Shelton, 1989; Zou et al., 2017). An early porosity network formed by early seawater dolomitization at certain intervals may have driven the initial flow of basinal and hydrothermal fluids. Reservoir quality in the porous intervals was later enhanced by carbonate dissolution and brecciation. The permeable intervals of the Potosi and Eminence are widespread in the Illinois basin and are encased in dense dolomite; thus, the formations have an excellent potential to serve as a combined reservoir and seal for storing anthropogenic CO_2 and waste material.

References

Buschbach, T. C., 1975, Cambrian system: Handbook of Illinois stratigraphy, Illinois State Geological Survey Bulletin 95, p. 34–46.

Freiburg, J. T., and Leetaru, H. E., 2012, Controls on porosity development and the potential for CO_2 sequestration or wastewater disposal in the Cambrian Potosi Dolomite (Knox Group): Illinois Basin: AAPG Eastern Section Meeting Abstracts.

Greb, S. F., Bowersox, J. R., Solis, M. P., Harris, D. C., Riley, R. A., Rupp, J. A., Kelley, M., and Gupta, N., 2012, Ordovician Knox carbonates and sandstones of the Eastern Mid-continent: Potential geologic carbon storage reservoirs and seals: AAPG Memoir 98, p. 1,077–1,101.

Gregg, J. M., and Shelton, K .L., 1989, Geochemical and petrographic evidence for fluid sources and pathways during dolomitization and lead-zinc mineralization in southeast Missouri: A review: Carbonates and Evaporites, v. 4, p. 153–175.

Kolata, D. R., 2005, Bedrock geology of Illinois: Illinois State Geological Survey, Illinois Map 14, 2 sheets, scale 1:500,000.

Lasemi, Y., and Askari, Z., 2020, Stratigraphic variability, secondary porosity development, and correlation of the Cambrian Potosi Dolomite across the Illinois basin: Geological Society of America Annual Meeting Abstracts with Programs.

Lasemi, Y., and Askari, Z., 2014, Stratigraphy of the Cambo-Ordovician Knox succession in Illinois: US DOE Knox Project Cooperative Agreement No. DE-FE0002068, Topical Report No. FE0002068-12, 43 p.

Lasemi, Y., Askari, Z., and Leetaru, H. E., 2012, Potential of the Cambro-Ordovician Knox carbonates of Illinois as combined reservoirs and seals for carbon sequestration: AAPG Eastern Section Meeting Abstracts.

Leetaru, H. E., Smith, V., Adushita, Y., and Freiburg, J. T., 2014, An integrated approach to evaluating the suitability of the Potosi Dolomite as a carbon sequestration target: Interpretation, v. 2, p. 125–133.

Palmer, J., Thompson, T. L., Seeger, C., Miller, J. F., and Gregg, J. M., 2012, The Sauk megasequence from the Reelfoot rift to southwestern Missouri: AAPG Memoir 98, p. 1,013–1,030.

Shaver, R. H., Ault, C. H., Burger, A. M., Carr, D. D., Droste, J. B., Eggert, D. L., Gray, H. H., Harper, D., Hasenmueller, N. R., Hasenmueller, W. A., Horowitz, A. S., Hutchison, H. C., Keith, B., Keller, S. J., Patton, J. B., and Rexroad, C. B., 1986, Compendium of Paleozoic rock-unit stratigraphy in Indiana — a revision: Indiana Geological Survey Bulletin 59, 203 p.

Thompson, T. A., Sowder, K. H., and Johnson, M. R., 2016, Generalized stratigraphic column of Indiana bedrock: Indiana Geological Survey, Bloomington, Indiana.

Zou, C., 2017, Other unconventional petroleum resources; *in* Unconventional Petroleum Geology: Elsevier Inc., Amsterdam, second edition, p. 405–451.

Timing of Hydrothermal Fluid Flow Events in Kansas and Tri-State Mineral District

Sahar Mohammadi[1], Andrew M. Hollenbach[1,2], Robert H. Goldstein[2], and Andreas Möller[2]
[1] Kansas Geological Survey, University of Kansas, Lawrence, Kansas, USA
[2] Department of Geology, University of Kansas, Lawrence, Kansas, USA

Introduction

The complex history of deformation and tectonic events in the Midcontinent of North America had a complex impact on the Paleozoic sedimentary rocks. They resulted in thermal alteration, Mississippi Valley-type (MVT) mineralization, and petroleum migration. Many researchers have suggested that tectonic drivers such as the Marathon-Ouachita/Ancestral Rocky Mountains or Laramide orogenies may have led to hydrothermal fluid flow in the Midcontinent (e.g., Shelton et al., 1992; Gregg and Shelton, 2012; Ramaker et al., 2015; Bailey, 2018; Goldstein et al., 2019; Mohammadi et al., 2019a, b; Temple et al., 2020). However, in this study, we will introduce new data supporting an event of hydrothermal fluid flow concurrent with the Sevier Orogeny and its foreland basin. More importantly, our new data reveal another event in a study area that is seismically active today and that is younger than 4.8 million years, indicating that continued seismicity without an obvious orogenic driver could cause hydrothermal fluid flow as well.

The Tri-State Mineral District (Missouri, Kansas, Oklahoma) is one of the largest and best-studied Pb-Zn deposits in North America. Typical for MVT deposits, fracturing and migration of warm brines deposited ore and gangue minerals (Leach et al., 2010). Ores in the district are mostly hosted in Mississippian rocks but also are known in lower Paleozoic and Pennsylvanian strata (e.g., Shelton et al., 1992; Gregg and Shelton, 2012; Wenz et al., 2012; Hagni, 1986). The widespread record of hydrothermal fluids and thermal alteration indicates a regionally advective system of fluid flow with stratigraphic and structural control (Goldstein et al., 2019).

In south-central Kansas, previously published geochemical and fluid inclusion data indicate paleotemperatures higher than normal burial temperature from Ordovician-Pennsylvanian strata, indicating advective fluid migration from the basin to foreland shelf (Goldstein et al., 2019). Later calcites with radiogenic $^{87}Sr/^{86}Sr$ also suggest fault pumping from the basement, perhaps during Laramide reactivation.

For a better understanding of controls on fluid migration in Paleozoic strata, we used laser ablation inductively coupled plasma mass spectrometry (LA-ICP-MS) for U-Pb dating on calcite cements from some of our previous studies (Mohammadi et al., 2019b; King and Goldstein, 2018; Goldstein et al., 2019) in the Tri-State Mineral District (a mine sample) in Neck City, Missouri, and the Berexco Wellington KGS 1-32 core from Sumner County, Kansas (fig. 1).

Methods and Results

This research was carried out using multiple methods, including (a) transmitted light and cathodoluminescence petrography to define the mineral and fracture paragenesis; (b) isotope geochemistry (carbon, oxygen, strontium) to determine temperature, fluid composition, rock-water interaction, and flow-paths of diagenetic fluids; (c) fluid inclusion microthermometry to determine the temperature and salinity of diagenetic fluids in cements and fractures; and (d) radiometric (U-Pb) dating of calcite cements by LA-ICP-MS.

A previously studied sample from the Tri-State Mineral District gives a mid-Cretaceous lower intercept at 122.3±5.5 Ma. A previously studied sample from the Wellington KGS 1-32 core (in Kansas) has Pb near the detection limit and the resulting age is 4.8±2.3 Ma (fig. 2a-b).

Discussion and Conclusions

Data were previously published (Mohammadi et al., 2019b) on the calcite sample from the Tri-State mine,

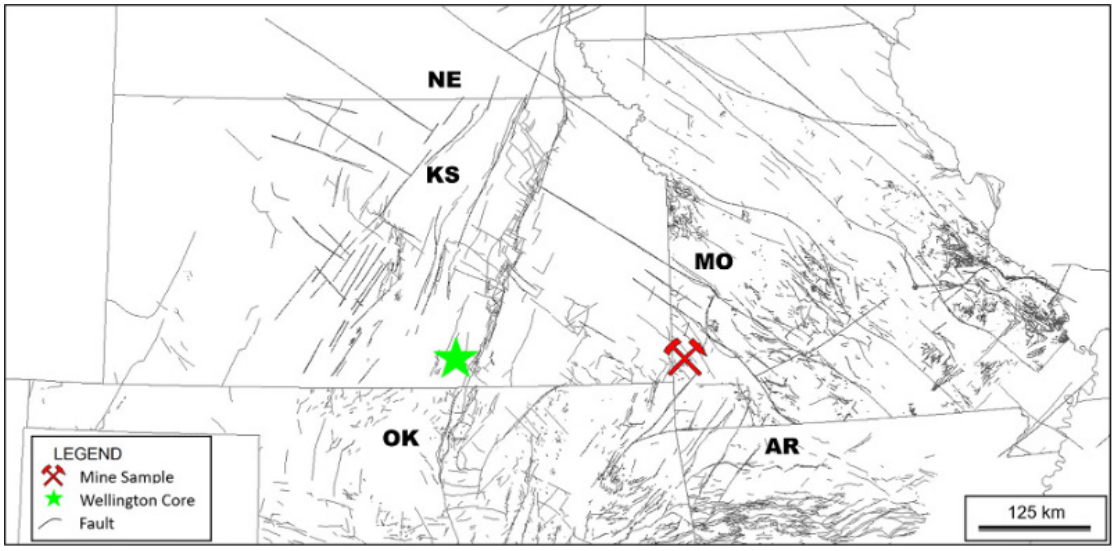

Figure 1. Basement faults map within the present study area, after Berendsen and Blair (1991), Northcutt and Campbell (1996), Dicken et al. (2001), and USGS (2020). Colored symbols show sample locations for this project.

Neck City, Missouri. The sample came from breccia pores in Mississippian strata. It yields primary fluid inclusions with T_h values ranging from 60 to 98° C, and T_m ice yielding salinities of 5.4–8.5 wt. % NaCl, as well as $^{87}Sr/^{86}Sr$ of 0.7099. Carbon and oxygen isotope values for this sample were -3.5 and -11.04 (‰ VPDB), respectively. These data indicate the calcite precipitated from hydrothermal fluids moving through the karst breccias. Previously, we suggested that these hot and moderately saline fluids most likely were associated with the Ouachita Orogeny. However, our new data from U-Pb analysis for that specific location gives the mid-Cretaceous age of 122.3±5.5 Ma. This age clearly is during the timing of the Sevier Orogeny along the west coast and development of its foreland basin well into the Midcontinent. The age is too old to be ascribed to the Laramide Orogeny and inconsistent with ages of various intrusives in the Midcontinent (Cox and Van Arsdale, 1997; Blackburn et al., 2008; Kjarsgaard et al., 2017).

Calcite cements from the Wellington KGS 1-32 core from previous studies (King and Goldstein, 2018; Goldstein et al., 2019) are one of the latest events in the paragenesis and are closely associated with the timing of sphalerite and galena precipitation. Cements toward the base of the Arbuckle Group have highly radiogenic $^{87}Sr/^{86}Sr$ around 0.716. The cements at this depth typically lack primary fluid inclusions but are crosscut by secondary fluid inclusions yielding T_h of 70.5–89.8º C, an indication of high temperatures after

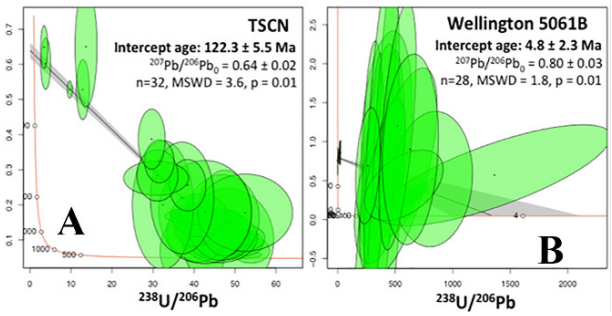

Figure 2. Tera-Wasserburg Concordia diagrams for preliminary U-Pb data from calcite with fluid inclusion evidence for hydrothermal processes. Samples from Missouri and Kansas. Results are interpreted as calcite precipitation ages. (a) Cretaceous age consistent with a Sevier Orogeny driver outside of the age envelope for Laramide or hotspot activity. (b) Remarkably young 4.8 Ma age for calcite precipitation, fracturing, and hydrothermal fluid flow, indicating continued seismicity unrelated to a known tectonic driver.

calcite precipitation. T_m ice of the secondary fluid inclusions yield salinities of 18.2–19.6 wt. % NaCl. $\delta^{18}O$ values range from -8.6‰ to -9.8‰. Based on the $\delta^{18}O$, $^{87}Sr/^{86}Sr$, and primary fluid inclusions higher in the section, it was argued that these late calcites resulted from a late stage of basement-involved fault pumping of hydrothermal fluids, where fluids were flowing vertically out of the basement into the overlying section during events of faulting. The paragenesis indicated that this deformation must have been after the Permian,

and it was hypothesized that far field stresses from the Laramide Orogeny may have caused the fluid flow. However, our new 4.8 Ma age on the calcite indicates the hydrothermal fluid flow that precipitated the calcite was not during the Laramide Orogeny but was at 4.8 Ma. The T_h of the secondary fluid inclusions indicate hydrothermal fluid flow younger than 4.8 Ma.

These results indicate that the paradigm of deformation and hydrothermal fluid flow being limited to major orogenic events with well-known far field stresses may not be correct. The development of the foreland basin for the Sevier Orogeny is one new tectonic event that must be considered, but continued deformation not linked to major orogenic events must also be considered.

References

Bailey, P. A., 2018, Diagenesis of the Arbuckle Group in northeastern and north-central Oklahoma, USA: M.S. thesis, Oklahoma State University, 75 p.

Berendsen, P., and Blair, K. P., 1991, Interpretive subcrop map of the Precambrian basement in the Joplin 1° x2° quadrangle: Kansas Geological Survey, Subsurface Geology Series 14, 10 p.

Blackburn, T., Stockli, D., Carlson, R. W., Berendsen, P., Walker, J. D., and Winters, N. D., 2008, (U-Th)/He dating of kimberlites; a case study from north-eastern Kansas: Earth and Planetary Science Letters, v. 275, p. 111–120.

Cox, R. T., and Van Arsdale, R. B., 1997, Hotspot origin of the Mississippi embayment and its possible impact on contemporary seismicity: Engineering Geology, v. 46, p. 201–216.

Dicken, C. L., Pimley, S. G., and Cannon, W. F., 2001, Precambrian basement map of the northern midcontinent, U.S.A. — A digital representation of the 1990 P.K. Sims map: U.S. Geological Survey Open-File Report 01-021, available online only. https://pubs.usgs.gov/of/2001/of01-021/

Goldstein, R. H., King, D. B., Watney, W. L., and Pugliano, T. M., 2019, Drivers and history of late fluid flow: Impact on Midcontinent reservoir rocks; *in* G. M. Grammer, J. M. Gregg, J. O. Puckette, P. Jaiswal, M. Pranter, S. J. Mazzullo, and R. H. Goldstein, eds., Mississippian Reservoirs of the Mid-Continent, U.S.A.: American Association of Petroleum Geologists Memoir 122, p. 417–450.

Gregg, J. M., and Shelton, K. L., 2012, Mississippi Valley-type mineralization and ore deposits in the Cambrian–Ordovician great American carbonate bank; *in* J. R. Derby, R. D. Fritz, S. A. Longacre, W. A. Morgan, and C. A. Sternbach, eds., The great American carbonate bank: The geology and economic resources of the Cambrian–Ordovician Sauk megasequence of Laurentia: AAPG Memoir, v. 98, p. 163–186.

Hagni, R. D., 1986, A summary of the geology of the ore deposits of the Tri-State district, Missouri, Kansas, and Oklahoma: A Guidebook to the Geology and Environmental Concerns in the Tri-State Lead-Zinc District, Missouri, Kansas, and Oklahoma, p. 30–54.

King, B. D., and Goldstein, R. H., 2018, History of hydrothermal fluid flow in the midcontinent, USA: The relationship between inverted thermal structure, unconformities and porosity distribution; *in* P. J. Armitage, A. R. Butcher, J. M. Churchill, A. E. Csoma, C. Hollis, R. H. Lander, J. E. Omma, and R. H. Worden, eds., Reservoir Quality of Clastic and Carbonate Rocks: Analysis, Modelling and Prediction: Geological Society, London, Special Publications, 435, first published online in 2016, p. 283–329.

Kjarsgaard, B. A., Heaman, L. M., and Pearson, D. G., 2017, The North America mid-Cretaceous kimberlite corridor: Wet, edge-driven decompression melting of an OIB-type deep mantle source: Geochemistry, Geophysics, Geosystems, v. 18, p. 2727–2747, doi:1002/2016GC006761.

Leach, D. L., Taylor, R. D., Fey, D. L., Diehl, S. F., and Saltus, R. W., 2010, A deposit model for Mississippi Valley-type lead-zinc ores: Scientific Investigations Report 5070-A, U.S. Geological Survey, Reston, Virginia, 64 p.

Mohammadi, S., Ewald, T. A., Gregg, J. M., and Shelton, K. L., 2019a, Diagenesis of Mississippian carbonate rocks in north-central Oklahoma, USA.; *in* G. M. Grammer, J. M. Gregg, J. O. Puckette, P. Jaiswal, M. Pranter, S. J. Mazzullo, and R. H. Goldstein, eds., Mississippian Reservoirs of the Mid-Continent, U.S.A.: American Association of Petroleum Geologists Memoir 122, p. 353–358.

Mohammadi, S., Gregg, J. M., Shelton, K. L., Appold, M. S., and Puckette, J. O., 2019b, Influence of late diagenetic fluids on Mississippian carbonate rocks

on the Cherokee–Ozark Platform, NE Oklahoma, NW Arkansas, SW Missouri, and SE Kansas; *in* G. M. Grammer, J. M. Gregg, J. O. Puckette, P. Jaiswal, M. Pranter, S. J. Mazzullo, and R. H. Goldstein, eds., Mississippian Reservoirs of the Mid-Continent, U.S.A.: American Association of Petroleum Geologists Memoir 122, p. 323–352.

Northcutt, R. A., and Campbell, J. A., 1996, Geologic provinces of Oklahoma: The Shale Shaker, v. 46, p. 99–103.

Ramaker, E. M., Goldstein, R. H., Franseen, E. K., and Watney, W. L., 2015, What controls porosity in cherty fine-grained carbonate reservoir rocks? Impact of stratigraphy, unconformities, structural setting and hydrothermal fluid flow: Mississippian, SE Kansas: The Geological Society of London, Special publications, v. 406, p. 179–208.

Shelton, K. L., Bauer, R. M., and Gregg, J. M., 1992, Fluid-inclusion studies of regionally extensive epigenetic dolomites, Bonneterre Dolomite (Cambrian), southeast Missouri: Evidence of multiple fluids during dolomitization and lead-zinc mineralization: Geological Society of America Bulletin, v. 104, p. 675–683.

Temple, B. J., Bailey, P. A., and Gregg, J. M., 2020, Carbonate diagenesis of the Arbuckle Group North Central Oklahoma to Southeastern Missouri: The Shale Shaker, v. 71, n. 1, 30 p.

USGS, 2020, GMNA Resources: Geologic Map of North America GIS database: https://ngmdb.usgs.gov/gmna/#gmnaDocs.

Wenz, Z. J., Appold, M. S., Shelton, K. L., and Tesfaye, S., 2012, Geochemistry of Mississippi Valley-type mineralizing fluids of the Ozark Plateau: A regional synthesis: American Journal of Science, v. 312, p. 22–80.

Regional Controls on Low-Latitude, Shallow-Water Heterozoan and Photozoan Carbonate Facies Distribution, Lower Mississippian, Continental U.S.

Diana Ortega-Ariza[1] and Evan K. Franseen[2,1]
[1] Kansas Geological Survey, University of Kansas, Lawrence, Kansas, USA
[2] KICC, Department of Geology, University of Kansas, Lawrence, Kansas, USA

Introduction

Under ideal photic zone conditions, low-latitude shallow-water carbonate systems are commonly dominated by photozoan association components (James, 1997). Increasingly, studies are documenting low-latitude shallow-water carbonate systems in which heterozoan association components are abundant and photozoan components are reduced or even absent (heterozoan-photozoan transitional carbonates, Halfar et al., 2006). These characteristics indicate factors that adversely affected the photic zone, commonly excess nutrients, turbidity, and cooler water from upwelling or land runoff. Low-latitude transitional carbonate systems can form significant reservoirs; however, compared to photozoan-dominated low-latitude carbonates, they are still not well recognized or understood. Further study is important because facies types and distribution, stratal architecture, dominant mineralogy, diagenetic potential, and resultant reservoir character can be significantly different from photozoan-dominated systems.

Early Mississippian carbonate systems form important reservoirs in the continental United States. During that time, most of the area was located in low latitudes and carbonates were widely deposited in a shallow tropical sea that covered much of the area (e.g., Gutschick and Sandberg, 1983). Our studies and others show shallow-water areas that are dominated by heterozoans (± biosiliceous facies), reflecting adverse photic zone conditions, whereas in other areas photozoans are abundant, reflecting more normal photic zone conditions. Our preliminary study is developing regional distribution patterns of shallow-water facies to provide a first-level understanding of controls on deposition and relevance to reservoir character.

Methods and Results

This project is part of our ongoing program on Lower Mississippian carbonates in the United States. This study incorporated data from our studies and that from the literature to document large-scale shallow-water carbonate facies distributions.

Shallow-water inner-to-outer ramp facies in areas bordering basins (Anadarko, Marathon, Arkoma, Illinois) south of the Transcontinental Arch (TA) and southeast areas flanking the Appalachians are dominated by heterozoans (echinoderms, bryozoans, and brachiopods) (fig. 1; e.g., Lasemi et al., 2003; Franseen, 2006; Kopaska-Merkel et al., 2013). Solitary rugose corals, siliceous sponges (including basin margin buildups; e.g., Kansas, Watney et al., 2001), and basin margin biodetrital and Waulsortian mounds (e.g., Kentucky, Lasemi et al., 2003; New Mexico, Kirkby and Hunt, 1996) are locally abundant. Notably, these areas lack abundant photozoans (minor occurrences of oolites locally). Other shallow-water inner-ramp facies in the areas south of the TA include evaporites (e.g., Kansas, Franseen, 2006; fig. 2a), crinoid-bryozoan biodetrital mounds (e.g., Illinois basin, Lasemi et al., 2003; fig. 2b), and small sponge-microbial mounds (e.g., southeast Appalachians, Kopaska-Merkel et al., 2013).

Heterozoan, biosiliceous, and mound facies are also found in shallow-water inner ramp and shelf areas west and north-northwest of the TA. However, those areas also show significant abundances of photozoans, consisting of red, green, and blue-green calcareous

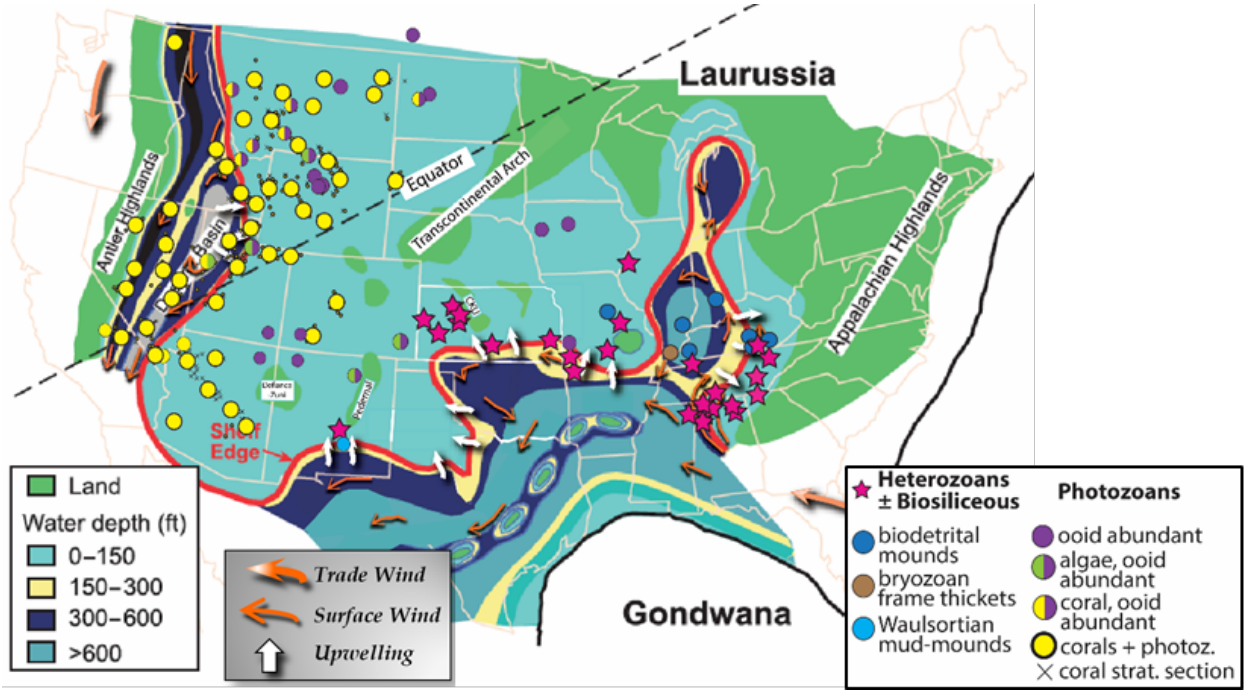

Figure 1. Paleogeographic map of the continental United States showing general distribution patterns of shallow-water carbonate facies (modified from Gutschick and Sandberg, 1983).

algae, stromatolites, benthic foraminifera, and oolites in shallow-water environments (figs. 1, 2c-d), including those surrounding basins (e.g., Williston basin) (e.g., Lindsay and Roth, 1982; Sando, 1980; Elrick and Read, 1991; Westphal et al., 2004). Osagean-Meramecian shallow-water colonial rugose and tabulate corals are also common in those areas (Sando, 1980; Sando and Bamber, 1985; fig. 2d).

Discussion and Conclusions

Previous paleogeographic and paleoceanographic studies interpreted upwelling in basinal areas, especially those south of the TA, during the Early Mississippian to account for the abundance of biosiliceous facies (including sponge buildups) and other types of buildups in basin margin areas (e.g., Lowe, 1975; Parrish, 1982; Gutschick and Sandberg, 1983; Lumsden, 1988; Lasemi et al., 2003). Subsequent documentation of heterozoan and biosiliceous facies in shallow-water (inner ramp) areas adjacent to basins south of the TA also interpreted upwelling as a dominant process that supplied nutrients, silica, and likely cooler water to those areas (e.g., Franseen, 2006).

The documentation in this study further shows dominance of shallow-water heterozoan-biosiliceous facies (and lack of photozoans) nearest basins south of the TA and abundance of photozoans in areas away from the basins (west, north-northwest of the TA). This is consistent with upwelling as a dominant process affecting shallow-water ramp environments adjacent to basins (fig. 1). Although nutrients derived from land runoff could have been a factor, initial data showing the presence of photozoan facies near land areas suggest that was not a major factor. Our ongoing studies will continue adding details to these large-scale distribution patterns, as well as internal finer-scale patterns of heterozoan and photozoan distributions, alternations, and cycles that may be tied to various processes, including sea-level fluctuations and climate changes.

References

Elrick, M., and Read, J. F., 1991, Cyclic ramp-to-basin carbonate deposits, Lower Mississippian, Wyoming and Montana; a combined field and computer modeling study: Journal of Sedimentary Research, v. 61, no. 7, p. 1,194–1,224.

Franseen, E. K., 2006, Mississippian (Osagean) shallow-water, mid-latitude siliceous sponge spicule and heterozoan carbonate facies: An example from Kansas with implications for regional controls and distribution

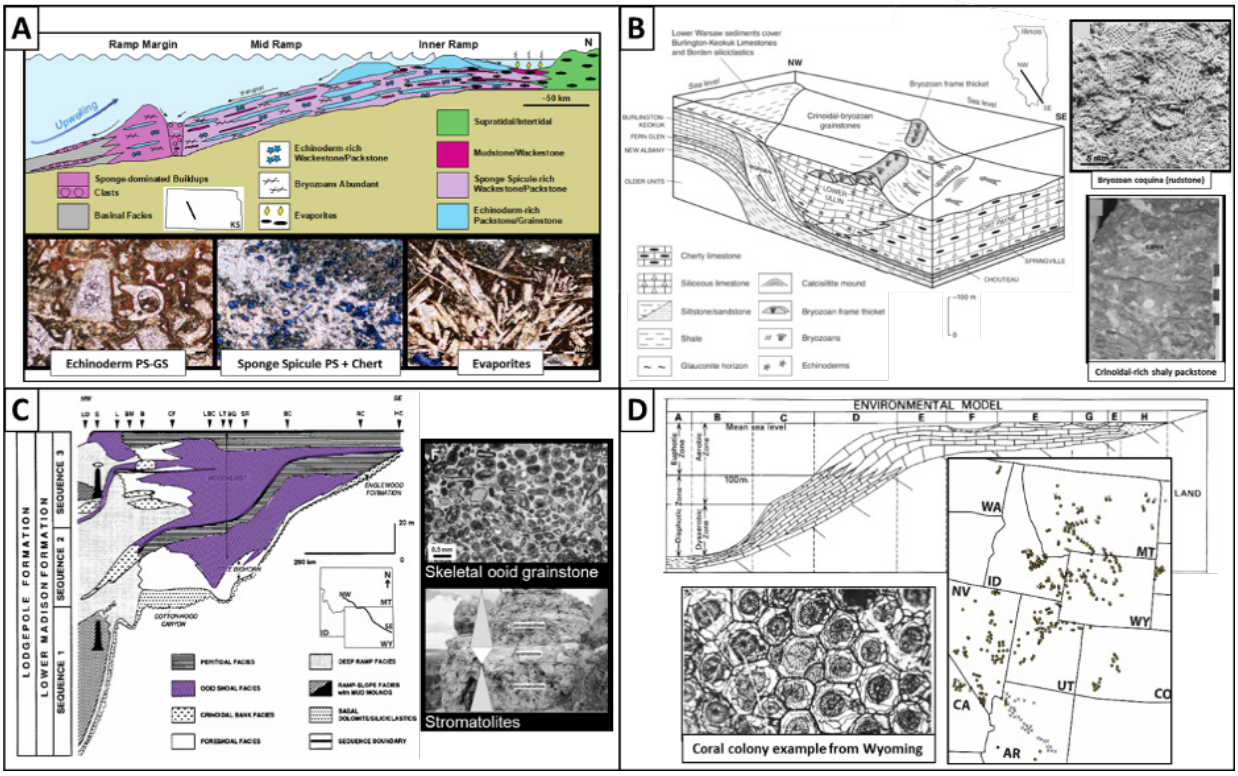

Figure 2. (a) Schematic inner-ramp to ramp-margin cross section and photomicrographs of representative heterozoan and biosiliceous facies from Kansas (Franseen, 2006). (b) Schematic block diagram and photographs showing inner-ramp to ramp-margin heterozoan facies from Illinois and Kentucky (Lasemi et al., 2003; Krause and Meyer, 2004). (c) Schematic ramp cross section, photomicrograph, and photograph highlighting photozoan facies components from Wyoming-Montana (Elrick and Read, 1991; Westphal et al., 2004). (d) Schematic ramp model for Mississippian coral occurrences in western areas (dots and x on map), including shallow-water corals (photo; lithofacies D, E), which are commonly associated with photozoan components (Sando, 1980; Sando and Bamber, 1985).

of potential reservoir facies: Current Research in Earth Sciences, Bulletin 252, part 1. http://www.kgs.ku.edu/Current/2006/franseen/index.html.

Gutschick, R. C., and Sandberg, C. A., 1983, Mississippian continental margins of the conterminous United States; *in* The Shelf-break Margin—Critical Interface on Continental Margins, D. J. Stanley and G. T. Moore: Society of Economic Paleontologists and Mineralogists, Special Publication 33, p. 79–96.

Halfar, J., Godinez-Orta, L., Mutti, M., Valdez-Holguin, J. E., and Borges, J. M., 2006, Carbonates calibrated against oceanographic parameters along a latitudinal transect in the Gulf of California, Mexico: Sedimentology, v. 53, no. 2, p. 297–320.

James, N. P., 1997, The cool-water carbonate depositional realm; *in* Cool-Water Carbonates, N. P. James and J. A. D. Clarke, eds.: Society of Economic Paleontologists and Mineralogists, Special Publication 56, p. 1–22.

Kirkby, K. C., and Hunt, D., 1996, Episodic growth of a Waulsortian buildup: the Lower Carboniferous Muleshoe Mound, Sacramento Mountains, New Mexico, USA: Geological Society, London, Special Publications, v. 107, no. 1, p. 97–110.

Kopaska-Merkel, D. C., Mann, S. D., and Pashin, J. C., 2013, Sponge-microbial mound facies in Mississippian Tuscumbia Limestone, Walker County, Alabama: AAPG bulletin, v. 97, no. 11, p. 1,871–1,893.

Krause, R., and Meyer, D., 2004, Sequence stratigraphy and depositional dynamics of carbonate buildups and associated facies from the lower Mississippian Fort Payne Formation of southern Kentucky, USA: Journal of Sedimentary Research, v. 74, no. 6, p. 831–844.

Lasemi, Z., Norby, R. D., Utgaard, J. E., Ferry, W. R., Cuffey, R. J., and Dever, G. R., Jr., 2003, Mississippian carbonate buildups and development of cool-water-like carbonate platforms in the Illinois basin, midcontinent U.S.A.; *in* Permo-Carboniferous Carbonate Platforms and Reefs, W. M. Ahr, P. M. Harris, W. A. Morgan, I. D. Somerville, and R. J. Stanton, Jr., eds.: Society of Economic Paleontologists and Mineralogists, Special Publication 78 and AAPG, Memoir 83, p. 69–95.

Lindsay, R. F., and Roth, M. S., 1982, Carbonate and evaporite facies, dolomitization and reservoir distribution of the Mission Canyon Formation, Little Knife Field, North Dakota; *in* J. E. Christopher and J. Kaldi, eds., 4th International Williston Basin Symposium Volume: Saskatchewan Geological Survey Special Publication 6, p. 153–179, Regina, Saskatchewan, Canada.

Lowe, D. R., 1975, Regional controls on silica sedimentation in the Ouachita System: Geological Society of America, Bulletin, v. 86, p. 1,123–1,127.

Lumsden, D. N., 1988, Origin of the Fort Payne Formation (Lower Mississippian), Tennessee: Southeastern Geology, v. 28, no. 3, p. 167–180.

Parrish, J. T., 1982, Upwelling and petroleum source beds, with reference to Paleozoic: AAPG Bulletin, v. 66, no. 6, p. 750–774.

Sando, W. J., 1980, The paleoecology of Mississippian corals in the western conterminous United States: Acta Palaeontologica Polonica, v. 25, no. 3–4.

Sando, W. J., and Bamber, E. W., 1985, Coral zonation of the Mississippian system in the western interior province of North America: USGS Professional Paper 1334, 61 p.

Watney, W. L., Guy, W. J., and Byrnes, A. P., 2001, Characterization of the Mississippian chat in south-central Kansas: AAPG bulletin, v. 85, no. 1, p. 85–113.

Westphal, H., Eberli, G. P., Smith, L. B., Grammer, G. M., and Kislak, J., 2004, Reservoir characterization of the Mississippian Madison formation, Wind River basin, Wyoming: AAPG bulletin, v. 88, no. 4, p. 405–432.

Geological Influences upon the Mississippian Pitkin Limestone/Caney Shale in the Arkoma Basin

Abbas Seyedolali[1], Kurt Rottmann[2], Emilio J. Torres Parada[3], William Full[4], and Brittany V. Stroud[5]
[1] Oklahoma Geological Survey, University of Oklahoma, Norman, Oklahoma, USA
[2] Consulting Geologist, Bethany, Oklahoma, USA
[3] Research Associate, University of Oklahoma, Norman, Oklahoma, USA
[4] GXStat LLC, Wichita, Kansas, USA
[5] University of Oklahoma, Norman, Oklahoma, USA

Introduction

In eastern Oklahoma–western Arkansas, two late Mississippian (Chesteran–lower Namurian) stratigraphic units are present: the Fayetteville Shale and the Pitkin Limestone. Pitkin Limestone outcrops are reported in the Ozark Mountains of northern Arkansas–eastern Oklahoma, and the zone is present in the subsurface northeast of Pittsburgh, Haskell, Latimer, Muskogee, and Le Flore counties of the Arkoma basin, Oklahoma. We interpret the Pitkin Limestone and Fayetteville Shale as being distinct facies of the Caney Shale farther west in the Arkoma basin. In the Arkoma basin, the Caney Shale has been subdivided into three members, with the upper and middle members being equivalent to the Pitkin Limestone and the lower being equivalent to the Fayetteville Shale. These members have unique gamma ray and deep resistivity well log responses, which allow them to be identified and correlated across the depositional fairway of the Arkoma basin. The members' lithologic composition may be controlled by water depth at the time of deposition. The electric well log features are similar throughout the Arkoma basin and Cherokee Platform.

Methods and Results

A total of almost 4,100 open-hole electric logs were used to correlate the tops of the Sylvan Shale; Hunton Group; Woodford Shale; Kinderhook Shale; Boone Limestone; Mayes Limestone; upper, middle and lower Caney Shale member markers; Caney Shale; Jefferson Shale; and the Pennsylvanian/Mississippian unconformity. A series of structure maps, cross sections, and isopach maps were generated for the interpretations discussed herein. Several theses were used to delineate the sedimentology of the Caney Shale in the Arkoma basin. Polished thin sections were made from multiple Caney Shale open-hole well cuttings/core and are undergoing petrographic and electron probe microanalyzer (EPMA) analyses.

Discussion and Conclusions

Correlations of the Caney Shale within the eastern part of the Arkoma basin have revealed a complex series of shales, organic shales, and limestones (fig. 1a). From the base upward is a hot gamma ray organic-rich Fayetteville Shale followed by the Pitkin carbonate-rich regressive systems tract (RST). A major east to west lateral facies change occurred during deposition of the Pitkin Limestone (upper and middle parts of the Caney Shale; fig. 1b). In the eastern part of the Arkoma basin, the Pitkin Limestone is dominated by skeletal crinoidal/bryozoans/brachiopods ooid-grainstone to packstone with its base highlighted by the presence of glauconite-rich sands. This indicates the transition from a lowstand to a highstand system tract. In the central part of the Arkoma basin, deposition contains both carbonate content and siliciclastic clay and is interpreted to be deposited in a depth-controlled transition zone. In the western part of the Arkoma basin, deposition is manifested by clay-rich mudstone and siltstone. This lateral change of facies within the Pitkin Limestone is interpreted to be controlled by sea-level depth during deposition and by access to more open marine waters and not by tectonic influences. Evidence for the lack of major tectonic activity during Silurian and Devonian Periods and the

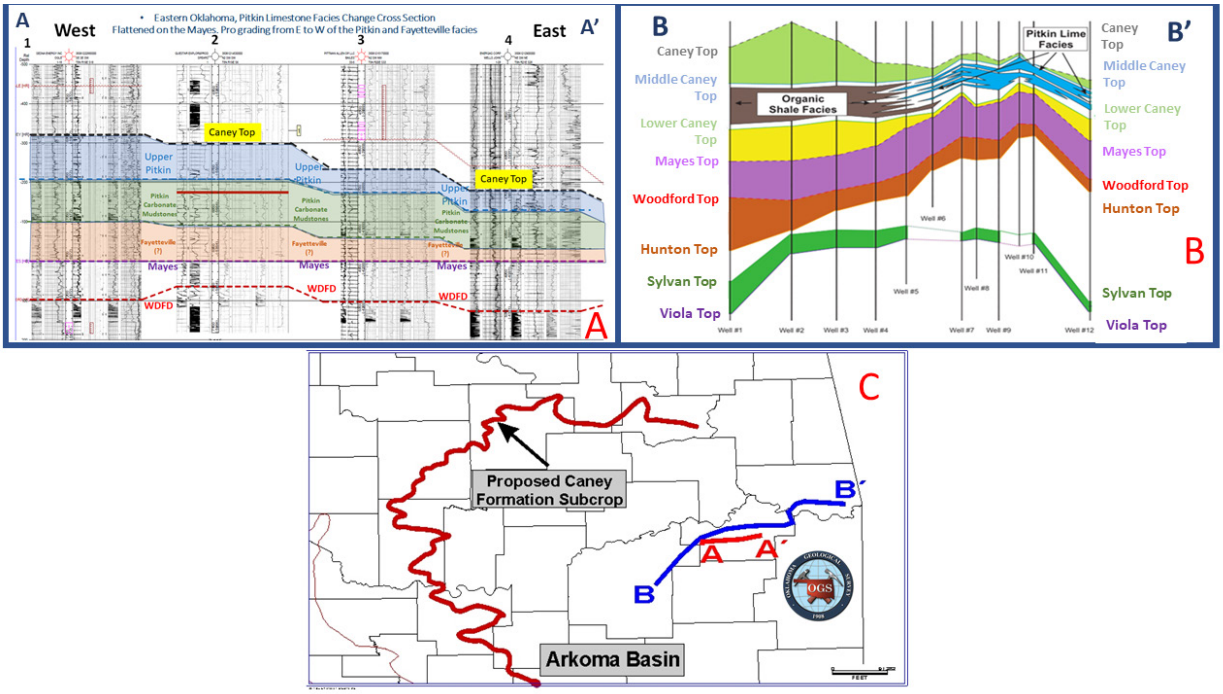

Figure 1. Lateral facies change of the Caney Shale toward a carbonate-rich, less-restrictive environment in eastern Oklahoma. (a) Cross section A–A' illustrates the stratigraphic relationship between the Caney Shale and Pitkin Limestone; (b) cross section B–B' is a colored diagram clearly showing this relationship; (c) location of the aforementioned cross sections along with the proposed limits of the Caney Shale subcrop around the Arkoma basin, Oklahoma.

Mississippian subperiod comes from the interpretation of an isopach of the time-stratigraphic surfaces of the top of the Mississippian to the top of Sylvan over the Arkoma basin and parts of the Cherokee Platform. Discounting regional dip, a lack of structural influences can be interpreted in those areas where the two time-stratigraphic markers are regionally parallel. Localized regional structural movement has occurred in those areas where the two surfaces are not parallel. This isopach suggests that the vast majority of the Arkoma basin and Cherokee Platform was essentially stable from Late Silurian through the Mississippian and possibly had a more restricted marine environment. Formation thicknesses within the two time-stratigraphic horizons vary considerably. Three significant unconformities controlled thicknesses of those formations within this interval: (1) the Devonian-aged post-Hunton/pre-Woodford unconformity, (2) the Osagean/Meramecian unconformity, and (3) the Mississippian/Pennsylvanian unconformity. In the eastern part of the Arkoma basin, the Hunton Group, Woodford Shale, and Mississippian Osagean deposits are thick, which resulted in the Mayes Limestone, Fayetteville Shale, and the Pitkin Limestone being deposited in relatively shallow water. In the western part of the Arkoma basin, the Hunton Group and the Woodford Shale are much thinner, which suggests the Mayes Limestone, Fayetteville Shale, and the Pitkin Limestone equivalent were deposited in much deeper water and possibly in a more restricted marine environment.

References

Magoon, A.M., 2011, Sequence stratigraphic framework of the Caney Shale, Arkoma Basin southeastern Oklahoma: M.S. thesis, University of Oklahoma, Norman, 97 p.

Schad, S.T., 2004, Hydrocarbon potential of the Caney Shale in southeastern Oklahoma: M.S. thesis, University of Tulsa, Oklahoma, 576 p.

Logging Reservoirs, Petroleum Systems, Wettability, and CCS Viability in Midcontinent Carbonates Using Gentle-Extraction Cryo-Trap Mass Spectrometry of Drill Cuttings' and Cores' Present-Day Volatiles

Michael P. Smith, Christopher Smith, Patrick Gordon, and Timothy Smith
Advanced Hydrocarbon Stratigraphy, Tulsa, Oklahoma, USA

Introduction

We discuss results of volatiles analyses of large numbers of drill cuttings and cores of carbonate formations from many oil wells in Oklahoma and two carbon capture and storage wells drilled by the Kansas Geological Survey in Kansas. We analyzed present-day volatiles — primarily C1–C10 hydrocarbons, formation water, formic and acetic acids, helium, CO_2, H_2S, sulfate as the SO+ ion, CS_2, COS, and methyl ethyl ketone — as well as various rock properties, including mechanical strength and permeability indices. Samples were analyzed using a gentle-extraction, cryo-trap mass spectrometry system designed and built at Advanced Hydrocarbon Stratigraphy (AHS). Data are used to evaluate reservoir quality, oil migration, potential CCS reservoir integrity, and oil versus water wettability.

Methods and Results

Analyses: Cuttings and core samples were analyzed using a patented gentle-extraction cryo-trap spectrometer system designed and built at AHS (fig. 1).

About 400 microliters of cuttings or core pieces were loaded into plastic tubes under normal atmospheric conditions and then inserted into brass tubes and sealed with a polymer plug at the bottom and a polymer cap on the top. Filled brass tubes were loaded onto an autosampler and connected to a pre-evacuated static vacuum system with a needle lowered through a black cap. The sample was then connected to the static vacuum inlet system at about 20 millibars of pressure, about 1/50th of an atmosphere. Lab-loaded samples were crushed by a piston exerting about 2 tons per square inch of force on the sample. The samples'

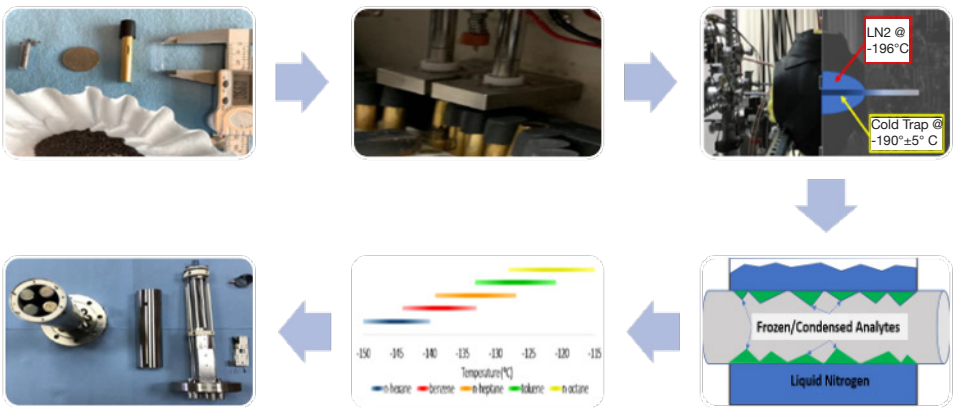

Figure 1. Components of AHS's gentle-extraction cryo-trap mass spectrometer system described in this section.

volatiles that had appropriate freezing points were vacuum extracted and frozen on a liquid nitrogen trap for 7.5 minutes. Non-condensable gases were trapped in sealed valves and burst by themselves into the mass spec for head space analyses. After 7.5 minutes, the liquid nitrogen trap was isolated from the sample and opened to the mass spectrometer at high vacuum. Gases that condensed onto the liquid nitrogen trap were liberated by sublimation in boiling point order by warming the LN_2 trap and were pumped through the mass spectrometer for analyses. This entire process was then repeated using the same piece of rock but extracting at 2 millibars pressure, or 1/500th of an atmosphere. The two data sets obtained from the same pieces of cuttings or core were then used to determine reservoir fluid properties as well as reservoir quality. Each sample takes about 15 minutes to run, so one machine can analyze about 100 samples a day.

Osage, Meramec, Woodford STACK, and SCOOP cores. More than 1,300 samples from nine cored wells drilled by Ovintiv in the Oklahoma STACK and SCOOP plays were analyzed. Figures 2 and 3 show some of the volatiles data work completed on these samples.

Figure 2 shows paraffins/(paraffins+naphthenes) and aromatics/(aromatics+naphthenes) logs (labeled "paraffins" and "aromatics," respectively) for the cores. The p/(p+n) logs show many samples have values close to 75%. This is the value obtained from whole oil samples produced in this play, which is usually close to 40 degrees API gravity. The p/(p+n) results indicate that these rocks are very tight and have not lost significant oil. Other samples show lower p/(p+n) values. These are the better-quality reservoir rocks. These rocks have lost more of the smaller non-cyclic paraffins that have about half the diameter of the larger-diameter cyclic naphthenes. This fractionation of smaller-diameter paraffins from larger-diameter naphthenes indicates limiting pore throat radii of about 5 nanometers in diameter. These changes in chemistry in the good-quality reservoir rocks occurred after the core was cut. This and the fact that the tight rocks show no chemical fractionation indicate that induration of these rocks followed oil migration and charging.

Figure 3 shows logs of total oil for each well. The samples showing high total oil are very tight and have maintained these high total oil values for the six years since coring. The samples showing low total oil

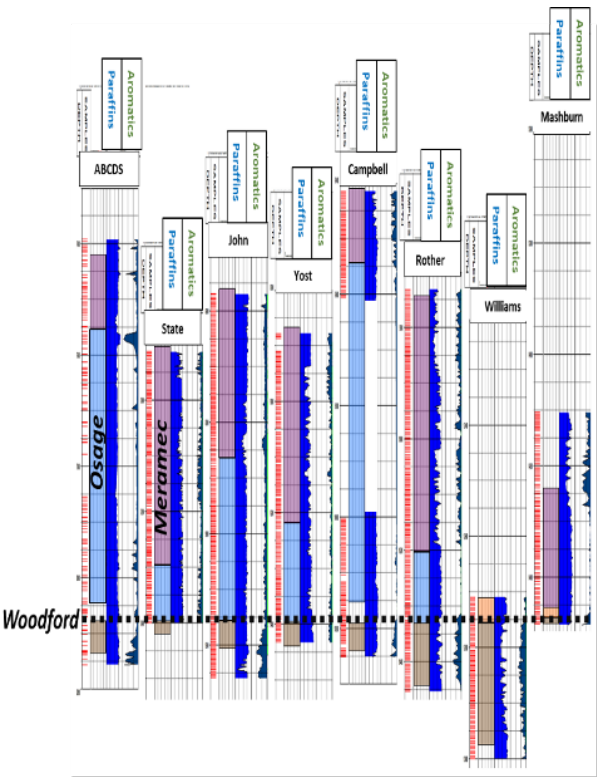

Figure 2. Cored Ovintiv wells: p/(p+n) and a/(a+n) logs.

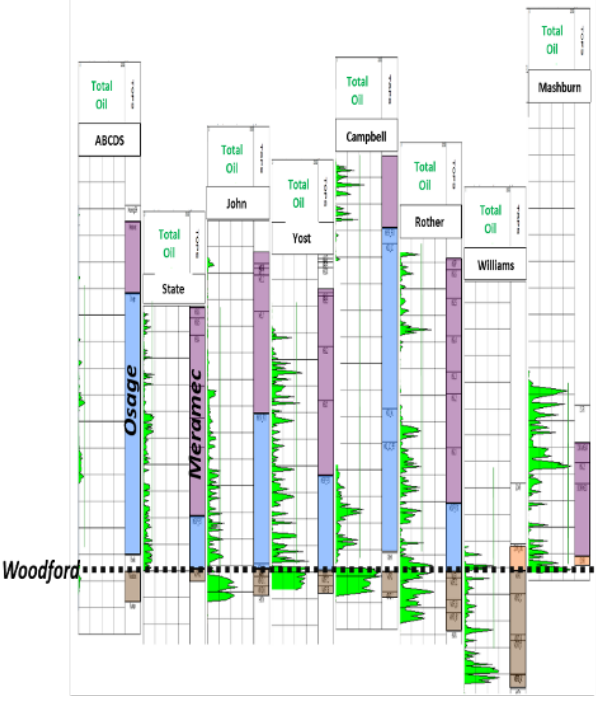

Figure 3. Cored Ovintiv wells: total oil logs.

are the good reservoir rocks. These samples have lost most of their oil since coring. An interesting feature of individual wells is that the maximum amount of total oil is repeated up and down the cored section. The data have the appearance of a comb with missing teeth. These data suggest very high oil saturations throughout the cored sections as indicated by the high values of total oil for each well's tight rocks. The data also indicate that these samples were indurated after oil migration and emplacement. Our assessment shows there is no way to fill the pore space in the tight rocks with the oil in their current state of induration. The inference that oil migration preceded induration was confirmed by mercury injection capillary pressure experiments, which failed to push mercury into these very tight rocks.

AHS's water data also indicate consistently low water saturations throughout these cored intervals, which is consistent with the water-free oil production from these reservoirs. It is also consistent with our interpretation based on our total oil assessment.

Osage and Meramec carbonates, northwest STACK, Oklahoma. Numerous Osage and Meramec laterals were analyzed in the northwest STACK play in Oklahoma. Some results are shown in figures 4 and 5.

Figure 4 shows high toluene/benzene ratios on a fault greater than that found in produced oils. This indicates oil migration, as more of the larger toluene molecules are left behind than the smaller benzenes. Cuttings oil is much higher, indicating tight rocks, on the heel side (left) of the fault than on the toe side (right). The heel side is the lower fault block; the toe side is the upper fault block. Oil migrated up the fault and into the upper fault block, charging the reservoir and stopping cementation. Oil-associated brines migrated down into the lower fault block and caused cementation. The upper orange track is cuttings' water. Water is lower toward the toe above the oil-migrating fault than toward the heel below the fault. Water increases away from the fault, indicating the highest oil saturations are near the fault. Figure 5 shows CO_2 logs for 10 one-mile Osage laterals in the northwest STACK. CO_2 is plotted on a log scale. Nine wells show similar CO_2 content, but the well circled in red shows massive CO_2 loss associated with a fault. These data show CCS reservoirs may not be viable near this fault.

KGS carbon capture and storage wells. Property logs of two KGS CCS wells are shown. Figure 6 shows

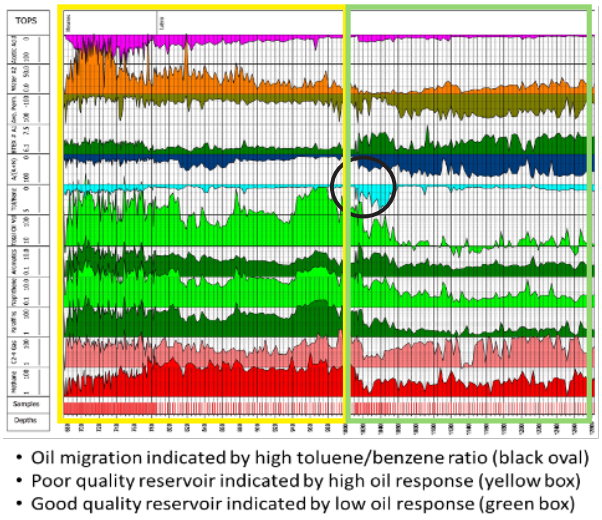

Figure 4. AHS property log for 1-mile Meramec lateral.

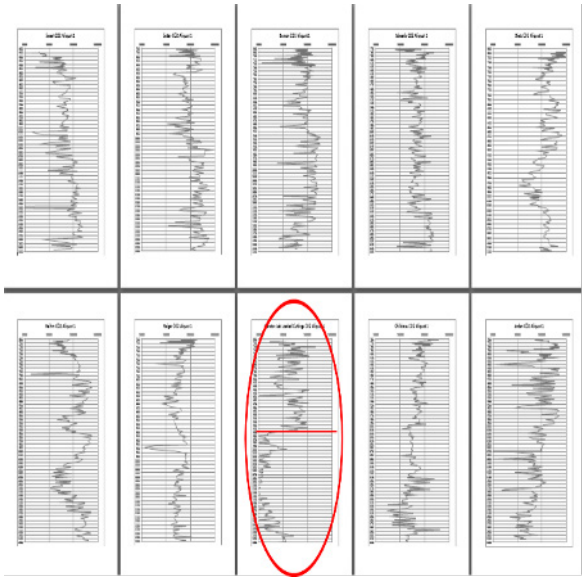

Figure 5. CO_2 log scales. Massive CO_2 loss at fault.

high CO_2, seen in both wells, indicating good CCS reservoir viability. Figure 7 shows the 20 millibar (black) and 2 millibar (red) water curves. The curves converge in the Morrow oil pay zone. Formations below the Morrow are water wetting. The Morrow is oil wetting. Formations above the Morrow are transitional from oil to water wetting. Water-wetting rocks hold their water tightly and have more 2 millibar water than 20 millibar water. Oil-wetting rocks are the opposite.

Discussion and Conclusions

Small quantities of formation fluids are held in the tight spaces of cuttings and core samples, even after

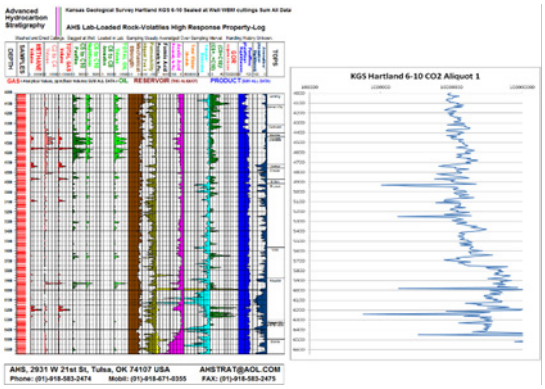

Figure 6. KGS Hartland well. Low CO_2 loss risk.

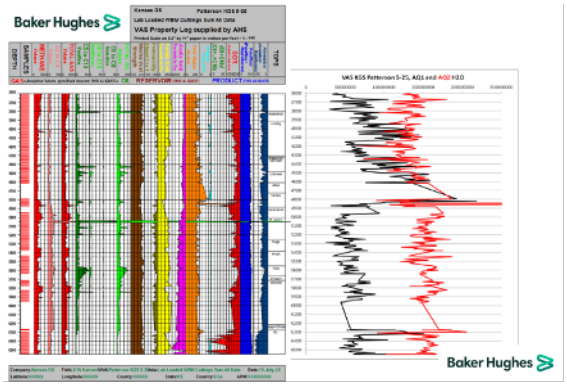

Figure 7. KGS Patterson well. Oil-wetting Morrow.

several to many years have passed since sample recovery during drilling. Gentle extraction and analyses of these trace volatiles allow many important features of carbonate systems to be ascertained. As discussed in this paper, these include reservoir quality, timing of oil emplacement relative to induration, the location of oil migration pathways and of charged permeable pay zones versus tightly cemented water legs, the viability of proposed CCS reservoirs, and oil- versus water-wetting strata.

The direct study of the fluids entrained in carbonate rocks is as important as the study of the composition and structure of carbonate rocks' solids. These fluids allow us to decipher parts of the history of these carbonates and identify the better reservoir zones. In the STACK and SCOOP Ovintiv cores, we determined that oil migration was vertical and preceded rock induration; that good reservoir rocks lose most of their oil and gas without compositions modified by fractionation, whereas tight rocks hold on to much of their oil and gas; and that the residual oil in these rocks was altered by preferential loss of smaller, lighter compounds. In the northwest STACK, away from the main Woodford oil-producing fairway, we see evidence of oil migration along faults and charging of reservoirs adjacent to and above oil-migrating faults. The reservoir quality of the oil-charged rocks is preserved, while the reservoir quality of rocks in the water leg may be destroyed. In the northwest STACK and in Kansas, we used CO_2 from cuttings to assess CCS reservoir viability. We also used the differential release of water from cuttings at different pressures to assess oil versus water wettability. Next, we must more fully integrate the fluids' and solids' stories.

Static Earth Modeling and CO_2 Storage in Lansing and Kansas City Groups, Huffstutter Field, Kansas, USA

Valerie Smith
Battelle, Columbus, Ohio, USA

Introduction

This study estimates the carbon dioxide storage potential of carbonate rocks and interbedded shales (cyclothems) in the Pennsylvanian Lansing and Kansas City (LKC) Groups at Huffstutter Field, Kansas. Located on the Central Kansas uplift in Phillips County, this field was selected because, geographically, it lies along a corridor near significant CO_2 sources to the northeast (corn ethanol plants) and potential CO_2 sinks (mature oilfields) to the southwest. The basis for this research stems from a goal of the Integrated Midcontinent Stacked Carbon Storage (IMSCS) Hub Project to develop a regional carbon storage hub connecting sources of captured carbon to existing oilfields for carbon storage and enhanced oil recovery (EOR).

The LKC Group is composed of Pennsylvanian cyclothems, and in this area, some of the LKC's carbonate units contain hydrocarbons. In this study, CO_2 resource estimates were simplified by treating the LKC units as saline aquifers. The two key research objectives were (1) to develop a 3-D static earth model (SEM) representing the petrophysical properties of the LKC groups so that (2) a quantitative CO_2 storage assessment could be performed on the carbonate reservoir units.

Huffstutter oilfield is the largest field in Phillips County, where many mature oilfields are still active. The largest structural trend in the area is the Central Kansas uplift, a southeasterly continuation of the Cambridge arch located in Nebraska. Together, these structural uplifts trend from the northwest to the southeast. Huffstutter Field is located on a very gentle anticline along the eastern portion of the Central Kansas uplift. Huffstutter contains more than 100 wells, and logs from 96 wells were digitized for this study. Most of these wells stop at or near the base of the LKC. Oil production for the field is generally limited to LKC stratigraphic zones "E" and "F" (using the lettering convention more commonly found in Nebraska [Smith and Joeckel, 2020]).

Methods and Results

The basic well log suite in this area generally includes gamma ray (GR), neutron-porosity (NPHI), and resistivity (R) logs. Unfortunately, core data were not available from the Huffstutter Field. However, LKC core from Sleepy Hollow Field to the northwest and Dopita Field (well A-16) to the south correlate with well log response through the LKC and serve as the basis for interpretations of LKC rock composition for this study. Interpretations from these core samples showed that the LKC rock units could generally be lumped into three categories: limestone-dominant, mudstone-dominant (commonly massive or blocky but not platy), and shale-dominant (commonly fissile) rock. Together, these three categories represent the fundamental facies for developing the SEM. Core from the limestone-dominant reservoir rock shows that porosity occurs in limestone textures, including packstone, grainstone, and oolitic units. Analysis of log responses from GR and NPHI logs reveals LKC interbedded shales and carbonates are cyclical and consistent with the "Kansas-type" cyclothem as described by Heckel (1986). The GR log was employed in SEM facies development to delineate limestone, mudrock, and shale using GR-thresholds. For developing effective porosity logs, adjustments to the NPHI logs required discriminating the clean limestones (reservoir units) from the mudrocks (seals).

The SEM was limited to an area of 6,000 ft by 6,000 ft and located in the northeast corner of Huffstutter Field, where well data was most concentrated and available (as obtained for CarbonSafe, Phase I [Battelle,

2018]). The SEM framework incorporates eight surfaces that are based on well tops from 96 wells in and around the field. Above the LKC, the Oread Member of the Douglas Group was included because it contains the Heebner Shale, a widely correlated unit in Kansas and Nebraska. The model comprised 2,548,800 cells. The SEM has a horizontal resolution defined by a grid cell XY-increment of 50 ft (15.23 m). Each model layer had 120 x 120 cells for a total of 14,440 cells per layer. About 285 feet thick, the petrophysical SEM included seven zones from the Oread Member of the Douglas Group down to the base of the Kansas City Group at approximately 3,500 feet measured depth. The LKC portion of this SEM measures about 216 feet thick and represents six of the seven model zones; the Oread portion is about 69 ft thick.

Facies modeling: The GR logs were used as the basis for a GR facies model. For 3-D facies modeling, the moving average modeling method was selected because GR log signatures were highly correlated and could usually be traced across the entire oilfield. The GR facies model was divided into three categories based on GR thresholds: (0) GR less than 70: Carbonate-dominated; oolitic, packstone, peloidal, and skeletal grainstones are of particular interest as reservoir rocks (Dunham classification); this category also includes other carbonate rock types, such as lime-mudstones and wackestones. Favorable porosity and permeability are associated with the cleaner carbonate units, where porosity development occurs. (1) GR greater than 70 and less than 120: Mudstone-dominated, includes illite-rich, reddish siliciclastic mudstones, often with pedogenetic features. (2) GR greater than 120: Shale-dominated, commonly black or dark gray transgressive marine shale. This GR facies model followed the approach used by Smith and Joeckel (2020).

Effective porosity modeling: Neutron porosity logs served as the key input for deriving effective porosity logs and required a shale volume correction. The arithmetic mean upscaling method was used to sample effective porosity logs into the 3-D grid cells along their well trajectories. These effective porosity values were interpolated into inter-well grid cells using a Gaussian Random Function Simulation while being conditioned by the GR facies model.

Pressure, temperature, and CO_2 density modeling: Pressure and temperature models were prepared for the LKC Group at Huffstutter Field and used drill-stem test results from Sleepy Hollow Field as proxy data. The density of supercritical CO_2 is dependent on reservoir pressure and temperature at reservoir conditions and was determined through a look-up table from NETLCO2-SCREEN (Goodman et al., 2016).

CO_2 storage resource assessment for the LKC Group: The CO_2 storage resource estimate for the LKC was computed using equation 1 and the 3-D SEM, which included models for the bulk volume (Vc), effective porosity (φ_e), pressure (P), temperature (T), CO_2 density (ρ_{CO2}(P,T)), and a storage efficiency factor of 0.1. M_{CO2} is the computed mass of supercritical CO_2 at reservoir conditions. Equation 1 is applied to the 3-D geocellular model. Estimates of CO_2 storage mass are computed directly on individual cells and added together to produce the total CO_2 storage mass estimate for 1 square mile of LKC.

$$M_{CO2} = Vc * \varphi_e * \rho_{CO2}(P, T) * E_{saline} \quad \text{eq. 1}$$

The storage efficiency factor was simplified to just the displacement terms: E_{saline} = (Ev * Ed), where E_v = volumetric displacement efficiency and Ed = microscopic displacement efficiency (Goodman et al., 2011). E_{saline} = 0.1 was used and represented the p10 confidence level for limestone per Peck et al. (2014). This level was selected because these carbonates are often tight; thus, the resource estimates reported here are conservative. Based on a 1-square mile of LKC section at Huffstutter Field, the computed M_{CO2} results are shown in fig. 1 and summarized in table 1. The storage resource estimations assume that all LKC carbonate units were accessible for CO_2 injection and are saline. Oil is diminishing for these mature fields, and saline LKC storage zones are likely more representative of what other sites may have to offer, especially for many corn ethanol plant locations.

Discussion and Conclusions

This study completed a CO_2 storage assessment for the LKC Group at Huffstutter Field and is based on a 3-D geocellular model representing midcontinent Pennsylvanian cyclothems. The storage capacity estimates are focused on regressive limestones representing key CO_2 storage intervals where GR log response of 70 gAPI or less was used to identify clean carbonate intervals that

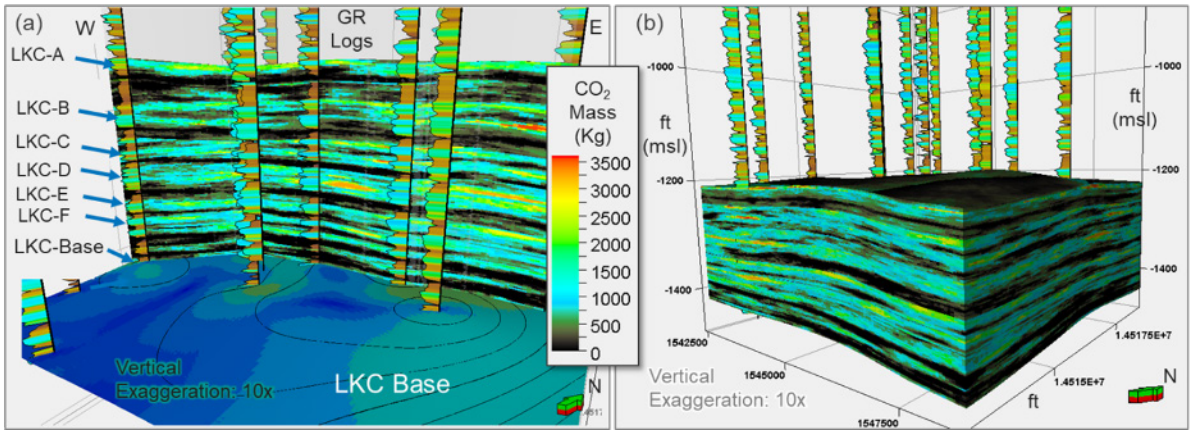

Figure 1. Computed CO_2 mass storage results, by cell, for the LKC. Light areas represent computed CO_2 storage resources based on CO_2 density and reservoir pore space accessibility. (a) Vertical slice through the SEM showing CO_2 mass; the dark areas represent mudrock intervals. (b) Oblique view of SEM with computed CO_2 mass storage, by cell, at an efficiency of 10%.

Table 1. Carbon storage resource estimated by zone for the LKC carbonate reservoir units where GR facies code = 0.

LKC unit	Effective reservoir (%) [a]	Tonnes CO_2/ mile^2	Tonnes CO_2/ km^2
LKC zone A	58	53,427	20,628
LKC zone B	66	92,092	35,557
LKC zone C	65	125,343	48,395
LKC zone D	71	61,815	23,867
LKC zone E	73	55,555	21,450
LKC zone F	36	55,123	21,283
Total:		443,355	171,180

[a] *Percent of zonal volume comprising carbonate reservoir rock; the remaining zonal portion is either mudrock or shale.*

are potentially accessible for CO_2 storage. Based on the SEM derived from Huffstutter well logs, the LKC here can potentially store 443,355 tonnes CO_2/mile^2 (171,180 tonnes CO_2/km^2) using a saline storage efficiency factor of 0.1. The workflow and SEM developed through this research can be applied to other oilfields in the area to manage hydrocarbon resources or can be used as the framework for saline storage estimates and the evaluation of CO_2 injection plans.

Acknowledgments

The research for the Integrated Midcontinent Stacked Carbon Storage Hub project is supported by the U.S. Department of Energy – NETL Agreement No. DE-FOA-0031623 and No. DE-FE0029264. The data supplied in this study were acquired in collaboration with the Conservation and Survey Division, School of Natural Resources, University of Nebraska–Lincoln, and through Great Plains Energy, Inc., Lincoln, Nebraska. Existing oilfield data were acquired through the Nebraska Oil and Gas Commission and the Kansas Geological Survey Oil and Gas database.

References

Battelle Memorial Institute, 2018, Integrated Midcontinent Stacked Carbon Storage Hub, Task 3 Sub-Basinal Geologic Assessment Topical Report, DOE Agreement/Project # DE-FE0029264, https://www.osti.gov/biblio/1478726-integrated-mid-continent-stacked-carbon-storage-hub-phase-final-report.

Goodman, A., Hakala, A., Bromhal, G., Deel, D., Rodosta, T., Frailey, S., Small, M., Allen, D.,

Romanov, V., Fazio, J., Huerta, N., McIntyre, D., Kutchko, B., and Guthrie, G., 2011, U.S. DOE methodology for the development of geologic storage potential for carbon dioxide at the national and regional scale: International Journal of Greenhouse Gas Control, v. 5, p. 242–249.

Goodman, A., Sanguinito, S., and Levine, J., 2016, Prospective CO_2 resource estimation methodology: Refinement of existing US-DOE-NETL methods based on data availability: International Journal of Greenhouse Gas Control, v. 54, p. 952–965.

Heckel, P. H., 1986, Sea-level curve for Pennsylvania eustatic marine transgressive-regressive depositional cycles along midcontinent outcrop belt, North America: Geology, v. 14, no. 4, p. 330–334, doi:10.1130/0091-7613(1986)14<330:SCFPEM>2.0.CO;2.

Peck, W. D., Glazewski, K. A., Klenner, R. C. L., Gorecki, C. D., Steadman, E. N., and Harju, J. A., 2014, A workflow to determine CO_2 storage potential in deep saline formations: Energy Procedia, v. 63, p. 5,231–5,238.

Smith, V. L., and Joeckel, R. M., 2020, Reservoir characterization and static earth model for potential carbon dioxide storage in Upper Pennsylvanian cyclothems, Nebraska, United States: Environmental Geosciences, v. 27, no. 2, p. 67–86.

Facies Architecture and Reservoir Characteristics of the Caney Shale, Ardmore Basin, Southern Oklahoma, USA

Yulun Wang[1], G. Michael Grammer[1], Jack Pashin[1], Jim Puckette[1], and Mileva Radonjic[2,1]
[1] Boone Pickens School of Geology, Oklahoma State University, Stillwater, Oklahoma, USA
[2] School of Chemical Engineering, Oklahoma State University, Stillwater, Oklahoma, USA

Introduction

The late Mississippian Caney Shale is an oil- and gas-producing unconventional hydrocarbon reservoir that has produced since the early 2000s (Andrews, 2007). Mostly found in southern Oklahoma, the subsurface Caney Shale produces in the Ardmore and Arkoma basins of the southern Midcontinent (fig. 1). Based on limited publication records (e.g., Kamann, 2006; Jacobi et al., 2009), the subsurface Caney Shale consists of organic-rich "shale" (or organic-rich, calcareous, siliceous, and silty mudstone) with siltstone and carbonate intervals. Despite petroleum industry efforts in the past decade, production from the Caney Shale has been relatively sparse and unpredictable, showing spatial variabilities across and within the Ardmore and Arkoma basins (e.g., Andrews, 2007; Cardott, 2017). Detailed published studies that focus on the relationship between facies distribution and production by integrating core and log data to evaluate the Caney Shale play in southern Oklahoma are lacking. Considering the limited recent research, we aim to conduct a comprehensive, interdisciplinary investigation of the Caney Shale play by collaborating with industrial and academic partners (Department of Energy Project DE-FE0031776; Field Evaluation of the Caney Shale as an Emerging Unconventional Play, Southern Oklahoma; 2019 to 2023). Our objective is to evaluate the reservoir and production potential of the Caney Shale play from the perspectives of geology, petrophysics, geomechanics, and engineering. In this study, we focus on core and log data from one Caney well within the Ardmore basin (fig. 1) with the goal to identify facies, establish depositional environments, define the stratigraphic framework using core and log data, and analyze reservoir distribution within this framework. By extrapolating the stratigraphic and petrophysical framework to nearby uncored wells, characterizing and predicting reservoir distribution at a regional scale can be enhanced. Core samples were examined to characterize the natural fracture system and rock strength tested using rebound hardness, both of which can provide insight into rock mechanical properties for production design.

Methods and Results

We propose an integrated, multiscale workflow. We conducted detailed core description (650 ft/200 m) and petrographic analysis (N = 93) to identify facies and depositional processes. Based on the vertical stacking of different facies, we defined a stratigraphic framework and tied this framework to the principal wireline log curves of the well, such as gamma ray (GR), resistivity,

Figure 1. The well of this study (red circle on map) is located within the Ardmore basin in southern Oklahoma.

photoelectric factor (PEF), neutron-density porosity, and sonic transit time. The primary objective is to evaluate whether individual facies, vertical facies succession, and the internal units of the stratigraphic framework show distinctive log responses and whether there is a relationship between the stratigraphic framework and potential reservoir distribution interpreted from logs. Ultimately, we aim to extrapolate this framework into nearby uncored wells to characterize the depositional system and predict reservoir distribution at a regional scale. To characterize the natural fracture system, the slabbed core surface was examined and nearly 1,000 naturally mineralized fractures were described and documented in terms of height, kinematic aperture, orientation, mineralization, and vertical termination. Fracture spacing data have also been acquired for fracture sets that contain at least two non-cross-cutting fractures. To understand the distribution of rock strength, rebound hardness testing was conducted on complete and polished core surfaces that are free of cracks. Nearly 2,100 rebound hardness data points were collected targeting all facies types and the finer-scale features, such as nodules, lenses, and millimeter-sized layers in various compositions. We aim to tie both fracture distribution and rebound hardness data to facies distribution to evaluate whether these two data types can be predicted by facies distribution and variations in mineralogy.

We identified 10 types of mixed carbonate-siliciclastic facies, including a variety of mudstone, siltstone, and carbonate facies (fig. 2). Based on the vertical variations in the stacking patterns of these facies, the entire core can be divided into four segments. When tied with log data, these four segments show distinctive, highly fluctuating responses in several log types among and within individual segments. In particular, the relatively thick layers of carbonate facies (e.g., packstone-grainstone [Ps-Gs], packstone to rudstone [Ps-Rs], dolomitic facies [DLM]; fig. 2) show distinctive log curve responses that can be readily identified relative to the mudstone and siltstone facies, such as lower GR, higher PEF, lower neutron and density porosity with closely tracked curves, and lower sonic transit time.

Mineralized natural fractures are present and are all filled with calcite cement (fig. 3). These fractures are concentrated in certain intervals, showing a

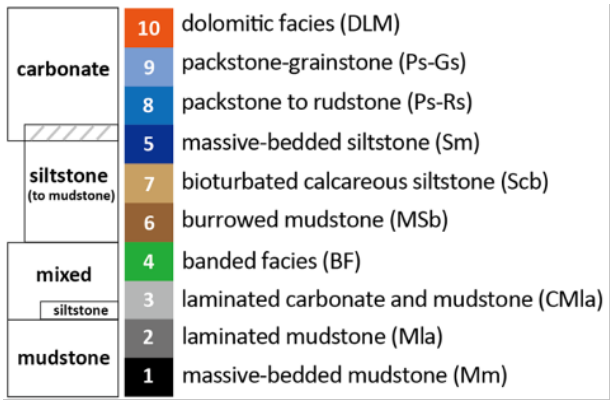

Figure 2. Caney facies types identified in the core of this study.

compartmentalized distribution pattern across multiple scales. In general, these fractures tend to be more abundant in carbonate facies, commonly creating a bed-bound fracture distribution in these layers (fig. 3a). At a finer scale, these fractures also can be confined by thin carbonate- and silica-rich layers (a few centimeters or less in thickness) that are enclosed by mudstone and siltstone (fig. 3b). At whole-core scale, a generalized trend is evident between rebound hardness data and the principal facies groups: mudstone, siltstone, carbonate, and chert (fig. 3). Overall, the highest rebound hardness values (RHN) tend to be observed in chert (greater than 800 HLD) and carbonate (700 to 800 HLD), followed by siliceous/calcareous mudstone-siltstone (500 to 700 HLD) and organic-rich mudstone (less than 500 HLD).

Discussion and Conclusions

The mixed carbonate-siliciclastic facies identified in core reflect a spectrum of energy conditions. Clay-rich mudstone and siltstone facies suggest low energy background sedimentation. Carbonate facies with planar and cross laminations, combined with chaotically arranged and poorly sorted (up to pebble-sized) clasts and grains in various compositions, point to intermittent high-energy event deposition (e.g., turbidity current, debris flow, longshore current, storm) that are likely sourced from a shallower water carbonate platform updip. Considering their vertical stacking in core, these facies are potentially part of axis (carbonate) and fringe (mudstone, siltstone) portions of a vertically stacked submarine fan system, being analogous to the Wolfcamp Formation in the Permian Basin (Kvale et al., 2020). In the four segments defined from core, their distinctive

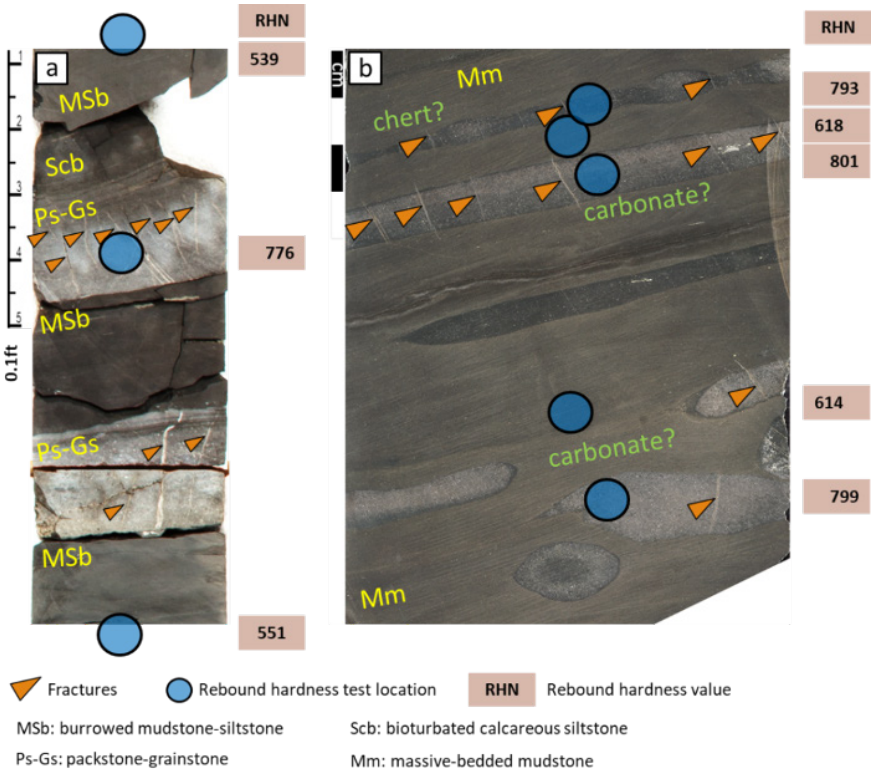

Figure 3. Core photographs showing the distribution of natural fractures (orange triangles) and rebound hardness data (RHN; testing locations marked by blue circles; values are noted by numbers on the right side of core photos). Facies acronyms are consistent with fig. 2. See text for discussion.

facies architecture and log response suggest that they may serve as fundamental units of a stratigraphic framework, which can potentially be extrapolated into nearby uncored wells for stratigraphic correlation and reservoir characterization at a regional scale. For the vertically stacked, highly heterogeneous reservoir properties (e.g., resistivity, porosity) among and within individual segments, they indicate variabilities in reservoir potential across multiple scales (e.g., meters to tens of meters) and can largely be tied with the vertical stacking of different facies and, at a finer scale, with mineralogical variations. Therefore, connecting facies architecture and reservoir properties within a hierarchical stratigraphic framework constructed by integrating detailed core observations and log response at a regional scale in 3-D can potentially allow for an enhanced delineation of reservoir distribution and improved exploration and production strategies.

From an overall reservoir perspective, the carbonate facies — which occur in relatively thick layers (e.g., more than 1 to 2 feet), show distinctive log responses such as low sonic transit time and low porosity, and can be readily identified in logs — are likely the seal facies. In contrast, the adjacent mudstone and siltstone are considered reservoir facies but overall lack a distinctive log response, making it challenging to predict these facies in detail and with high confidence using logs alone. In particular, because they tend to show the most abundant fractures and the highest rebound hardness values among all facies (fig. 3), carbonate facies are potentially favorable targets for creating the hydraulic fractures required to produce from the adjacent organic-rich mudstone and siltstone intervals. Therefore, understanding the distribution and geometry of these carbonate layers in the context of a core-based stratigraphic framework from a 3-D perspective can be beneficial for targeting and predicting these seal-reservoir zones at a regional scale. Further, considering the distinctive log response of these carbonate layers, it is feasible to map their spatial distribution in 3-D to guide exploration and production, which has been achieved in the Wolfcamp Formation in the Permian Basin (e.g., Kvale et al., 2020). Doing so will enhance the understanding of not only the origin of these carbonate intervals but also the geometry of the regional depositional system, which will, in turn, enhance the prediction of the associated reservoirs. Therefore, such a direct tie among facies architecture, petrophysical and rock mechanical properties, fracture distribution, and stratigraphic framework can potentially provide insight

for constructing a regional reservoir model to optimize exploration and production.

References

Andrews, R. D., 2007, Stratigraphy, production, and reservoir characteristics of the Caney Shale in southern Oklahoma: Shale Shaker, v. 58, p. 9–25.

Cardott, B. J., 2017, Oklahoma shale resource plays: Oklahoma Geology Notes, v. 76, no. 2, p. 21–30.

Jacobi, D., Breig, J., LeCompte, B., Kopal, M., Hursan, G., Mendez, F., Bliven, S.. and Longo, J., 2009, Effective geochemical and geomechanical characterization of shale gas reservoirs from the wellbore environment: Caney and the Woodford shale: Society of Petroleum Engineering (SPE) Annual Technical Conference and Exhibition, New Orleans, Louisiana, USA, 4–7 October, paper 124231.

Kamann, P. J., 2006, Surface-to-subsurface correlation and lithostratigraphic framework of the Caney Shale (including the "Mayes" Formation) in Atoka, Coal, Hughes, Johnston, Pittsburg, and Pontotoc counties, Oklahoma: Unpublished M.S. thesis, Oklahoma State University, Stillwater, USA, 259 p.

Kvale, E. P., Bowie, C. M., Flenthrope, C., Mace, C., Parrish, J. M., Price, B., Anderson, S., and DiMichele, W. A., 2020, Facies variability within a mixed carbonate–siliciclastic sea-floor fan (upper Wolfcamp Formation, Permian, Delaware basin, New Mexico): American Association of Petroleum Geologists (AAPG) Bulletin, v. 104, p. 525–563.

Northcutt, R. A., and Campbell, J. A., 1996, Geologic Provinces of Oklahoma: Transactions of the 1995 AAPG Mid-Continent Section Meeting, p. 128–134.